

STUDIES ON THE GENETICS OF RETINITIS PIGMENTOSA

Marian M Humphries, MSc

**A thesis submitted for
the degree of
Doctor of Philosophy
1999**

University of Szeged

**József Attila University,
Egyetem u. 2,
POB 659, Szeged, H-6722,
Hungary.**

Declaration

I hereby certify that this thesis, "Studies on the genetics of Retinitis Pigmentosa", submitted for the degree of Doctor of Philosophy to the József Attila University, Hungary, has not been previously submitted for a degree or diploma in this or any other university. The work presented in this thesis is my own, except where explicitly stated to the contrary.

Marian Humphries

Marian M Humphries

30th November, 1999.

DEDICATION

To Pete and Jeremy

ACKNOWLEDGEMENTS

I would like to thank Drs. Denise Sheils, Jane Farrar, Paul Kenna and all my colleagues in the Ocular Genetics Unit and throughout the world for their continued help, support and encouragement throughout the years.

I would like to say a special thank you to members of RP-Ireland Fighting Blindness, DEBRA-Ireland for their constant fund-raising to support our research.

To the RP and EB family members for their support, interest and endless co-operation throughout the years.

Special thanks to my parents, parents-in-law, and family for their support and encouragement throughout the years.

NOTATIONS AND ABBREVIATIONS

AAV	Adeno Associated Virus
adMD	Autosomal Dominant Macular Degeneration
ADS	Antibody Diluting Solution
adRP	Autosomal Dominant Retinitis Pigmentosa
ARMD	Age Related Macular Degeneration
arMD	Autosomal Recessive Macular Degeneration
arRP	Autosomal Recessive Retinitis Pigmentosa
bp	Base-pair
BTMD	Best's Vitelliform Macular Dystrophy
BSA	Bovine serum albumin
cGMP	Cyclic 3',5'-guanosine Monophosphate
cM	centiMorgans
DAB	Diaminobenzidine
dNTP	Deoxynucleotide triphosphate
EDTA	Ethylenediaminetetra-acetic acid
EM	Electron Microscope
EOG	Electro-oculogram
ERG	Electroretinogram
ES	Embryonic Stem Cells
FFM	Fundus Flavimaculatus
GAPDH	Glyceraldehyde-3-phosphate dehydrogenase
GDNF	Glial Derived Neurotrophic Factor
GFP	Green Fluorescence
H&E	Haemotoxin and Eosin
G	Ganglion Cell Layer
HGM9	Human Gene Mapping Nine
IN	Inner Nuclear Layer
IP	Inner Plexiform Layer
IS	Inner Segment
kb	kilobase
kD	kiloDalton
Lod	log of odds
NIH-NIGMS	National Institute of Health-National Institute of General Medicine
θ	Recombination fraction
OP	Outer Plexiform Layer
ONL	Outer Nuclear Layer
OS	Outer Segment
PCR	Polymerase Chain Reaction
PDE	Phosphodiesterase
PIC	Polymorphic information content
PBS	Phosphate Buffered Saline
PVP	Poly vinyl prolene
RCS	Royal College of Surgeons
RDS	Retinal Degeneration Slow
RFLP	Restriction fragment length polymorphism
Rho	Rhodopsin
RIS	Rod Inner Segments
ROS	Rod Outer Segments
RP	Retinitis Pigmentosa
RPE	Retinal Pigment Epithelium
RPGR	Retinitis Pigmentosa GTPase Regulator
RT-PCR	Reverse Transcriptase Polymerase Chain Reaction
SDS	Sodium dodecyl sulphate
SSC	Standard saline citrate

STGD	Stargardt Disease
TAE	Tris Acetate
TCD-M	Irish Pedigree Displaying Retinitis Pigmentosa
TE	Tris/EDTA
TIMP3	Tissue Inhibitor of Metalloproteinases
TK	Thymidine Kinase
UCLA-RP1	American Pedigree Displaying Retinitis Pigmentosa
xIRP	X-linked Retinitis Pigmentosa

TABLE OF CONTENTS

DEDICATION		i
ACKNOWLEDGEMENTS		ii
NOTATIONS AND ABBREVIATIONS		iii-iv
TABLE OF CONTENTS		v-vi
Chapter 1	RETINITIS PIGMENTOSA: ON THE ETIOLOGY OF THE DISEASE AND ON THE DEVELOPMENT OF THERAPEUTIC STRATAGIES.	
1.1	Background	1
1.2	The Structure of the Human Eye.	4
1.3	Visual Transduction	7
1.4	Clinical Features of Retinitis Pigmentosa and Methods for diagnosis of the disease.	9
1.5	Clinical Features of Macular Degeneration	13
1.6	Genetics of Degenerative Retinopathies	16
Chapter 2	LINKAGE ANALYSIS OF HUMAN CHROMOSOME 4: EXCLUSION OF AUTOSOMAL DOMINANT RETINITIS PIGMENTOSA (adRP) AND DETECTION OF NEW LINKAGE GROUPS: SYSTEMATIC LINKAGE STUDIES REPRESENTATIVE OF THOSE THAT LEAD TO THE LOCALISATION OF THE FIRST adRP GENE.	
2.1	Introduction	19
2.1:i	Families	21
2.1:ii	Genetic Markers	24
2.2	Materials and Methods	25
2.2:i	Materials	25
2.2:ii	Genomic DNA Preparation, Probe Preparation, Restriction Digestion and Southern Blotting Analysis	25
2.2:iii	Data Analysis	26
2.3	Results	28
2.3:i	Linkage Strategy	28
2.3:ii	Between-marker Linkages	29
2.3:iii	Haplotype Analysis	31
2.3:iv	adRP Exclusion	31
2.4	Discussion	32

Chapter 3 RETINOPATHY INDUCED IN MICE BY TARGETED DISRUPTION OF THE RHODOPSIN GENE

3.1	Introduction	34
3.2	Materials and Methods	38
3.2:i	Materials	38
3.2:ii	Purification of Phage DNA from Single Plaque Forming Units.	38
3.2:iii	DNA Digestion and Gel Electrophoresis of Phage and Genomic DNAs	38
3.2:iv	Southern Blotting	39
3.2:v	Nick Translation	39
3.2:vi	Prehybridization and Hybridization Conditions	40
3.2:vii	Membrane Washes	40
3.2:viii	Ligations, Packaging and Titering Reactions	40
3.2:ix	Large Scale Phage Preparation	41
3.2:x	Large Scale Plasmid Preparation	42
3.2:xi	Polymerase Chain Reaction	42
3.2:xii	Isolation of Total RNA using SV Total RNA Isolation System (Promega)	42
3.2:xiii	Reverse Transcriptase Polymerase Chain Reaction (RT-PCR)	43
3.2:xiv	Histology	43
3.2:xv	Immunocytochemical Analysis of Rhodopsin in Retinal Sections	44
3.2:xvi	Electroretinographic Recordings	45
3.3	Results	46
3.3:i	Construction of Rhodopsin Targeting Vector, ES Cell Selection, Generation and Analysis of Chimeric Mice	46
3.3:ii	Reverse Transcriptase PCR (RT-PCR)	48
3.3:iii	Retinal Pathology of Rho ^{-/-} and Rho ^{-/-} Mice	49
3.3:iv	Immunocytochemical Analysis of Rhodopsin in Retinal Sections	50
3.3:v	Electroretinographic Analysis of Rho ^{+/-} and Rho ^{-/-} Mice	51
3.3:vi	Breeding of Rho ^{-/-} Mice onto pure C57 and 129 Genetic Backgrounds	53
3.3:vii	Generation of Rho ^{-/-} -c-fos ^{-/-} Mice	53
3.4	Discussion	55
4.1	Summary	60
5.1	References	64

CHAPTER 1

RETINITIS PIGMENTOSA: ON THE ETIOLOGY OF THE DISEASE AND ON THE DEVELOPMENT OF THERAPEUTIC STRATEGIES.

1.1 Background.

Retinitis pigmentosa (RP) is a heritable degenerative disease of the retina (retinopathy) in which the photoreceptors gradually die. Patients initially experience night blindness owing to the early loss of rod cells, a symptom usually followed by the development of tunnel vision and eventually, in many cases, total blindness as the cone photoreceptors subsequently degenerate. RP occurs with an approximate frequency of 1:3000 and a prevalence, world-wide of approximately 1.5 million (Heckenlively, 1988; Pagon, 1988). The condition is incurable, and hence a first step towards the development of therapies is the determination of the cause of the disease. Ten years ago we knew that at least two genes would turn out to be implicated in disease etiology since the condition was known to be inherited either in an autosomal dominant, autosomal recessive or X-linked mode (McKusick, 1983). As will be emphasised in this introduction the genetics of RP turned out to be considerably more complex. Two large pedigrees were initially available to us, one of Irish and the other of American origin, which were, in principle, sufficiently large to enable the genes involved to be localised by genetic linkage analysis. There were relatively few genetic markers available at that time. However we were able to put together a set of markers on chromosome 4 which, hopefully, would enable coverage of much, if not all of that chromosome. In Chapter 2 of this thesis the exclusion studies carried out with these markers are presented as an example of the very large amount of work which was undertaken to eventually localize the gene in the Irish family. As a group, we covered at least 60% of the genome in the

search for this gene, the location of which was eventually established in 1989. The marker in question, C17 (D3S47), which was located on the long arm of chromosome 3, co-segregated with the disease locus in this family at zero recombination and with a lod score of 13.7, which was at that time and probably remains to this day, the largest single lod score ever reported as a result of genetic linkage studies in a single family (McWilliam, et al 1989). As an immediate consequence of this study we were able to establish the existence of genetic heterogeneity in autosomal dominant retinitis pigmentosa: there was no evidence for linkage on chromosome 3 in another large family of Irish origin that had become available to us (Farrar, et al. 1990). The gene in that family was localized to the short arm of chromosome 6 (Farrar et al. 1991a; Farrar et al. 1991b). Also in 1991 the gene in the original American family was eventually localized in the pericentric region of chromosome 8 by Dr. Stephen Daiger and colleagues (Blanton, et al 1991). Since those early days many genes have been localized as a result either of genetic linkage studies in families with RP and related retinal dystrophies, or by direct mutation screening of potential candidate genes in affected cases. In total, 35 genes have now been isolated and characterized, as summarised below.

In respect to the chromosome 3 study, the gene encoding Rhodopsin, the light sensitive pigment of the rod photoreceptors turned out to map within the disease interval. From the published sequence of the rhodopsin gene we found a microsatellite which could be amplified by PCR. Again this genetic marker co-segregated with the disease locus at zero recombination, providing a very strong indication that the rhodopsin gene was probably implicated in disease etiology. To date up to 100 mutations have been encountered within the rhodopsin gene, mostly in cases of adRP although some have also been found in autosomal recessive RP and in congenital night blindness (Humphries, et al 1992a; Sullivan and Daiger, 1996).

The generation of a mouse model carrying a targeted disruption of the rhodopsin gene, which is the major component of this thesis, was undertaken for two reasons. The first is historical. As described above the rhodopsin gene was the first to be implicated in the cause of RP in man. The protein constitutes the major component of the rod photoreceptors. Clearly it would be of immense intrinsic interest to ask the fundamental question - what is the functional and histological consequence to the rod cells of losing their major protein component?. Secondly, a mouse model for RP based on a targeted disruption of the rhodopsin gene would serve as a useful model for studies on therapeutic gene intervention.

In this Chapter, an outline is provided of the structure of the human eye, the mechanisms of visual transduction and of our current knowledge of the molecular pathology of degenerative diseases of the human retina. As will become apparent, many genes involved both in visual transduction and in the structure of the rod photoreceptors are involved. In Chapter 2, I present my data on the genetic linkage studies carried out, using as an example the exclusion studies undertaken on chromosome 4, in the Irish and American adRP pedigrees, studies which eventually yielded the localization of the causative gene on chromosome 3. These studies typify the difficulties associated with early genetic linkage studies, largely employing restriction fragment length polymorphism (RFLP) markers of relatively low information content and requiring the use of the tedious Southern blotting technique (Southern, 1975). Later studies were rendered less tedious owing to the development of high information content microsatellites (CA repeats) which involved the use of the very much more rapid polymerase chain reaction (PCR) technique (Weber and May, 1989). Chapter 3 is devoted to the construction of a mouse model for adRP based on the work I have undertaken on a targeted disruption of the rhodopsin gene (Humphries, et al 1997). Progress in the development of a second dominant model for RP will also be described. Animal

models of this sort will be essential for the development of gene therapies for this prevalent group of conditions. I will also present data on the effects of genetic background on rates of photoreceptor degeneration in $Rho^{-/-}$ retinas. Specifically, the progression of the retinopathy in $Rho^{-/-}$ mice has been followed both on pure C57B6 and 129 strains, preliminary data suggesting a significant retardation of photoreceptor degeneration in C57B6 mice. Such observations may hopefully result in the identification of “modifier” genes, the products of which may influence the rate of degeneration of photoreceptor cells. Clearly, knowledge of such genes bears direct relevance to the eventual development of optimal preventative therapies. Data are also presented on the effects of photoreceptor degeneration in the rhodopsin knockout crossed onto a *c-fos* knockout mouse. The latter study was undertaken in view of the fact that apoptotic cell death is known to be substantially inhibited on a *c-fos*^{-/-} background.

1.2 The Structure of the Human Eye

The human eye is anatomically composed of three layers, an outermost sclera-cornea, a middle or uveal layer and an innermost layer, the retina (Dowling, 1987; Heckenlively, 1988). The sclera is a tough, collagenous, fibrous and opaque tissue providing the eye with much of its mechanical strength. Anteriorly this layer is referred to as the white of the eye (Figure 1.1). The cornea is a continuation of the sclera. It is positioned at the front of the eye and is completely transparent due to the very regular orientation of its collagen fibres. The cornea, together with the lens, act to bring light rays to a focus on the retina. The uveal layer consists of the choroid, the ciliary body and the iris. The choroid is suffused with blood capillaries called the choriocapilaris which supplies blood to the retinal pigment epithelium (RPE) and outer one-third of the retina, the remaining two-thirds being supplied by superficial retinal blood

vessels. The RPE is a single row of pigmented cells which absorb light that gets through the retina. Between this single layer of cells and the choroid is a collagenous basement layer referred to as Bruch's membrane. The ciliary body, composed mainly of smooth muscle, is attached to the lens via the suspensory ligament. It controls the shape of the lens allowing more fine focusing of the corneal image onto the retina. The iris extends from the ciliary body and lies wholly in front of the lens, creating the anterior and posterior chambers. The anterior and posterior chambers are filled with aqueous humor, a watery substance which is produced by the ciliary body and secreted into the posterior chamber. This fluid circulates via the pupil into the anterior chamber where it drains through the trabecular meshwork via the canal of Schlemm. The aqueous humor provides nutrients to the cornea and lens and maintains the shape of the cornea. The circulation of the aqueous humor also plays a very important function in maintaining intraocular pressure (Dowling, 1987). The amount of iris pigment varies, blue eyed people having less pigment than brown eyed people. The iris also regulates the amount of light reaching the retina.

Figure 1.2 illustrates the retina as seen through the lens using an ophthalmoscope (photograph kindly provided by Dr. P. Kenna). The yellowish coloured disc represents the optic nerve head from which both nerve fibres and blood vessels radiate. Sectioning of the retina reveals a number of clearly defined morphological and cellular layers (Figure 1.3). As described above, the base of the retina is lined by a single row of pigmented epithelium cells (the RPE). As the name suggests, these cells are highly pigmented and absorb excess light that has travelled the thickness of the retina without having been absorbed by the photoreceptor cells. In addition the RPE phagocytoses shedded photoreceptor outer segment discs (see below) and also provides nutrients for the photoreceptors. The photoreceptor layer is immediately adjacent to the RPE and consists of three clearly distinguishable layers, the outer segment layer (OS), the inner segment layer (IS), and the outer nuclear

layer (ON). Examination of the structure of the rod and cone photoreceptors reveals the composition of these layers, each cell being composed of a nuclear sector, an inner segment and an outer segment. In rods, which are responsible for vision in low light, the outer segments contain disc-like structures that carry the photoreceptor pigment rhodopsin (see Figure 1.4). The outer segment discs are continuously being renewed, approximately 10% being phagocytosed by the RPE each day (Dowling, 1987). The outer segments of the cone photoreceptors do not form individual discs. The membrane carrying the cone pigments folds as a continuous stacked layer. The human eye contains approximately 120 million rods and 6 million cones. While there is only one type of rod cell, ie that which contains rhodopsin, there are three types of cones, carrying either the blue, red or green photoreactive opsin pigments. The cone pigments are less sensitive to light than the rod pigments and are responsible for daytime vision. Light travels directly through the lens and impinges on the central part of the retina, a region called the macula. This region carries the highest density of cone photoreceptors, and is approximately 4.5 mm in diameter. The centre of the macula, termed the fovea is approximately 1.5 mm in diameter, and is identifiable by the presence of a slight depression on the retinal surface, approximately 0.4mm diameter, which is termed the foveolar pit. This area is composed entirely of cone photoreceptors (see Figure 1.1).

Moving out from the photoreceptor cell layer, other retinal layers are clearly identifiable using conventional staining procedures. These layers include the outer plexiform layer (OP) , the inner nuclear layer (IN), the inner plexiform layer (IP) and the ganglion cell layer (G) (Dowling, 1987). Figure 1.3 illustrates a section of mouse retina stained with haematoxylin and eosin (H+E) in which these layers are visible (Humphries, et al. 1997). The OP layer is a synaptic region. Here the axons of the photoreceptors synapse with the termini of three other retinal neurons, the bipolar, horizontal and interplexiform cells (Dowling, 1987), (Figure 1.5). The inner nuclear layer represents the nuclei of these three

neuronal cells. It is within the outer plexiform layer that the signals from the photoreceptors are primarily processed and the bipolar cells carry the processed output to the inner plexiform layer, where further processing takes place. Here again four neurons synapse, namely bipolar, amacrine, interplexiform and ganglion cells, and further processing of the visual signal takes place (see Fig. 1.5). The ganglion cells are the final output cells of the retina and carry their information to the brain via their axons, which traverse the surface of the retina, converging at the optic disc to form the optic nerve. The optic disc itself has no photoreceptors and is referred to as the physiological 'blind spot'. The optic nerve carries the visual signals to the visual cortex, which resides at the back of the brain. One additional type of neuron is present in the retina, namely Muller or glial cells (see Fig. 1.5). These cells extend vertically through the retina from the inner to the outer limiting membranes and their nuclei reside in the inner nuclear layer. Muller cells are responsible for potassium homeostasis in the retina. Neuronal activity releases potassium into the outer retina and Muller cells remove the potassium via active pumps located in their villi (Ogden, 1989). Thus, not only is the retina responsible for the absorption of light, but it is truly part of the brain itself, being responsible for the first two steps in visual processing. Figure 1.6 illustrates a retinal section which has been subjected to electron microscopy (magnification 1.2K). Layers described above are clearly visible, notably the outer segment discs of the rod photoreceptors. This photograph was kindly provided by Dr. E. Fekete.

1.3 Visual Transduction

Rhodopsin (a 40kD protein) is the light sensitive pigment of the photoreceptor cells. It comprises approximately 90% of the membrane protein of the rod outer segment discs. The chromophore 11-cis retinal, a derivative of vitamin A, is bound to rhodopsin through a Schiff base at codon 296 (lysine) in



the 7th transmembrane domain of the protein. When a photon of light is absorbed by the chromophore it isomerizes from the 11-cis, to the all-trans form (Stryer, 1986). As a result, the structure of rhodopsin changes to its active catalytic form metarhodopsin III and it is now capable of interacting with transducin, an enzyme in the cytoplasm of the rod photoreceptor cells. Transducin is composed of three polypeptide chains, alpha, beta and gamma, 39kD, 36kD and 8kD respectively (Stryer, et al. 1981). The interaction between activated rhodopsin (R*) and transducin causes a dissociation of the beta and gamma subunits of transducin from its alpha subunit. In addition, the alpha subunit has a GDP/GTP binding site. In the inactive form, this site is charged with GDP. When activated by interaction with rhodopsin, the site becomes charged with GTP. Activated transducin (alpha transducin-GTP) now reacts with cGMP phosphodiesterase (PDE). The latter is composed of an alpha, beta and two gamma subunits, 88kD, 84kD and 11kD respectively (Baehr, et al 1979). Phosphodiesterase is inhibited by its gamma subunits and as such is referred to as being in the dark state. Activated transducin (alpha-GTP) activates PDE by causing the gamma subunits to dissociate from the protein. Activated PDE now cleaves cyclic cGMP which is bound to the membrane-associated protein, the cGMP-gated channel. When cGMP is bound to the channel protein the channel is maintained in an open configuration, allowing passive transport across the rod cell membrane of mono- and divalent cations eg. Na⁺, Ca²⁺, K⁺ and Mg²⁺. Cleavage of cGMP causes the channel to close, thus preventing the flow of ions into and out of the cell. However, active pumps continue to expel ions from the photoreceptor, resulting in a build-up of positive charge on the outside of the cell. It is this positive charge that triggers an electrical impulse to the outer plexiform layer via the synapses of the photoreceptor cells (Stryer, 1986). Deactivation of the visual cascade must also rapidly take place. Lowering of Ca²⁺ levels results in activation of recoverin, a 23.3 kD protein, which in turn activates guanylate cyclase which regenerates

cGMP, in turn resulting in a re-opening of the gated channel. In addition, rhodopsin kinase phosphorylates serine and threonine residues at rhodopsin's carboxy-terminus (Kuhn et al, 1984). In the phosphorylated state, rhodopsin is recognised by arrestin (S-antigen), a 48kD protein which binds to the rhodopsin molecule and prevents it from reacting with transducin (Zuckerman, et al 1985). Phosphatases subsequently dephosphorylate rhodopsin and the chromophore is restored to the 11-cis retinal form, thus restoring rhodopsin to the deactivated state (Figure 1.7). The visual transduction cycle is a cascade, in that a single activated rhodopsin molecule is capable of activating many transducin molecules. Similarly, each transducin can activate many PDE molecules. Thus, at each of these two stages the signal from the activated rhodopsin molecule is amplified. The process is extremely rapid, the time elapsing from photoactivation of rhodopsin to transmission of the amplified signal to other neurons at the outer plexiform layer being in the order of a few milliseconds (Stryer, 1986). As outlined later, mutations within genes encoding a variety of proteins involved in visual transduction have now been identified.

1.4 Clinical Features of Retinitis Pigmentosa and Methods for Diagnosis of the Disease.

Retinitis pigmentosa (RP) is a clinically and genetically heterogeneous group of diseases resulting in photoreceptor degeneration. Clinical features of RP are night blindness, a gradual loss of peripheral vision, retinal pigmentary deposits and tunnel vision, which in many cases may lead eventually to total blindness. Age of onset is variable, ranging from early childhood to late adulthood. In addition, electroretinographic recordings are invariably abnormal or non-recordable (Heckenlively, 1988). In the later stages of the disease fundus examination usually reveals a pale optic nerve head, bone-spicule pigmentary deposits and attenuated retinal vessels (Figure 1.2 and 1.8 illustrate a normal

and RP affected eyes). RP is an inherited disease manifesting as autosomal dominant (adRP), autosomal recessive (arRP) and X-linked (xLRP) (McKusick V 1983). RP may also be associated with a number of syndromes, for example, Usher syndrome, or recessive Bardet-Biedl syndrome. The prevalence of RP is approximately 1:3000, affecting approximately 1.5 million individuals worldwide. Autosomal recessive and sporadic cases of RP account for approximately half of all cases (Humphries, et al., 1992b). There are at least five clinically distinct types of retinitis pigmentosa, including rod-cone degeneration, cone-rod degeneration, sectoral RP, congenital RP and retinitis punctata albescens (Heckenlively, 1988). Clinical diagnosis of the disease may be effected using several diagnostic criteria, including best-corrected visual acuity, colour visual acuity, visual fields, dark adaptometry and electrophysiology (Newell, 1982). Pedigree information may often determine the mode of inheritance of the condition.

Best-corrected visual acuity measures the function of the fovea centralis (where the highest number of cone photoreceptors reside) exploiting small differences between and within objects, such as the letters of the alphabet. This is referred to as the Snellen test.

Colour vision testing assesses whether cone degeneration is involved in the retinopathy. This is performed using the Farnsworth-Munsell 100 hue test. This consists of 84 coloured caps, split into four groups of different hue, with a reference cap at each end (e.g. deep purple at one end and pale pink at the other end). Each group spans a different spectral range and the patient is asked to place the caps in the correct order. The test is carried out in a Macbeth light box to ensure standardized illumination of the colour caps (Rose, 1983). This test is useful in determining the type and severity of the colour defect.

In visual field assessment the patient is placed in front of a Goldman bowl perimeter in such a way that the eye is 33cm from the centre of the bowl.

Throughout examination the testing distance of 33cm remains constant. The patient is asked to identify at which point a moving target, which is brought in from the periphery to the centre at a constant speed, can be identified. Targets of three different sizes may be used, e.g. IV4e, I4e and 04e in decreasing size. The points are then graphically plotted and the individual's field of vision can be evaluated. Particular attention is paid to possible mid-peripheral field defects, which are a classic feature of early RP (Newell, 1982). Figure 1.9 illustrates the visual fields of a normal individual (A), an individual with early-to-mid onset RP (B), and an individual with advanced RP (C). (Kindly provided by Dr. Paul Kenna).

Two colour dark adaptometry is a measurement of the threshold of the sensitivity of the retina to light. Rods and cones have different spectral sensitivities, rods being more sensitive to blue light and cones more sensitive to red light. Prior to the test the patient's pupil is fully dilated to standardize the amount of light reaching the retina. The patient is placed in front of a Goldmann-Weekers bowl and subjected to an intense bright light for 5 minutes. This is to essentially bleach all the patient's rhodopsin. All lights are extinguished and the patient is asked to fixate on a small dim red target positioned 15° of arc above the centre of the bowl in order to stimulate a retinal area of good rod/cone mixture. The targets used are 2° in diameter, one red and the other blue. Each target is presented until the patient indicates that he or she appreciates the target flashing and this is taken as the "on" threshold. The brightness of the target is then reduced until the patient can no longer appreciate the flashing, this is referred to as the "off" threshold. The true threshold for detection is taken as mid way between the on and off thresholds. This procedure is repeated every 2.5 minutes for 30 minutes (Sondheimer, et al. 1979). Initially, mediation of the targets is exclusively by cones, as the 5 minute bleach has essentially suppressed all of the rods. This is demonstrated by the thresholds at 0 and 5 minutes in Figure 1.10 (bottom panel) where the red target

is detected at a lower threshold than the blue. As dark adaptation progresses and rod function recovers the blue target is eventually detected at a lower threshold than the red as evidenced by the thresholds at 10 minutes and subsequently, indicating that target detection has been mediated by the rods. In normal individuals this “cross-over” occurs somewhere between 5 and 10 minutes of dark adaptation. In individuals with type I RP this crossing over never occurs, indicating absence of rod activity, as shown in figure 1.10. Whereas, in type II RP the threshold pattern is normal but at a higher intensity, suggesting the presence of some impaired rod function.

An electroretinogram (ERG) can be used in a dark adapted (scotopic, rod mediated response) or light adapted (photopic, cone mediated response) manner to gain information about the retina (Heckenlively, 1988). After dark adaptation for approximately 30 minutes to maximize rod sensitivity, contact lens electrodes are placed on the corneal surface, and an electrical response is evoked from the retina in response to a flash of light. The stimulating light can be altered in intensity, wavelength and flicker frequency, and is presented in a Ganzfeld bowl to ensure even retinal illumination. Figure 1.11a illustrates an example of dark adapted rod-isolated ERG tracings from a normal and an RP-affected individual. The RP-affected individual shows no response to the light stimulus. The photopic ERG is carried out after 10 minutes of light adaptation and the flashes are presented against a rod suppressing background light. This is to ensure that the rods are bleached out and will not react to the light stimulus, thus a response will be derived only from the cones. (Heckenlively, 1988). Figure 1.11b illustrates cone-isolated responses from a normal and an RP affected individual.

An electro-oculogram (EOG) analyses the standing potential between the front and back of the eye which is generated by the retinal pigment epithelium (RPE). Amplitudes are measured after 10 minutes of dark adaptation as the patient alternatively observes two points 20° apart. The same amplitudes are

measured after 10 minutes of light adaptation. In normal people the amplitude from the light adapted response is twice that of the dark adapted response and is referred to as the light/dark, or Arden ratio, and is calculated by dividing the largest light-adapted signal by the smallest dark-adapted signal and multiplying by 100. The Arden value in the normal population generally exceeds 160%, while individuals suffering from RP generally have values less than 160% (Arden, et al. 1962) (see Figure 1.12 for illustration of an EOG).

The fundus can also be viewed in detail by direct or indirect ophthalmoscopy. Direct ophthalmoscopy gives a monocular, magnified view of the fundus, while indirect ophthalmoscopy enables a stereoscopic wide angle examination of the entire retina. Photography is usually performed to provide a record of any fundus changes (Heckenlively, 1988).

1.5 Clinical Features of Macular Degeneration

While RP represents the most prevalent mendelian retinopathy, it is by no means the most prevalent degenerative retinal disease in man, being eclipsed in prevalence by the age related macular degenerations, which as a group, are responsible for visual handicap in up to one in ten persons in Europe over the age of 65 years (for Review see Humphries, et al 1994). This group of conditions represents the most common cause of registered blindness in many developed countries, and the most common form of visual impairment in individuals over the age of 65, for example, currently affecting approximately 1 million and 6 million persons respectively in the United Kingdom and the USA (populations approximately 60 and 240 million respectively). While macular dystrophies do not, except in very rare instances, segregate according to mendelian ratios, there are nevertheless strong genetic factors associated with their etiologies (Meyers and Zachary, 1988; Klein, et al. 1994; Silvestri, et al. 1994; Meyers, et al 1995), and indeed there are now indications of mutations

within the Rim glycoprotein gene that may contribute to the phenotype (see below).

Macular degenerations, as the name implies, primarily affect the macular area, which is predominantly cone photoreceptor-rich. As described above, macular degenerations are usually late onset multifactorial conditions (age related macular degeneration, ARMD), except in rare instances, where an autosomal dominant (adMD) or recessive (arMD) inheritance pattern can be identified. Among the latter are Best's vitelliform (adMD), Sorsby's fundus (adMD), Butterfly-shaped pigment (adMD) and North Carolina (adMD) macular dystrophies, and Stargardt's disease (arMD).

Genetic and environmental factors such as smoking, diet and exposure to sunlight may possibly play a role in the onset of the disease (Cruickshank, et al. 1993; Smith, et al. 1997). There are two forms of ARMD, the dry or atrophic form, which involves thinning of the macula, and the wet or exudative form, which results from growth of fragile blood vessels which gain access to the sub-retinal space through breaks in Bruch's membrane and may result in sub-retinal haemorrhage and subsequent scarring of the macula (Figures 1.13 and 1.14). ARMD is also characterized by the accumulation of debris within Bruch's membrane, referred to as drusen. The latter material is composed of extracellular debris, varies in size, shape and hardness, and is yellowish in colour (Gass, 1987; Sarks, 1980). The dry form of the disease affects approximately 90% of all ARMD sufferers, and the condition usually progresses slowly, resulting in disturbance and loss, predominantly, of central vision, i.e. reading vision. It is very rare for individuals to lose all their vision. The wet form accounts for the remaining 10% of cases of the disease (Sarks and Sarks, 1989).

Best's vitelliform macular dystrophy (BTMD) is a juvenile onset autosomal dominant condition, which is progressive in nature. Clinically the disease is initially characterized by a yellowish, lipid containing, sub-retinal blister which is

often described as resembling a “fried egg, sunny side up”. As the condition progresses, the blister flattens, and in appearance, resembles a “scrambled egg”. The patient at this stage notices significant visual disturbance, and as the disease progresses, an atrophic scar forms on the macula (Best, 1905). At-risk patients can be presymptomatically tested before the appearance of the retinal blister by carrying out an electro-oculogram (EOG) which shows a reduced or absent light response.

Stargardt disease (STGD) is the most common hereditary recessive macular dystrophy, with an incidence of 1:10,000. The disease is characterized by juvenile-to-young adult onset, patients presenting with central visual impairment, and bilateral atrophy of the macular retinal pigment epithelium (RPE). Orange-yellow fishtailed flecks may also be distributed around the macula and the midretinal periphery of the retina. A clinically similar condition, with later onset and slower progression, is fundus flavimaculatus, (FFM). Both Stargardt disease and fundus flavimaculatus have long been thought to be variants of the same clinical entity (Fishman, 1976).

Sorsby’s fundus dystrophy is an autosomal dominant disorder, involving loss of central vision. Clinically it is characterized by atrophy of the choriocapillaris, retinal pigment epithelium (RPE) and retina in the third or fourth decade of life (Sorsby, et al. 1949).

Butterfly-shaped pigment dystrophy of the fovea, is an autosomal dominant condition, which is characterized by a bilateral accumulation of pigmented material in the region of the retinal pigment epithelium (RPE). This material varies in colour (black, white or yellow), and forms an unusual configuration that resembles the shape of a butterfly (Nichols, et al 1993). The disease manifests itself in the late twenties or early thirties. As outlined above, these mendelian forms of macular disease are very rare in comparison to the age-related forms of the disease.

1.6 Genetics of Degenerative Retinopathies.

During the past 10 years enormous progress has been made in our understanding of the genetic causes of RP and related degenerative retinopathies. As previously outlined, RP may segregate either in autosomal dominant (adRP), autosomal recessive (arRP) or X-linked (xlRP) modes. The first RP gene to be localized, in 1984, was on the X chromosome (Bhattacharya, et al. 1984), subsequent studies revealing the presence of two closely linked genes (RP2 and RP3), (Ott, 1985). The first autosomal dominant RP gene was localized in 1989 on the long arm of chromosome 3 as a result of genetic linkage studies in a large adRP pedigree of Irish origin (McWilliam, et al. 1989), and chapter 2 of this thesis describes some of the linkage studies that resulted in this localization. These studies led to the implication of the gene encoding rhodopsin in disease etiology and the first mutation within the rhodopsin gene in adRP was identified by Dryja, et al (1990). The second autosomal dominant RP gene to be characterized encoded *RDS-peripherin*, again following its location in 1991, by genetic linkage studies in a large Irish kindred (Farrar, et al. 1991b; Jordan, et al. 1992). Over the last seven years many additional retinopathy loci have been identified either as a result of genetic linkage studies or of direct mutational analysis of candidate genes, and to date, mutations within approximately 35 genes have been identified in various types of RP and other retinal degenerations. These data are summarised in Table 1.1 based on RetNet (Daiger SP, 1999).

From the above summary, it will be noted that many of the genes that have been implicated in RP are expressed solely in the photoreceptor cells, and encode either structural elements of these cells or proteins of the visual transduction cascade. *RDS-peripherin*, and *Rom 1* are structural components

of the rod outer segment disc membranes although these proteins might also have some as yet undetermined transporter function. Rhodopsin also represents a major structural component of the discs, being by far the most abundant protein of the rod photoreceptor cells. Enzymatic components of the visual transduction cascade that have been implicated in RP include Rhodopsin, S-antigen (arrestin) (Fuchs, et al. 1995), the alpha sub-unit of rod transducin (Dryja, et al. 1996), the α and β sub-units of cyclic GMP phosphodiesterase (α,β PDE) (Huang, et al. 1995; McLaughlin, et al. 1995), the alpha sub-unit of the cGMP-gated channel protein (Dryja, et al. 1995), rhodopsin kinase (Yamamoto, et al. 1997), and the retina-specific guanylate cyclase (Perrault, et al. 1996). Other well characterised proteins have also been implicated in disease etiology. These include, for example, myosin 7A, implicated in Usher syndrome type 1B, (Well, et al. 1995) and the cellular retinaldehyde binding protein (Maw, et al. 1997). Other less well characterised proteins have also been implicated in RP disease etiology, for example, an RPE-expressed protein (Gu, et al 1997; Marlhens, et al 1997), a retina-expressed Tubby homologue (Banerjee, et al 1998), otx-like photoreceptor-specific homeobox transcription factor (Bellingham, et al 1997) and RPGR, a possible guanine nucleotide exchange factor (Andreasson, et al 1997). It is of interest to note that a form of digenic RP, involving the combined effects of mutations within both the *Rom1* and *RDS* genes has also been identified, representing the first example of the complete elucidation of the genetic etiology of a multifactorial disease (Kajiwara, et al 1994). It should also be noted that genes implicated in a number of rare dominant or recessive macular dystrophies have also been identified. These include a tissue inhibitor of metalloproteinases (TIMP3) in Sorsby's macular dystrophy (Weber, et al 1994), *RDS*-peripherin in Butterfly foveal dystrophy (Nichols BE et al 1993) and the *rim* glycoprotein (ABC transporter) in Stargardt disease (Allikmets, et al. 1997). It is also of interest to note that a number of mutations have been identified within the latter gene in patients with age-related

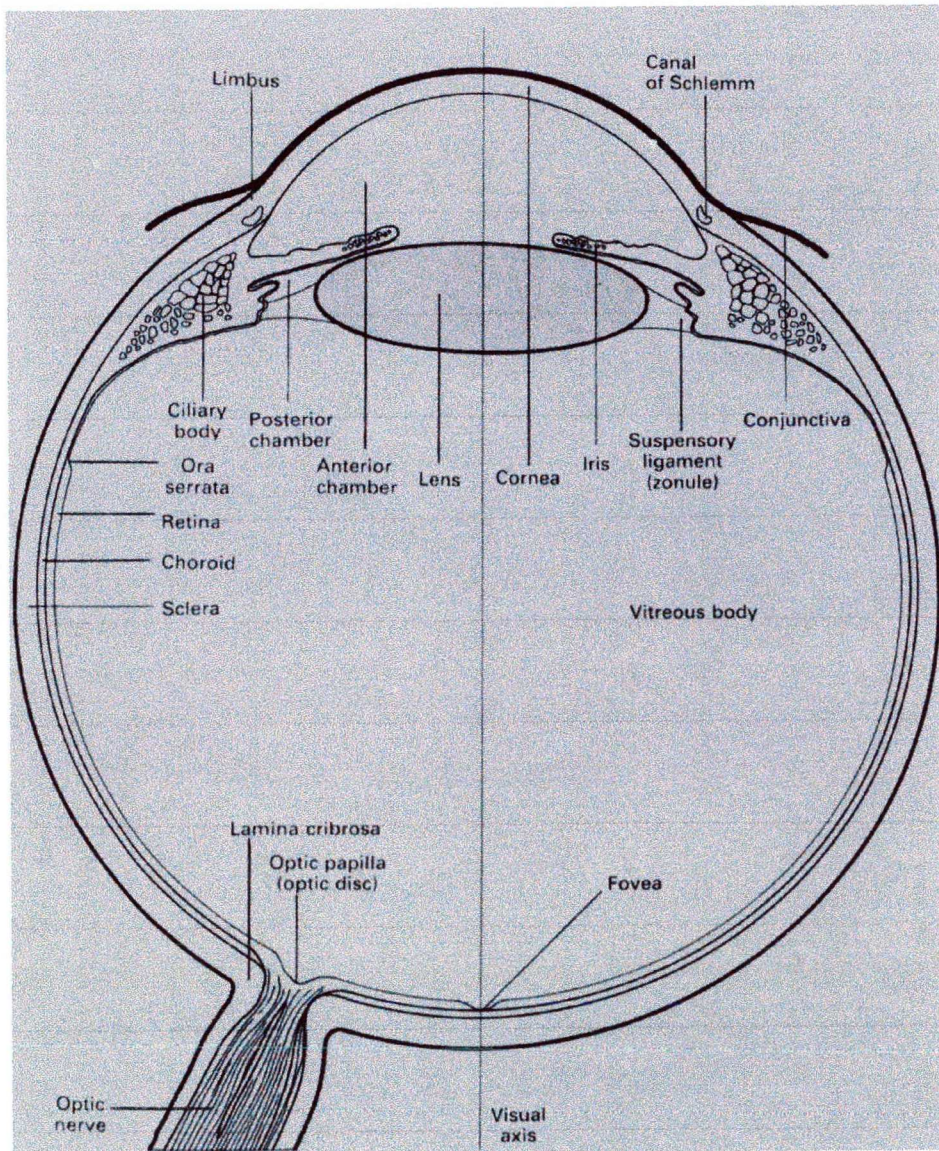
macular degeneration (ARMD) (Allikmets, et al 1997). However, at the time of writing there is some discussion as to whether such mutations are truly disease specific or simply rare polymorphic variants.

Another feature of the etiology of RP is the occurrence, in some instances, of extensive intragenic mutational heterogeneity, the best known examples being rhodopsin and *RDS*-peripherin, where up to approximately 100 and 30 disease-causing mutations respectively have been identified. The majority of mutations are single amino acid substitutions, although in a number of cases small deletions have been identified (see figures 1.15 and 1.16). For example, the first *RDS* mutation to be encountered, in a large Irish pedigree, was a three base-pair deletion removing a cysteine residue at codons 118/119 of the protein (Farrar, et al. 1991b).

In respect to disease pathology, the mechanisms by which such mutations lead to photoreceptor cell death remain to be fully elucidated. In the case of rhodopsin, at least two classes of mutation have been identified, according to whether or not mutant protein is transported to the outer segment disc membranes (Sung, et al. 1991). However, all studies in animal models conducted so far suggest that photoreceptors carrying disease-causing mutations undergo apoptosis (programmed cell death) (Portera-Cailliau, et al. 1994; Chang, et al. 1993). Therefore, therapies for such diseases may eventually be based on targeting the primary mutation, or suppression of apoptotic cell death, or a combination of both.

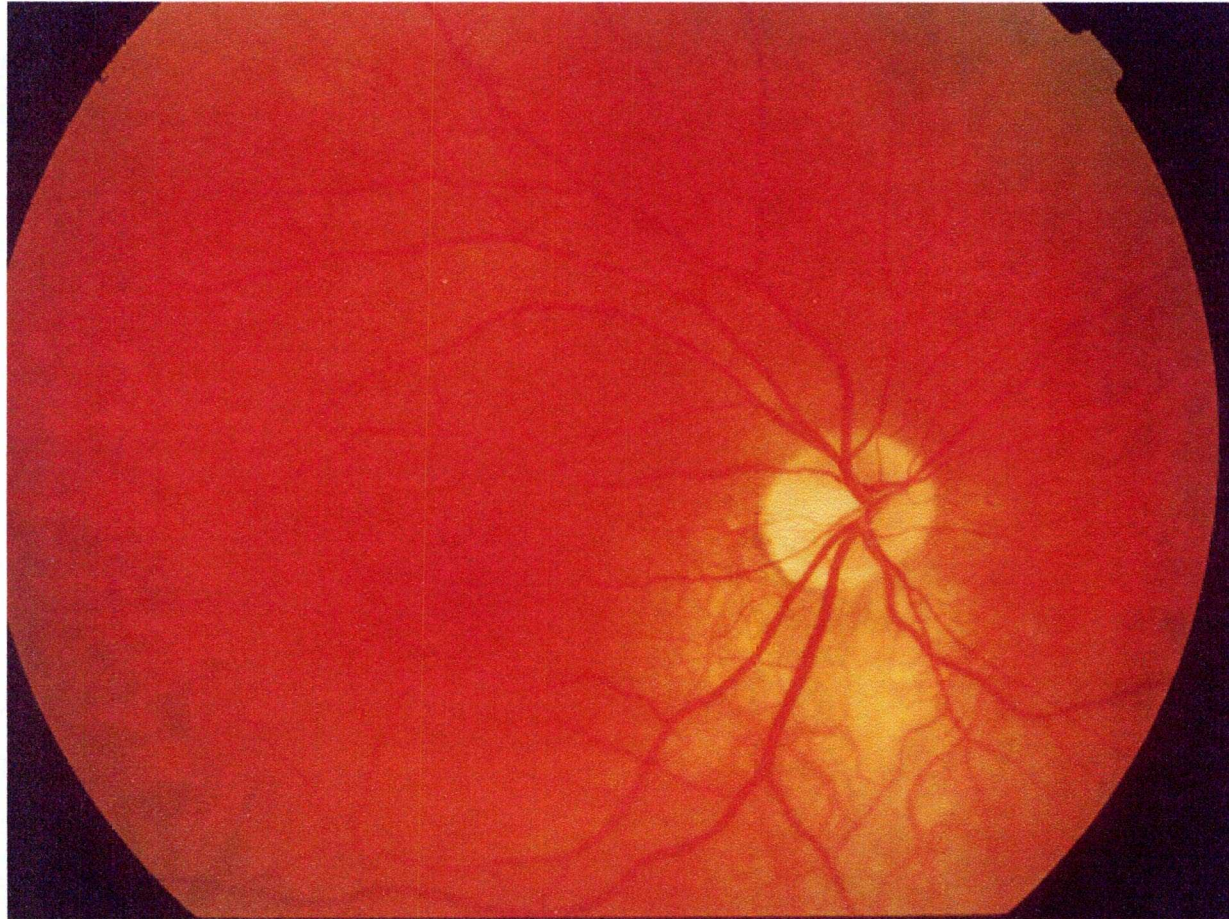
Clearly, our knowledge of the etiologies of RP and related degenerations is now such that therapies, based upon rectification of genetic defects, or indeed suppression of apoptosis, are a realistic possibility. Studies both of the molecular genetics of RP, and of the development of a mouse model for the disease based upon the targeted knockout of the rhodopsin gene are reported here, in the form of a PhD research thesis, for the first time.

Figure 1.1



Drawing of a cross section of the human eye from Dowling, JE, 1987

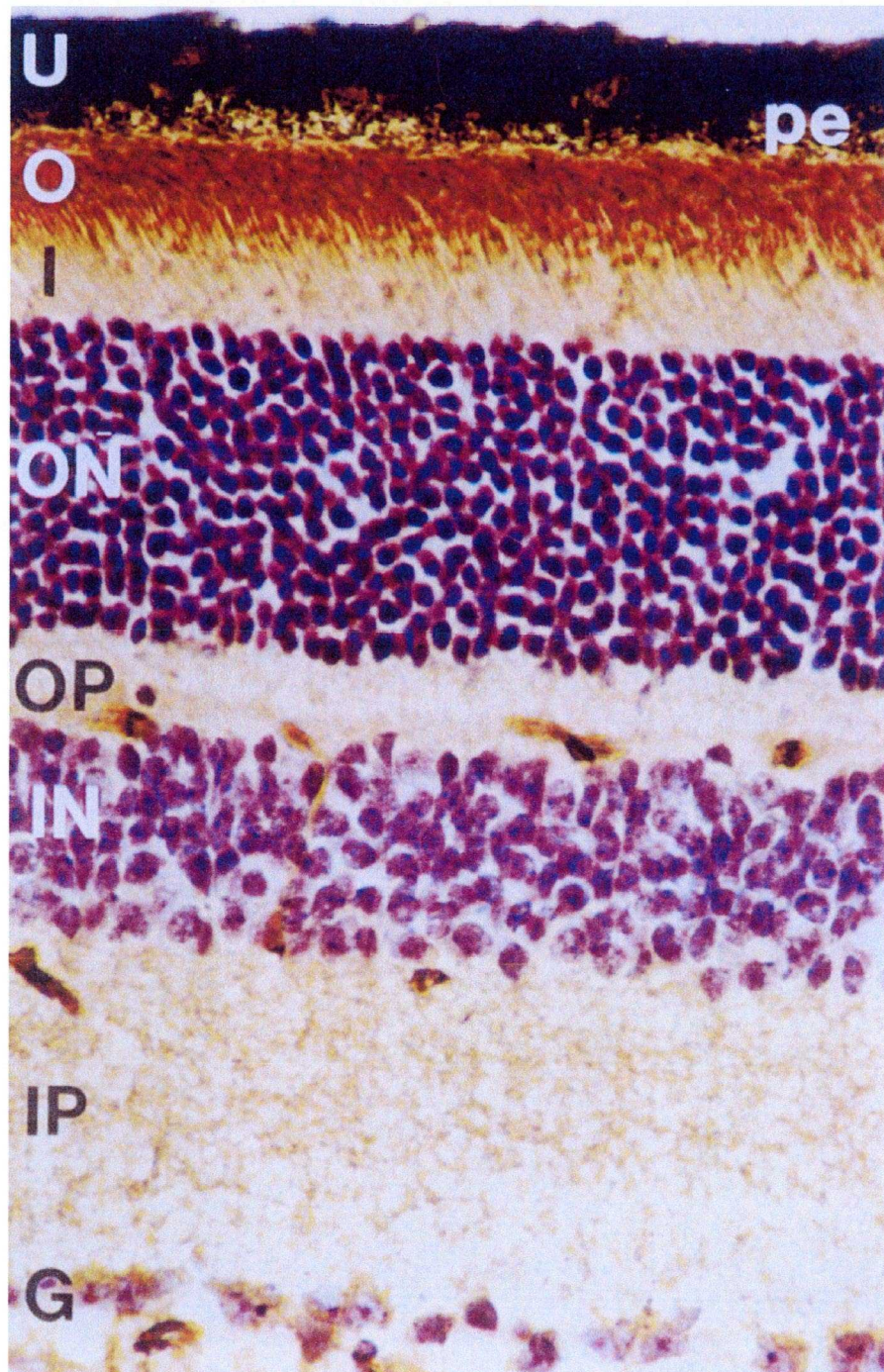
Figure 1.2



Photograph of the fundus of a normal human eye (kindly provided by Dr. P. Kenna). The yellowish disc is the optic nerve head from which the optic nerve fibres and blood vessels emanate and the darker avascular area to the left of the optic disc is the macula.

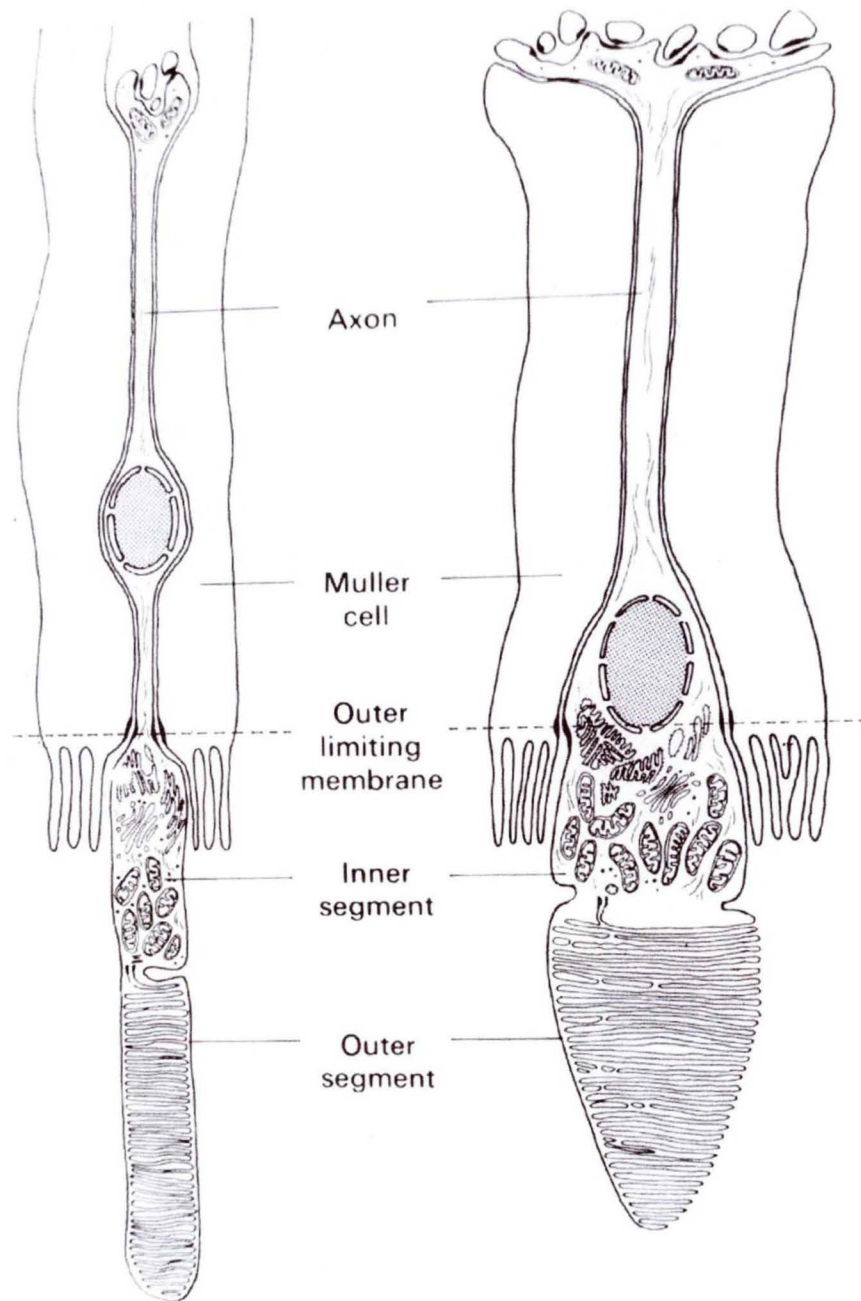


Figure 1.3



Haematoxylin and eosin stained cross section of a normal mouse retina. The layers are as follows: uveal layer (U), retinal pigment epithelium (PE), photoreceptor outer segment layer (O), inner segment layer (I), outer nuclear layer (ON), outer plexiform layer (OP), inner nuclear layer (IN), inner plexiform layer (IP) and the ganglion cell layer (G).

Figure 1.4



Schematic diagram of rod and cone photoreceptors taken from Wheater's Functional Histology, Third Edition, 1993

Figure 1.5

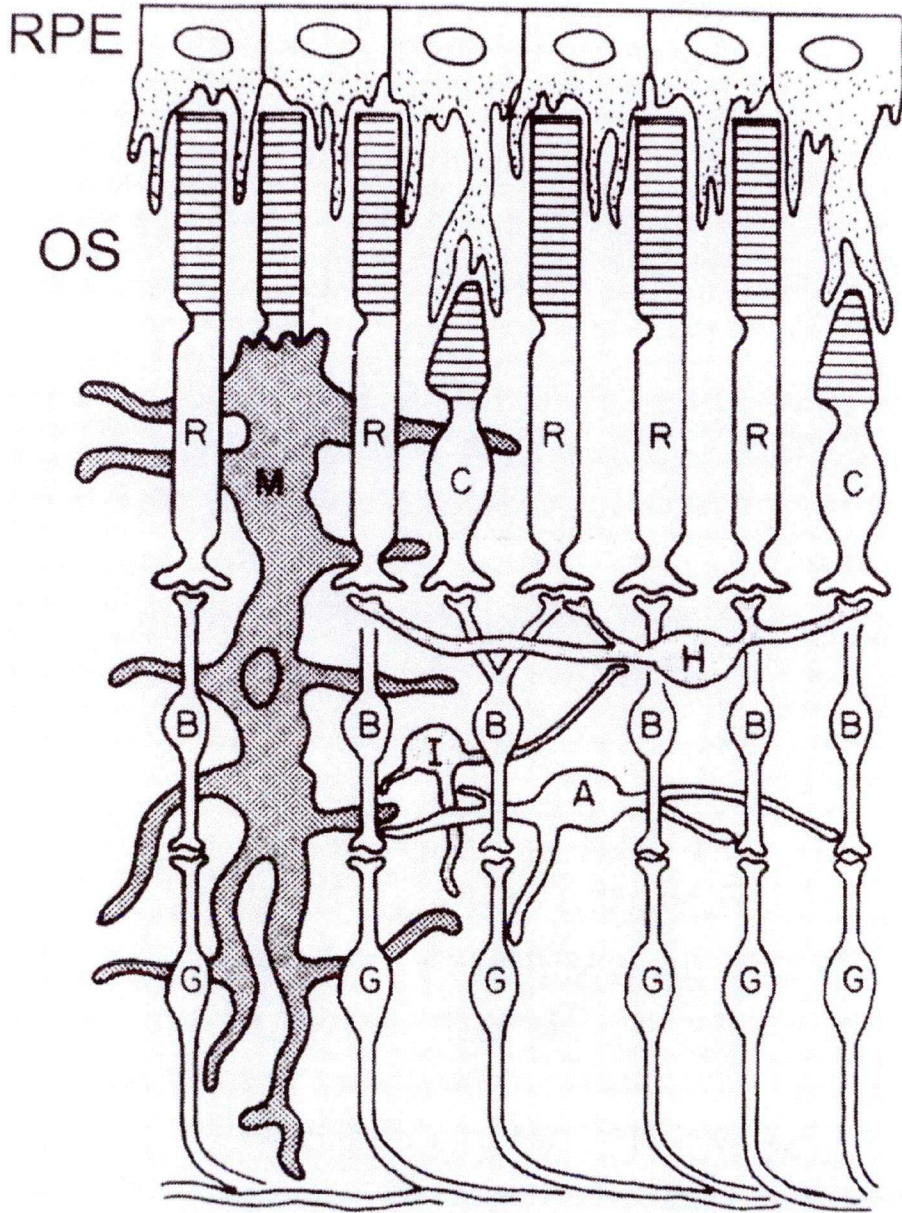


Diagram of a retinal section illustrating the RPE and the structural organization of retinal neurons, (taken from Travis GH 1998). B = bipolar, H = horizontal, I = interplexiform, A = amacrine, G = ganglion and M = Müller or glial cells.

Figure 1.6

Outer segment layer

Inner segment layer

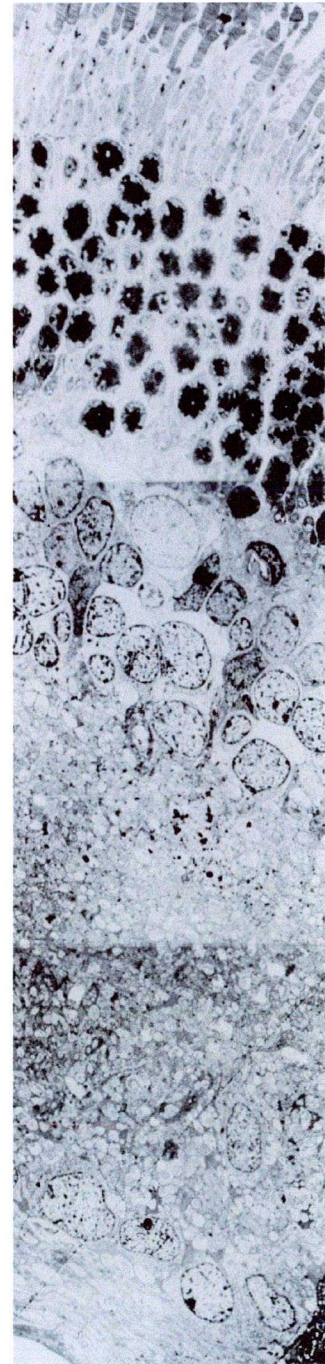
Outer nuclear layer

Outer plexiform layer

Inner nuclear layer

Inner plexiform layer

Ganglion cell layer



Electron micrograph of mouse retinal section kindly provided by Dr. E. Fekete

Figure 1.7

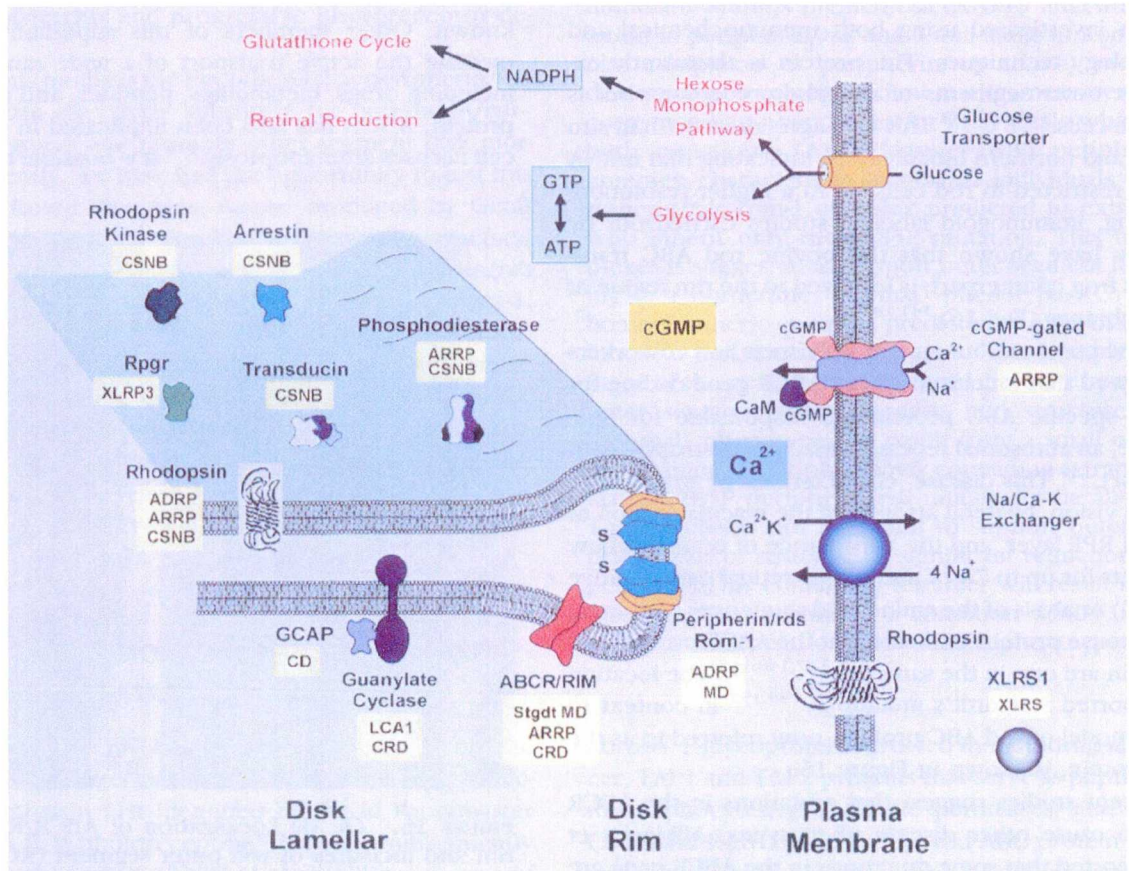
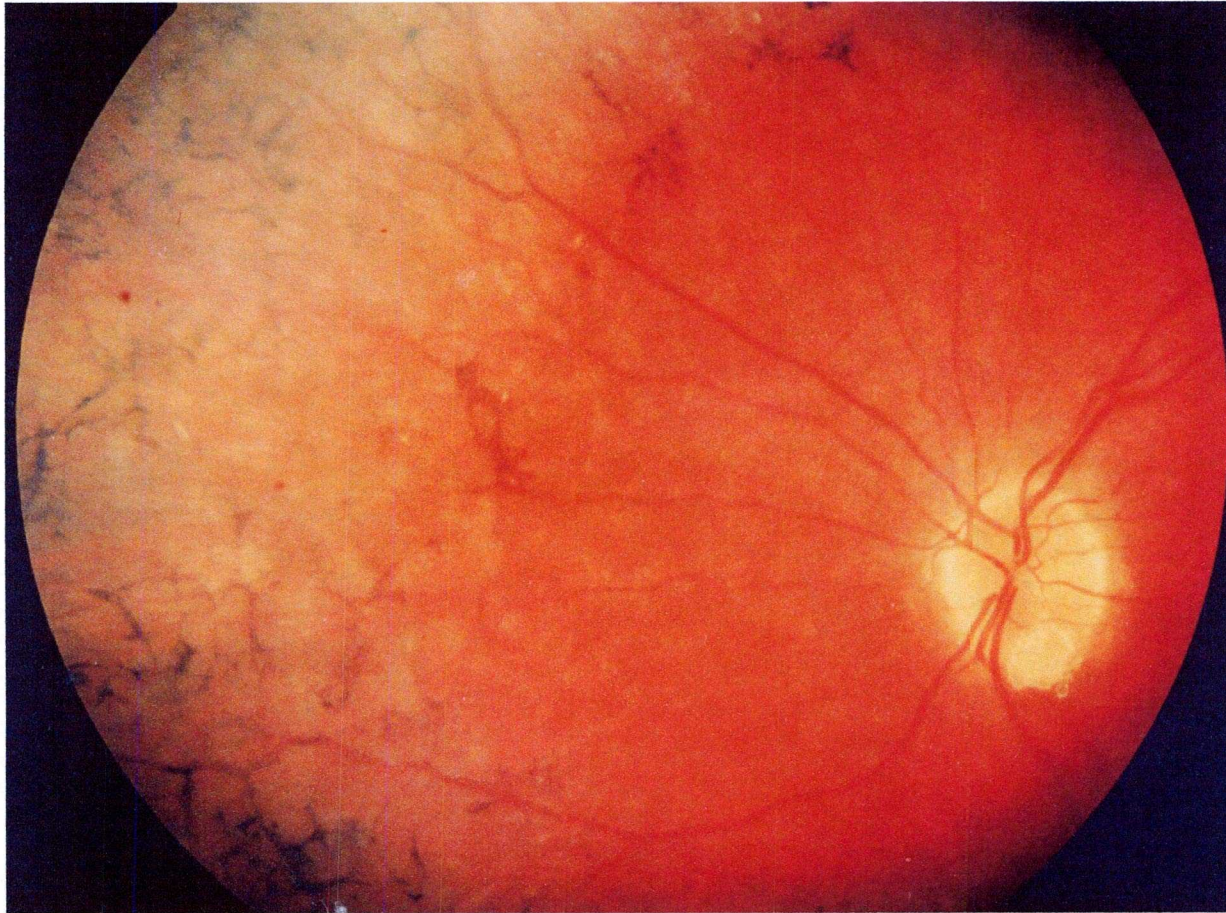


Diagram of visual transduction taken from Molday R, IOVS, Vol 39, (1999), 2493 - 2513

Figure 1.8



Retinal photograph of an individual with advanced Retinitis Pigmentosa, kindly provided by Dr. Paul Kenna.

Figure 1.9

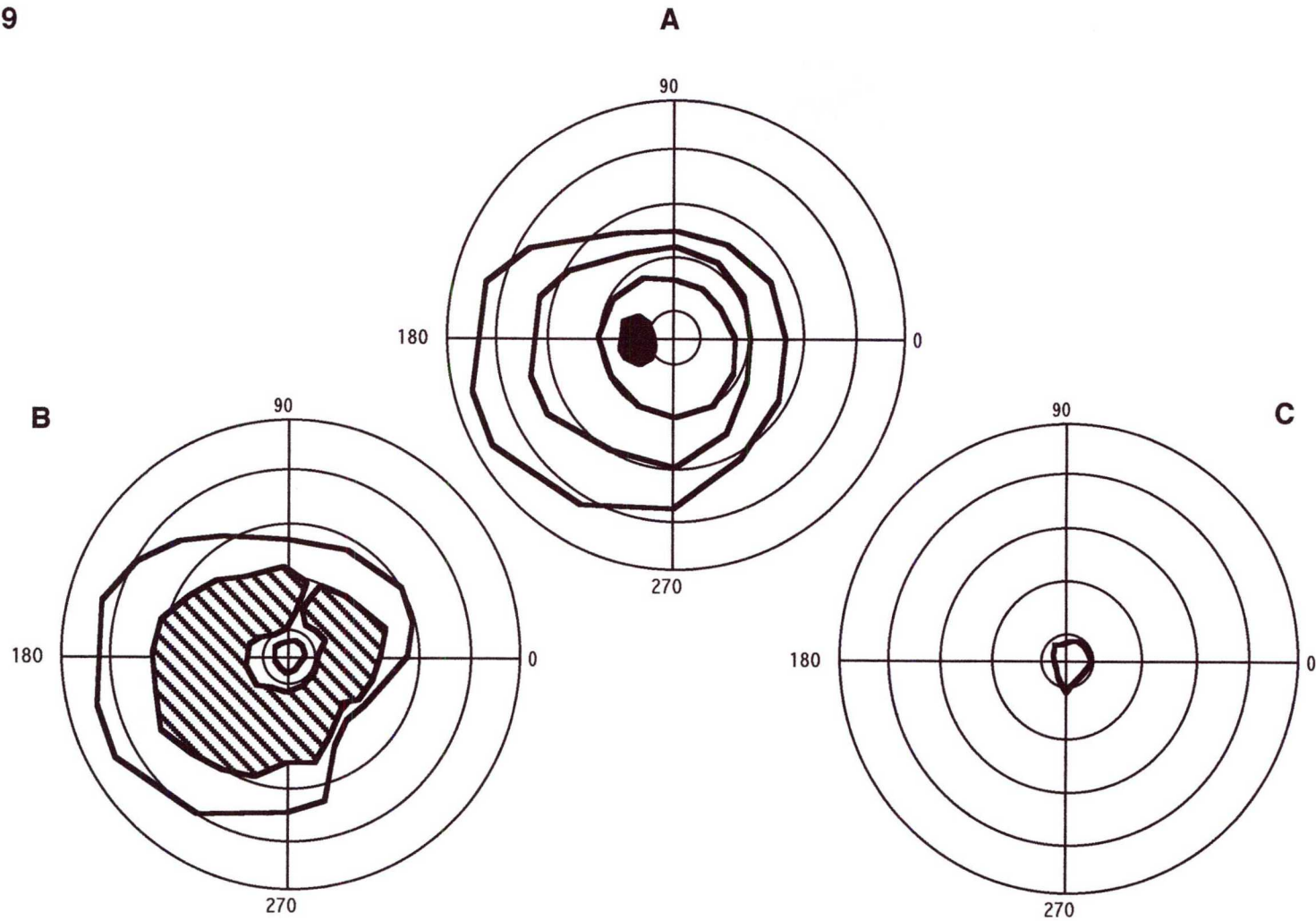
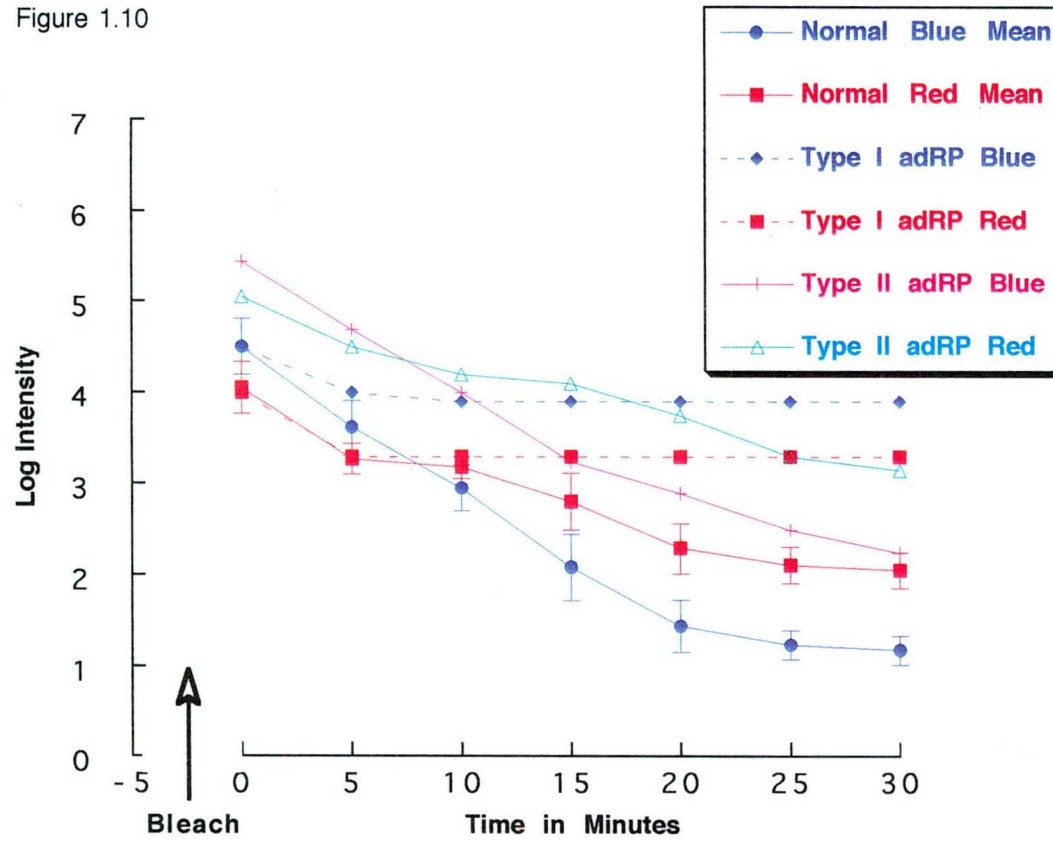


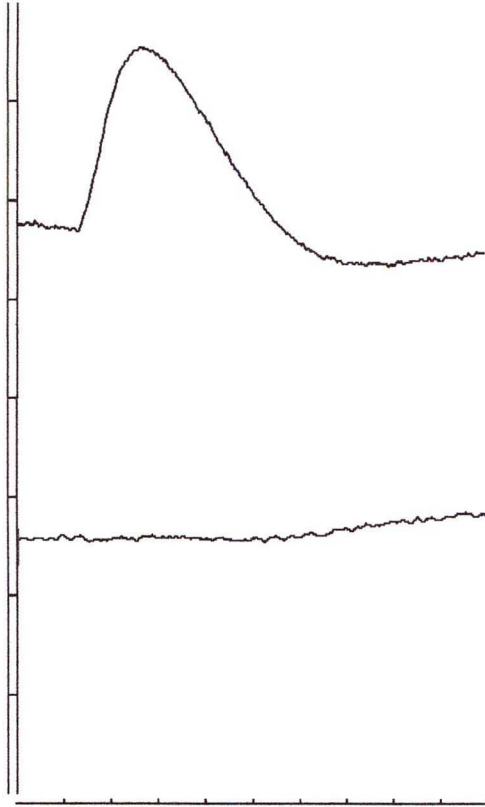
Diagram of visual fields from a normal individual (A), an individual with early-to-mid stage RP (B), and an individual in the advanced stages of RP (C).

Figure 1.10



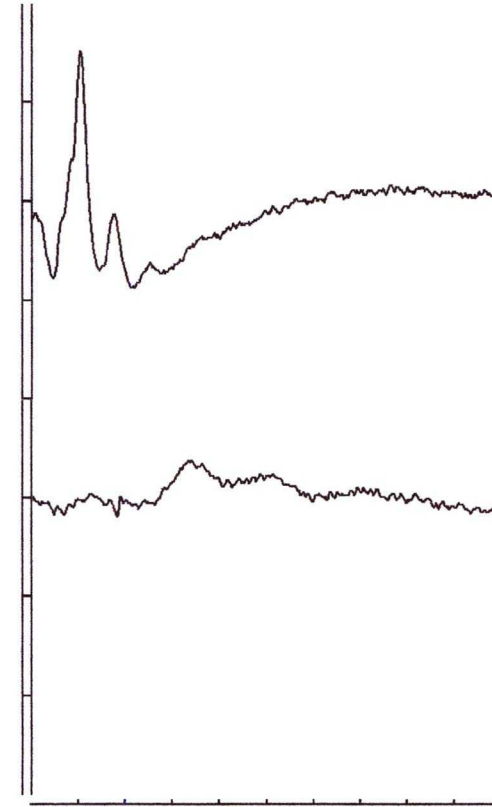
Normal, Type I and Type II 2 Colour Dark Adaptation Patterns

Figure 1.11a



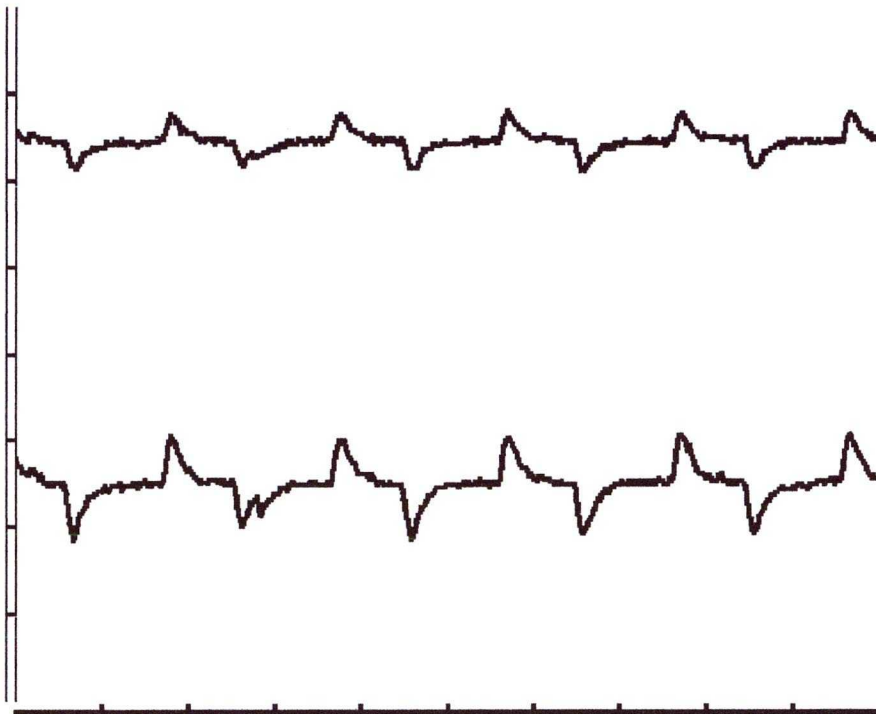
Example of dark adapted rod-isolated electroretinogram (ERG) tracings. Top, normal tracing; bottom, non-recordable response from an RP patient.

Figure 1.11b



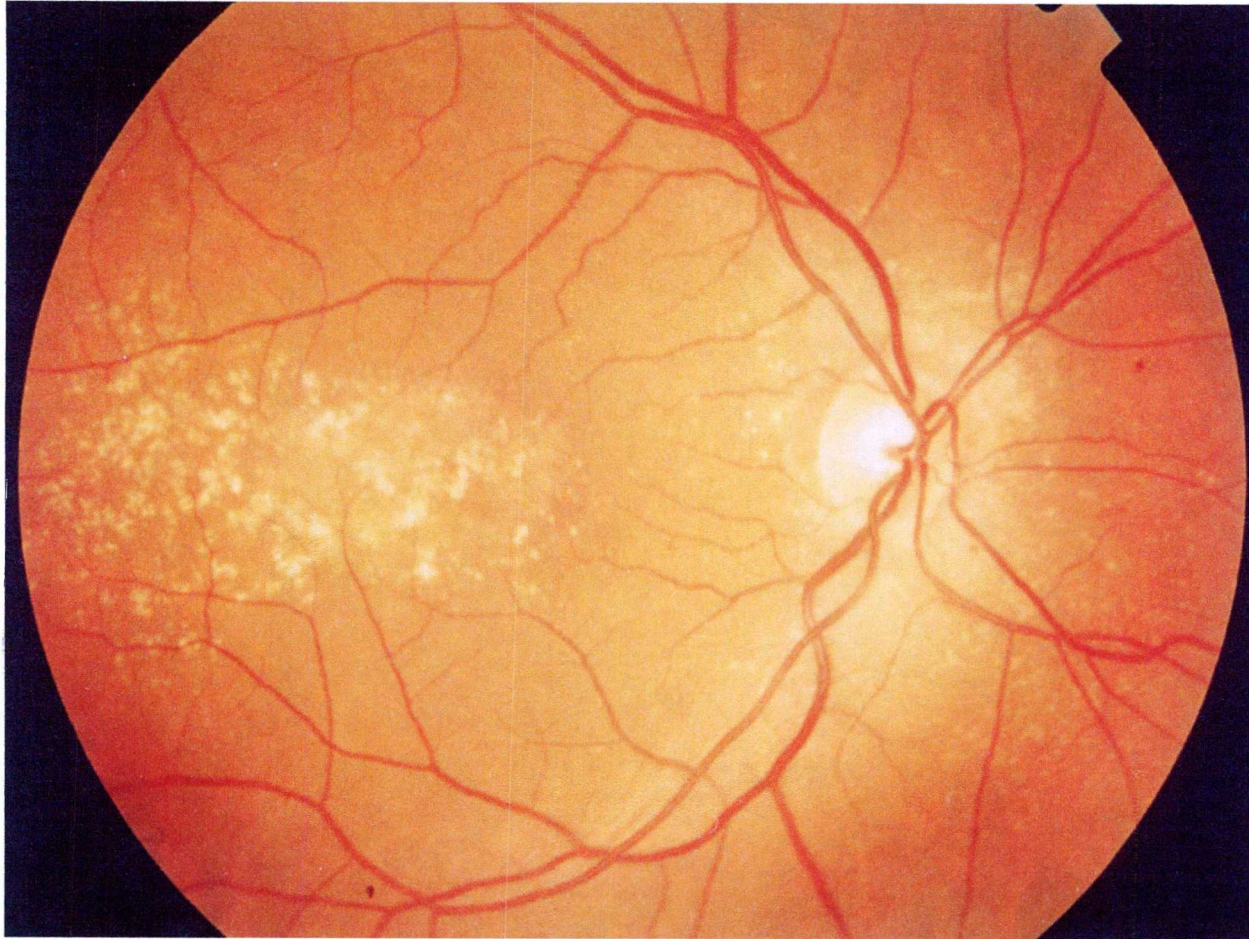
Example of light adapted cone-isolated electroretinogram (ERG) tracings. Top, normal tracing; bottom, very delayed and grossly reduced amplitude generated by an RP patient.

Figure 1.12



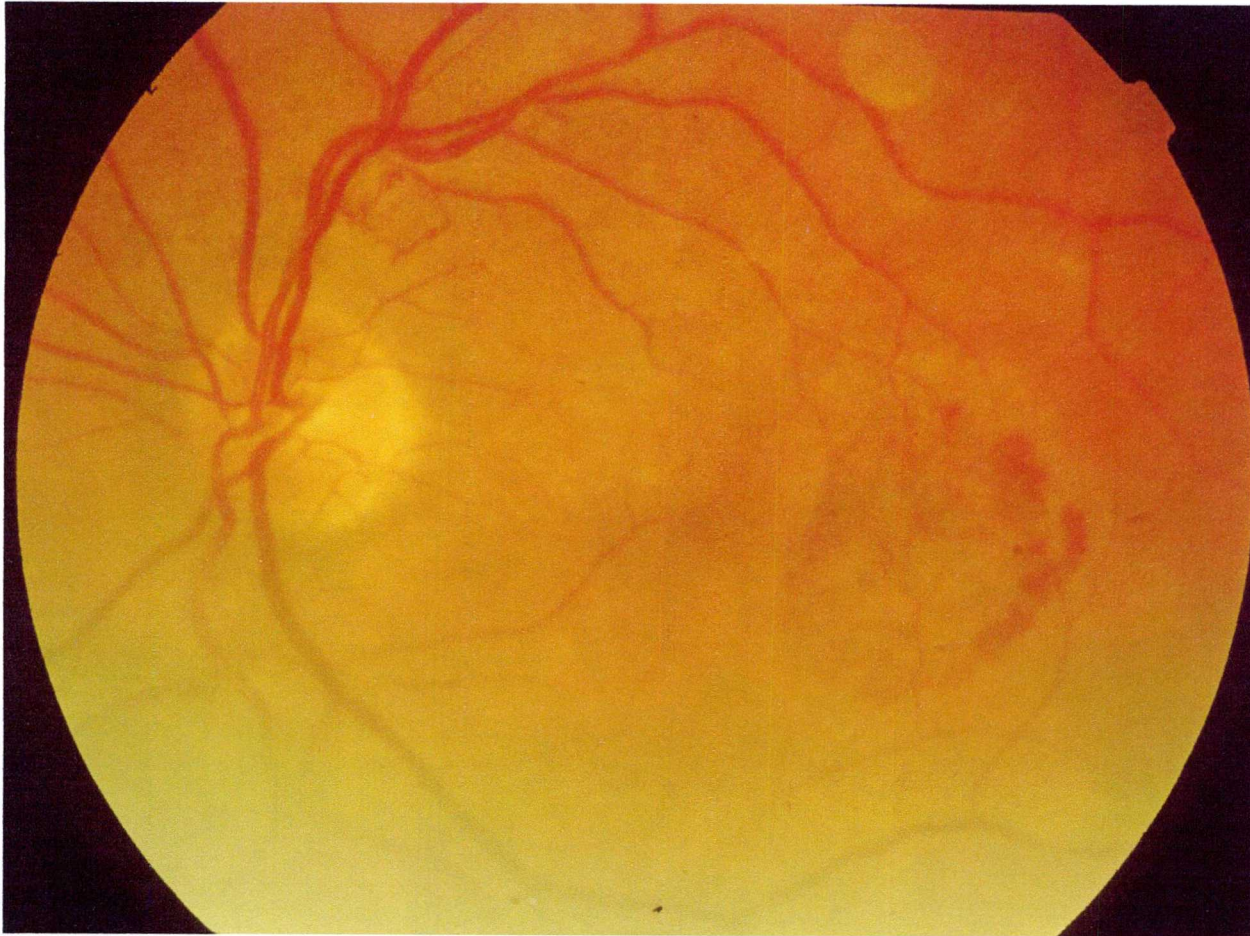
Electro-oculogram (EOG) tracings in the dark (top tracing) and in the light (bottom tracing) in a normal individual.

Figure 1.13



Fundus photograph of an individual with the dry or atrophic form of age-related macular degeneration (ARMD). This photograph was kindly provided by Dr. Paul Kenna

Figure 1.14



Fundus photograph of an individual with the wet or exudative form of age-related macular degeneration (ARMD), kindly provided by Dr. Paul Kenna

Figure 1.15

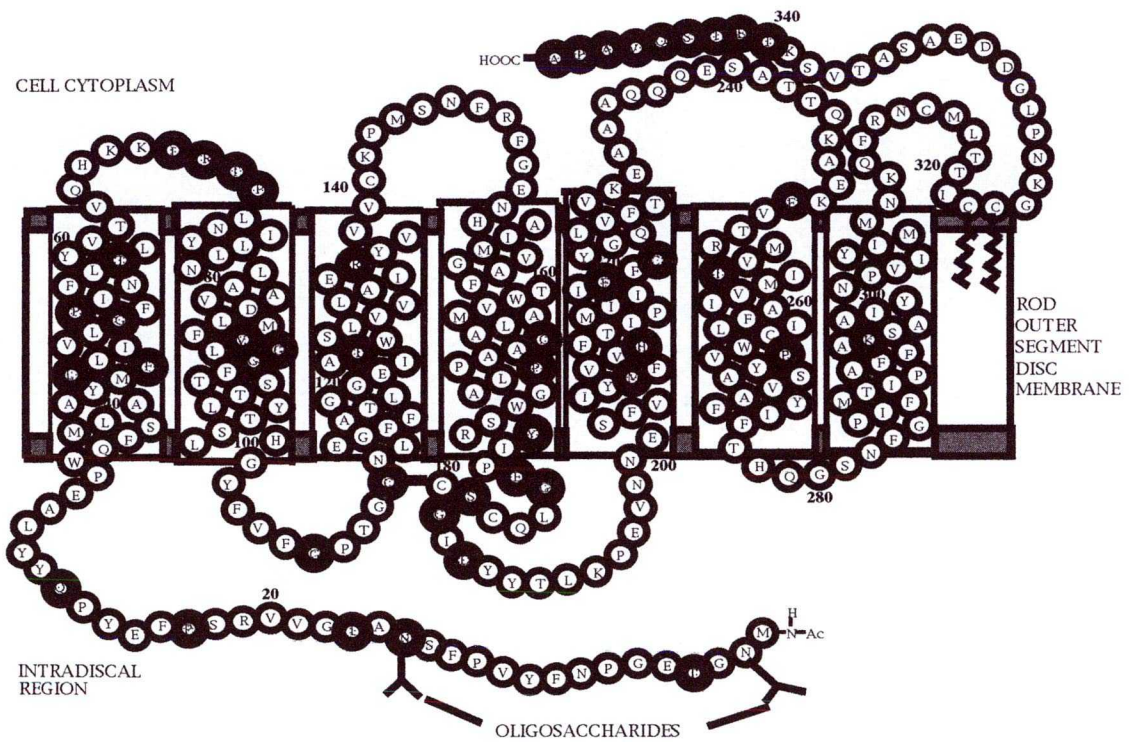


Diagram of the Rhodopsin protein illustrating approximately 100 disease-causing mutations (thick dark circles) in individuals suffering from Retinitis Pigmentosa.

Figure 1.16

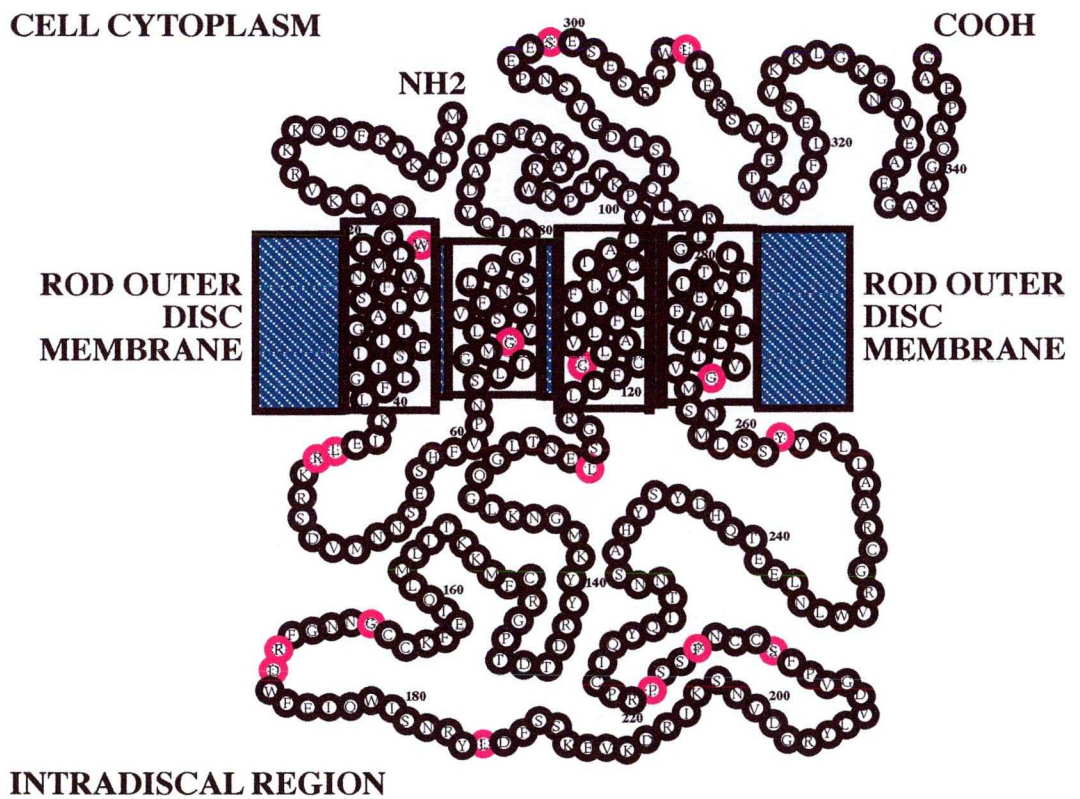


Diagram of the RDS-peripherin protein indicating approximately 40 disease-causing mutations (pink circles) in patients suffering from Retinitis Pigmentosa or macular degenerations.

Table 1. (Adapted from 'Ret-Net', 1998)

GENES MAPPED AND/OR CLONED WHICH ARE INVOLVED IN RETINAL DISEASE

<u>SYMBOL</u>	<u>DISEASE</u>	<u>MAP LOCATION</u>	<u>PROTEIN</u>	<u>REFERENCE NO.</u>	<u>OMIM</u>
LCA2, RP20	recessive Leber congenital amaurosis	1p31	retinal pigment epithelium-specific 65 kD protein	Gu 97; Marthens 97; Morimura 98	204100
STGD1, RP19	recessive Stargardt disease (fundus flavimaculatus), juvenile and late onset; recessive MD; recessive RP; recessive combined RP and cone-rod dystrophy	1p21-p13	ATP-binding cassette transporter - retinal	Allikmets 97;97a Anderson 94;Cremers 98;Gerber 95;98; Kaplan 93;94; Martinez-Mir 97; Martinez-Mir 98; Nasonkin 98; Sun 97	248200
RP18	dominant RP	1q13-q23	not known	Xu 96a	601414
RP12	recessive RP with para-arteriolar preservation of the RPE (PPRPE)	1q31-q32.1	not known	Heckenlively 82; Leutelt 95; van Soest 94	600105
USH2A	recessive Usher syndrome, type 2a	1q41	not known	Kimberling 90 Kimberling 95; Lewis 90	276901
DHRD, MTLV	dominant radial drusen; dominant Doyme honeycomb retinal degeneration (malattia leventinese)	2p16	not known	Héon 96; Heon 96a; Gregory 96	126600
ACMH2	recessive achromatopsia	2p11.2-q12	not known	Arbour 97	216900
----	recessive RP	2q31-q33	not known	Bayés 98	----
SAG	recessive Oguchi disease	2q37.1	arrestin (s-antigen)	Fuchs 95; Maw 95; Wada 96	258100
USH3	recessive Usher syndrome, type 3	3q21-q24	not known	Joensuu 96; Sankila 94; Sankila 95	276902
RHO, RP4	dominant RP; dominant CSNB; recessive RP	3q21-q24	rhodopsin	Dryja 90; Dryja 90a; Dryja 91; Farrar 90a; McWilliams 89; Nathans 84	180380
SCA7, OPCA3, ADCA2	dominant spinocerebellar ataxia w/MD or retinal degeneration	3p21.1-p12	SCA7 protein	Benomar 95; David 97; Del Favero 98; Gouw 95; Holmberg 95	164500
GNAT1	dominant CSNB, Nougaret type	3p21	rod transducin alpha subunit	Dryja 96; Maumenee-Hussels 96	139330
BBS3	recessive	3q	not known	Sheffield 94	;

600151	Bardet-Biedl syndrome				Kwitek-Black 94	
RP5	not distinct from RHO/RP4	3q	not known		Farrar 92	180102
OPA1	dominant optic atrophy, Kjer type	3q28-q29	not known		Bonneau 95; Brown 97a; Eiberg 94; Johnston 97; Lunkes 95; Votruba 97; Votruba 98	165500
CSNB3, PDE6B	recessive RP; dominant CSNB;	4p16.3	cGMP phosphodiesterase beta subunit		Altherr 92; Bateman 92; Bayes 95; Bowes 90; Collins 92; Farber 92; Gal 94; Gal 94a; McLaughlin 93; McLaughlin 95; Piriev 98; Pittler 91; Riess 92; Suber 93; Valverde 95	163500
CNGC	recessive RP;	4p14-q13	rod cGMP-gated channel alpha subunit		Dryja 95; McGee 94	123825
ABL, MTP	recessive abetalipoproteinemia	4q22-q24	microsomal triglyceride transfer protein		Narcisi 95; Sharp 93; Shoulders 93	200100
WGN1, ERVR	dominant Wagner disease and erosive vitreoretinopathy	5q13-q14	not known		Brown 95	143200
PDE6A	recessive RP	5q31.2-q34	cGMP phosphodiesterase alpha subunit		Huang 95	180071
RP14, TULIP1	recessive RP	6p21.3	tubby-like protein 1		Banerjee 97; Banerjee 98; Banerjee 98a; Hagstrom 98; Knowles 94; Shugart 95	600132
RDS, RP7	dominant RP; dominant MD; digenic RP with ROM1; dominant adult vitelliform MD	6p21.2-cen	peripherin/RDS		Arikawa 92; Connel 91; Farrar 91; Felbor 97a; Jordan 92a; Kajiwarra 91; Kajiwarra 94; Travis 91; Travis 91a	179605
COD3, GUCA1A	dominant cone dystrophy	6p21.1	guanylate cyclase activating protein 1A		Payne 97; Payne 98	602093
STGD3	dominant MD, Stargardt-like	6q11-q15	not known		Stone 94	600110
MCDR1, PBCRA	dominant MD, North Carolina type; dominant Belize MD; dominant progressive bifocal chorioretinal atrophy	6q14-q16.2	not known		Keisell 95; Small 92; Small 93	136550

RCD1	dominant retinal-cone dystrophy 1	6q25-q26	not known	OMIM 98	180020
CYMD	dominant MD, cystoid	7p21-p15	not known	Inglehearn 94a; Kremer 94	153880
RP9	dominant RP	7p13-p15	not known	Inglehearn 93; Inglehearn 94b; Keen 95; Kim 95	180104
RP10	dominant RP	7q31.3	not known	Daiger 97; Jordan 93; McGuire 95; McGuire 96; Millan 95; Mohamed 96	180105
CBT	dominant tritanopia	7q31.3-32	blue cone opsin	Fitzgibbon 94; Nathans 86; Nathans 92; Nathans 93; Weitz 92; Weitz 92b	190900
RP1	dominant RP	8q11-q13	not known	Blanton 91; Daiger 97; Roderick 97; Sadler 93; Xu 96	180100
TTPA	recessive RP and/or recessive or dominant ataxia	8q13.1-q13.3	not known	Yokota 96	600415
VMD1	dominant MD, atypical vitelliform	not 8q24	not known	Daiger 97; Ferrell 83; Leach 96; Sohocki 97	153840
RP21	dominant RP with sensorineural deafness	9q34-qter	not known	Kenna 97	601850
USH1F	recessive Usher syndrome, type 1f	10	not known	Wayne 97	602083
RDPA, PAHX, PHYH	recessive Refsum disease	10p	phytanoyl-CoA hydroxylase	Jansen 97; Jansen 97a; Mihalik 97; Nadal 95	266500
USH1D	recessive Usher syndrome, type 1d	10q	not known	Wayne 96	601067
OAT	recessive gyrate atrophy	10q26	ornithine aminotransferase	Valle 95	258870
AA	dominant atrophy areata; dominant chorioretinal degeneration. helicoid	11p15	not known	Fossdal 95	108985
USH1C	recessive Usher syndrome, Acadian	11p15.1	not known	Ayyagari 95; Heckenlively 95; Keats 94; Noun 93; Nouri 94; Smith 92	276904
VMD2	dominant MD, Best type	11p12-q13	not known	Forsman 92; Graff 94;	153700

					Nichols 94; Stone 92a; Wadeilus 93; Weber 93; Weber 94a; Weber 94c; Zhaung 93	
BBS1	recessive Bardet-Biedl syndrome	11q13	not known	Bruford 97; Cornier 95; Leppert 94; Wright 95	209901	
ROM1	dominant RP; digenic RP with RDS	11q13	retinal outer segment membrane protein 1	Bascome 92; Bascom 92a; Bascom 93; Bascom 93a; Connell 90; Kajiwara 94; Nichols 94; Sakuma 95	180721	
EVR1, FEVR	dominant familial exudative vitreoretinopathy	11q13-q23	not known	Li 92; Ki 92a; Muller 94	133780	
VRNI	dominant neovascular inflammatory vitreoretinopathy	11q13	not known	Stone 92	193235	
MYO7A, DFNB2, USH1B	recessive Usher syndrome, type 1	11q13.5	myosin VIIA;	Adato 97; Bonne-Tamir 94; El-Amraoui 96; Gibson 95; Kelley 97; Kimberling 92; Levy 97; Liu 97; Liu 97a; Smith 92; Weil 95; Weil 97; Weston 95; Weston 96	276903	
STGD2	dominant MD, Stargardt type	13q34	not known	Zhang 94	153900	
RHOK, RK	recessive CSNB, Oguchi type	13q34	rhodopsin kinase	Cideciyan 98; Khani 98; Maw 98; Yamamoto 97	180381	
(RP16)	recessive RP (possible)	14	not known	Bruford 94	not known	
RMCH, AMCH1	recessive rod monochromacy or achromatopsia	14	not known	Pentao 92	216900	
USH1A, USH1	recessive Usher syndrome, French	14q32	not known	Kaplan 91; Larget-Piet 94	276900	
BBS4	recessive Bardet-Biedl syndrome	15q22.3-q23	not known	Bruford 97; Carmi 95	600374	
RLBP1, CRALBP 180090	recessive RP	15q26	cellular retinaldehyde-binding protein	Maw 97		
RP22	recessive RP	16p12.1-p12.3	not known	Finckh 98	not known	
BBS2	recessive	16q21	not known	Bruford 97;	209900	

	Bardet-Biedl syndrome, type 2			Kwitek-Black 93; Kwitek-Black 94; Kwitek-Black 96; Wright 95	
CACD	dominant central areolar choroidal dystrophy	17p	not known	Lotery 96	215500
LCA1, GUC2D, GC1, RETGC	recessive Leber congenital amaurosis	17p13	retinal-specific guanylate cyclase	Camuzat 95; Camuzat 96; Perrault 96; Semple-Rowland 98	204000
RP13	dominant RP	17p13.3	not known	Goliath 95; Greenberg 94; Kojis 96; Tartelin 96	600059
CORD5, RCD2	dominant cone dystrophy, progressive	17p13-p12	not known	Balciuniene 95; Small 95	600977
CORD6	dominant cone-rod dystrophy	17p13-p12	not known	Kelsell 97	601777
CORD4	cone-rod dystrophy	17q	not known	Klystra 93	not known
RP17	dominant RP	17q22	not known	Acland 98; Bardien 95; Bardien 97	600852
PDEG	mouse recessive retinal degeneration	17q25	cGMP phosphodiesterase gamma subunit	Dollfus 93; Tsang 95	180073
CORD1	cone-rod dystrophy; de Grouchy syndrome (multiple organs)	18q21.1-q21.3	not known	Manhant 95; Warburg 91	600624
(MGA3)	recessive optic atrophy with ataxia and 3-methylglutaconic aciduria	19q13.2-q13.3	not known	Nystuen	98258501
CORD2, CRX	dominant cone-rod dystrophy; dominant and 'de novo' Leber congenital amaurosis; dominant RP	19q13.3	otx-like photoreceptor-expressed homeobox transcription factor	Bellingham 97; Evans 94; Evans 95; Freund 97; Freund 98; Gregory 94; Li 98; Swain 97	120970
RP11	dominant RP	19q13.4	not known	Al-Magtheth 94; Al-Magtheth 96; Nakazawa 95	600138
AGS, PLCB4	dominant Alagille syndrome	20p12-p11.23	phospholipase-C-beta-4	Alvarez 95; Rao 95	600810
USH1E	recessive Usher syndrome, type1	21q21	not known	Chäib 97	602097
SFD, TIMP3	dominant Sorsby's fundus dystrophy	22q12.1-q13.2	tissue inhibitor of metalloproteinases-3	Felbor 95; Felbor 97; Jacobson 95; Peters 95; Stohr 95; Weber 94; Weber 94b; Wijesuriya 96	136900
RS, XLRS1	retinoschisis	Xp22.3-p22.1	X-linked retinoschisis 1 protein	Bergen 93a; Huopaniemi 97;	312700

				Sauer 97; Sieving 90	
RP15	X-linked RP, dominant.	Xp22.13-p22.11	not known	McGuire 95a	300029
----	RP with mental retardation	Xp21-q21	not known	Aldred 94	not known
RP6	X-linked RP	Xp21.3-p21.2	not known	Musarella 90; Ott 90	312612
DMD	Oregon eye disease	Xp21.2	dystrophin	D'Souza 95; Pillers 93; Ray 92	310200
RP3, RPGR	X-linked RP; X-linked CSNB	Xp21.1	RPGR protein, homologous to RCC1 guanine nucleotide exchange factor	Andréasson 97; Buraczynska 97; Fujita 97; Hermann 96; Meindl 96; Musarella 90; Ott 90; Roepman 96; Roepman 96a	312610
COD1	X-linked cone dystrophy, 1	Xp11.4	not known	Bartley 89; Bergen 93 Dash-Modi 96; Hong 94; Meire 94; Seymour 98	304020
(CSNB4)	X-linked CSNB	Xp11.4-p11.3	not known	Berger 95; Hardcastle 97	not known
NDP, EVR2	Norrie Disease; familial exudative vitreoretinopathy	Xp11.4-p11.3	Norrie disease protein	Berger 92; Berger 92a; Chen 92; Chen 93; Chen 93a; Fuchs 94; Fuchs 96; Fullwood 93; Isashiki 95; Meindl 92; Meindl 95; Rehm 97; Schuback 95; Shastry 95; Shastry 97; Shastry 97a; Shastry 97b; Strasberg 95	310600
CSNB1	X-linked CSNB	Xp11.4-p11.3	not known	Aldred 92; Bech-Hansen 92; Boycott 98; Gal 89; Musarella 89	310500
OPA2	X-linked optic atrophy	Xp11.4-p11.2	not known	Assink 97	311050
AIED, OA2	Åland island eye disease	Xp11.4-q21	not known	Alitalo 91; Glass 93; Schwartz 91	300600
RP2	X-linked RP	Xp11.3	not known	Bhattacharya 84; Teague 94; Thiselton 96	312600
PRD	retinal dysplasia, primary	Xp11.3-p11.23	not known	Ravia 93	312550
CSNB2, CSNBX2	X-linked CSNB,	Xp11.23	not known	Boycott 98; Bergen 94; Bergen 95; Bergen 96	300071
PGK1	RP with myopathy	Xq13.3	phosphoglycerate	Tonin 93	311800

kinase

CHM, REP1	choroideremia	Xq21.1-q21.3	geranylgeranyl transferase Rab escort protein 1	Andres 93; Beaufre 96; Cremers 90; Seabra 93; van Bokhoven 94; van Bokhoven 94a; van den Hurk 92; van den Hurk 97	303100
COD2, XLPCD	X-linked progressive cone dystrophy, 2	Xq27	not known	Bergen 97	300085
CBP, RCP 303900	protanopia and rare dystrophy in blue cone monochromacy	Xq28	red cone opsin	Nathans 86 Nathans 92	;
CBD, GCP	deuteranopia and rare retinal dystrophy in blue cone monochromacy	Xq28	green cone opsin	Nathans 86; Nathans 92; Neitz 95; Winderickx 92	303800
KSS	Kearns-Sayre syndrome including retinal pigmentary degeneration	mitochondrion	not known	Puddu 93; Wallace 92	530000
LHON	Leber hereditary optic neuropathy	mitochondrion	several mitochondrial proteins	Brown 92; Brown 97; Hofmann 97; Howell 97; Howell 98; Huoponen 93; Mashima 93; Nikoskelainen 96; Riordan-Eva 95; Torroni 97; Wallace 88	535000

CHAPTER 2

LINKAGE ANALYSIS OF HUMAN CHROMOSOME 4: EXCLUSION OF AUTOSOMAL DOMINANT RETINITIS PIGMENTOSA (adRP) AND DETECTION OF NEW LINKAGE GROUPS: SYSTEMATIC LINKAGE STUDIES REPRESENTATIVE OF THOSE THAT LEAD TO THE LOCALIZATION OF THE FIRST adRP GENE

2.1 Introduction

The chromosome 4 study was the first systematic one that we embarked upon to cover the genome chromosome by chromosome in two large adRP families in the search for the causative gene. The study I have described in this Chapter was a team effort, involving daily input from myself, Beth Sharp, Nan Giesenschlag (who is sadly now deceased), Peter Humphries and Stephen Daiger over a period of 3 months. After preparing the probes in Dublin we took them to the Houston laboratory where we did the work up (June-August 1988). I either ran myself, or had a major hand in running and analysing all markers described in this Chapter

The first part of this study - the localization of the adRP gene in the Irish family was concluded, again as a team effort, at the Dublin laboratory the following summer (May 1989). Those involved in this study, including myself, are as shown in the list of authors on the manuscript entitled "Autosomal dominant retinitis pigmentosa (adRP): localization of an adRP gene to the long arm of chromosome 3". The RFLP, C17, mapping on chromosome 3q, showed zero recombination with the disease locus, generating a lod score of 13.7, conclusive evidence of linkage.

The second part of this study, localization of the adRP gene in the US pedigree was concluded by Dr S Daiger and colleagues in 1991, the gene mapping to the pericentric region of chromosome 8.

Following a multilocus analysis undertaken by Dr Jane Farrar (Dublin), linkage of the disease locus in the Irish pedigree was firmly established (1990). A mutation within the rhodopsin gene in adRP families was first reported by Dryja et al (1990). The mutation in the Irish family, a met-207-arg substitution, was also reported (Farrar et al., 1992). To date up to 100 mutations have been reported within the rhodopsin gene in autosomal dominant RP (Humphries P et al, 1992b).

As part of our ongoing linkage studies of degenerative retinal diseases, we tested seven DNA markers and two classical genetic markers from chromosome 4 in two extended families with autosomal dominant retinitis pigmentosa (adRP). Our goals were (1) to detect or exclude linkage of adRP to markers spanning most of chromosome 4 and (2) to contribute useful new information regarding the linkage map of this chromosome. Our results excluded linkage of adRP from more than 82% of chromosome 4. We detected four new linkage relationships: loose linkage of K082 (D4S10) and G1E5 (D4S21) at a distance of 21 cM; loose linkage of 4F2 (D4S18) and GC protein at a distance of 19cM; tight linkage (i.e., no recombinants) between B3D (D4S44), B5A (D4S40), and the MNS blood group; and tight linkage between 4F2 and GDS5 (D4S23). These data, combined with previously reported data, excluded adRP from approximately 35% of the human genome.

No significant linkages for the autosomal forms of retinitis pigmentosa had been reported at this time; however, there was suggestive evidence for linkage of at least one form of autosomal dominant retinitis pigmentosa (adRP) to the Rh blood group on chromosome 1p (Spence et al., 1977; Field et al., 1982; Daiger et al., 1987c) and for linkage of Usher syndrome, a recessive form of retinitis pigmentosa accompanied by congenital deafness, to GC protein on chromosome 4q (Daiger et al., 1987a; Pelias et al., 1989).

As part of our ongoing linkage studies of degenerative retinal diseases, we adopted a strategy of testing for linkage using a number of genetic markers from a single chromosome (Daiger et al., 1987b; Bradley et al., 1989). This approach took advantage of previously established multipoint linkage groups to establish or exclude linkage to the disease locus and increased the likelihood of detecting useful new linkage relationships among the genetic markers themselves.

Following this strategy, we tested for linkage in two large, Caucasian families with adRP using nine genetic markers spanning most of chromosome 4. We chose chromosome 4 for this investigation because of the availability of a number of well-characterised restriction fragment length polymorphisms (RFLPs) mapped to this chromosome (Gusella and Wasmuth, 1987) and because of the suggestion of linkage of Usher syndrome to GC (Daiger et al., 1987a). The two families tested were an Irish kindred, TCD-M, with over five affected generations and a Kentucky family, UCLA-RP01, with over seven affected generations. UCLA-RP01 was the subject of earlier linkage studies using classical genetic markers (Spence et al., 1977; Field et al., 1982; Heckenlively et al., 1982). In independent studies, adRP had also been excluded from much of chromosome 1 (Bradley et al., 1989).

2.1:i Families

The Irish TCD-M pedigree encompasses more than five generations known to be affected with adRP, with at least 50 living, affected members. The pedigree is shown in Figure 2.1. Most family members live within 100 km of Dublin, Ireland. For purposes of this study, blood samples and DNAs were acquired from 76 family members, including 42 affected individuals. An additional 11 individuals were included in the linkage analysis as parents or as links between individuals from whom samples had been drawn.

The Kentucky adRP pedigree, UCLA-RP01, is part of a seven-generation family described by Spence et al. (1977) and Field et al. (1982). The pedigree is shown in Figure 2.2. (Specifically, the family included in this study is family UCLA-RP01 in Field et al. (1982) plus additional members ascertained since 1982. The pedigree in Figure 2.2 differs from the pedigree in Field et al. (1982) because of the addition of new members and because the order within sibships has been rearranged to reflect birth order). There are over 100 known affected members in the extended UCLA-RP01 family. For this study, blood samples were collected from 103 family members, 45 of whom are affected. An additional 47 individuals were included in the analysis as links between sampled individuals. Of the total 156 individuals included in the analysis, classical genetic markers had been tested in 68 individuals as part of earlier studies (Spence et al., 1977; Field et al., 1982). TCD-M and UCLA-RP01 share no surnames in common, and there is no evidence of Irish ancestry in UCLA-RP01.

DNAs from the TCD-M family were prepared directly from blood samples at Trinity College, Dublin. Blood samples from UCLA-RP01 were collected as part of the Support Program for DNA Linkage Studies of Degenerative Retinal Diseases, established jointly by the National Retinitis Pigmentosa Foundation Fighting Blindness, USA; the George Gund Foundation; and the National Institute of Health - National Institute of General Medicine (NIH-NIGMS) (Daiger et al., 1987c). Under the auspices of this program, samples from UCLA-RP01 were provided to the NIGMS-Human Genetic Mutant Cell Repository, Camden, NJ, for transformation and long-term storage of lymphoblasts (Daiger SP, 1988). DNAs from these cell lines were subsequently prepared at the University of Texas Health Science Center at Houston, TX.

In both families, all individuals from whom blood samples were collected were given a comprehensive ophthalmological examination, following the diagnostic criteria proposed by Marmor (1983), including a clinical history,

funduscopy evaluation, determination of visual fields, and, where possible, ERGs. In addition, a number of affected individuals from both families were given more extensive examinations at either the Royal Victoria Eye and Ear Hospital, Dublin (TCD-M), or the Jules Stein Eye Institute, Los Angeles (UCLA-RP01). These extended ophthalmological examinations included full-field ERGs and retinal photography. The disease status of individuals who were included in the analysis but from whom samples were not drawn, and who were not otherwise available for testing, was established from the medical history.

Both families display classical features of adRP (Farber et al., 1985). Characteristic findings include diffuse retinal pigmentation, a progressive decrease in recordable ERGs, and concentric visual field loss. Both families manifest relatively early development of symptoms, typically between the ages of 5 and 25, with members of TCD-M showing an earlier onset than those of UCLA-RP01. There are no known "skipped generations" in TCD-M. In UCLA-RP01, two deceased obligate heterozygotes, both with affected children, had no history of RP. One obligate heterozygote died at age 95 without an ophthalmologic examination. The other died at age 35 and did not show symptoms at an examination two years prior to death. (See generation III in Figure 2.2.) Otherwise, the RP gene is highly penetrant in both families.

Although the two families are clinically similar, members of TCD-M are more severely affected than members of UCLA-RP01. The average age of onset is earlier in TCD-M than in UCLA-RP01 (10-20 years of age versus 20-30 years); the rate of progression is faster (10-15 years for development of severe visual impairment versus 20-30 years); and pigmentation is less diffuse and ERGs more abnormal at comparable stages of disease in TCD-M than in UCLA-RP01. These differences in severity are consistent with the clinical subtypes proposed by Farber et al. (1985), with TCD-M being type I (more severe) and UCLA-RP01 being type II (less severe). The possibility of genetic heterogeneity was incorporated into our linkage analysis, as discussed in the Results section.

Blood and cell lines were collected from all living family members shown in Figures 2.1 and 2.2. Age at the time of examination of at-risk, unaffected individuals (and the age at death of two obligate carriers in UCLA-RP01) is given at the upper right of the pedigree symbol. Cell line numbers assigned to UCLA-RP01 by the Cell Repository can be found in the Cell Repository Catalog (Daiger, 1988).

2.1:ii Genetic Markers

Table 2.1 lists the chromosome 4 markers included in this study and gives their relevant characteristics, including references. Markers are listed in physical order, where known. Symbols are those assigned at the Human Genome Mapping meeting 9 (HGM9 1987) or at earlier workshops. DNA probes were kindly provided by Drs James Gusella and Conrad Gillian, Massachusetts General Hospital, Boston, MA. MNS and GC subtyping for TCD-M were performed by Terry Bertin and Victoria Cortessis at the Graduate School of Biomedical Sciences, The University of Texas. MNS and GC typing for UCLA-RPO1 were performed in the Department of Medicine, University of California at Los Angeles, as part of earlier studies (Spence et al., 1977; Field et al., 1982).

All DNA RFLPs tested were of the simple two-allele variety, except KO82 (D4S10). KO82, a subclone of the G8 probe linked to Huntington disease, detects several independent RFLPs (Youngman et al., 1986). For this study two independent KO82 polymorphisms, both detected with Hind III , were combined to make four haplotypes. The two Hind III RFLPs are known to be in linkage equilibrium, making this a highly informative locus (Youngman et al., 1986). Figure 2.3 shows the patterns produced by the seven DNA RFLPs. An appropriate map of chromosome 4 is shown in Figure 2.4.

2.2 Materials and Methods

2.2:i Materials

Sources of all materials are described in Chapter 3.

2.2:ii Genomic DNA Preparation, Probe Preparation, Restriction Enzyme Digestion and Southern Blot Analysis

Genomic DNAs were prepared from either whole blood (TCD-M) or lymphoblast pellets (UCLA-RP01) using either SDS lysis, proteinase K digestion, phenol/chloroform extraction, ethanol precipitation, and aqueous resuspension or an Applied Biosystems Nucleic Acid Extractor. Restriction digests of genomic DNA were performed using a four-fold excess of enzyme and 16 h digestion following the manufacturers directions for temperature and buffer conditions. Southern gel electrophoresis, transfer to charged nylon membranes, nick translation, hybridization, and autoradiography was performed as described in Chapter 3. The 8 DNA probes used in Southern blots were prepared by restriction digestion of the plasmid or phage carrying the human genomic insert. DNA fragments were separated on preparative 1% agarose gels and the human fragments excised in the form of strips of agarose. The strips were placed into dialysis tubing (8/32) filled with electrophoresis buffer and sealed at each end. Dialysis tubes were placed in a horizontal electrophoresis tank and the DNA electroeluted into the walls of the tubing. Electroelution of the fluorescent (ethidium bromide stained) DNA could be followed using a hand-held long wave ultra violet (UV) lamp. DNA was released from the dialysis tubing by a 30 second reversal of current. The solution of DNA was extracted several times with methoxyethanol and then pressure-dialysed to a volume of approximately 100 μ l. The concentrated DNAs were then nick-

translated to produce $\alpha^{32}\text{P}$ -labelled probes. The optimal amount of DNA labelled was determined empirically - we usually arrived at 50% incorporation of label in a 100 μCi nick-translation assay as determined by Sepharose G50 gel filtration of the reaction.

2.2:iii Data Analysis

Linkage analysis was performed on a 80386-based microcomputer with a math coprocessor or on a VAX8850 mainframe computer made available by the School of Public Health of the University of Texas Health Science Center at Houston by Dr S Daiger. Two-point recombination fractions were calculated using LIPED (Ott, 1985). Multipoint analysis, using fixed genetic distances between linked markers (K082-G1E5 and GC-MNS), was performed using version 4.8 of the LINKMAP program in the LINKAGE program set (Lathrop et al., 1984). Note that UCLA-RP01 contains two inbreeding loops (Fig. 2.2.) The LINKAGE programs will accept pedigrees with no more than one loop, whereas LIPED will accept any number of loops, although computation time increases exponentially. Thus the loop in generation III of UCLA-RP01 was broken for multipoint analysis but left intact for two-point calculations. Comparable analyses, with and without this loop, differed by no more than 20%. The allele or haplotype frequencies used are those given in Table 2.I. Finally, to account for unknown phase in double heterozygotes at the K082 and MNS loci, the two possible genotypes (ab x cd versus ad x bc) were coded as having identical phenotypes. The same strategy was followed in analyzing B3D-B5A haplotypes.

To correct for delayed age-of-onset of RP in at-risk, unaffected individuals, the following strategy was adopted. Individuals under 20 years were coded as "unknown" and those over 40 as "unaffected". Those between 20 and 29 years were assigned a probability of 20% of carrying the adRP gene and those

between 30 and 39 were given a 10% probability. At-risk, “unaffected” individuals had a limiting risk of 1% of carrying the adRP gene. Implementation of this strategy in LIPED is slightly different from implementation in LINKAGE, but comparison of two-point analyses produced similar results.

Two-point exclusion ranges and maximum likelihoods were determined by calculating lod (log-odd) scores at 1% intervals, with identical male and female recombination rates. Recombination rates were converted to genetic distances in centiMorgans (cM), using Haldane’s formula, $x = -100 \times [1n(1 - 2\theta)]/2$, assuming no interference (Ott, 1985). For multipoint analysis, the distance between K082 and G1E5 was fixed at 21 cM and that between GC and MNS at 60 cM (Keats et al., 1979).

Sex-averaged distances were used throughout. We felt that the linkage map of chromosome 4 is not sufficiently refined nor are our family sizes sufficiently large to justify more complicated approaches.

2.3 Results

2.3:i Linkage Strategy

Linkage analysis proceeded in two phases. First, we tested for linkage between all nine genetic markers with the goal of establishing useful new linkage relationships. Second, we tested for linkage between adRP and the nine markers, taking advantage of new or previously known linkage groups for multipoint analysis. Both types of analysis involved potential pitfalls that were dealt with in the following manner.

First, regarding between-marker linkages, a maximum lod score of 3.0 or greater is generally regarded as significant evidence for linkage between two randomly selected genetic markers. This convention is based on the argument that if (1) the *a priori* probability that two randomly selected markers are linked is 1/50, (2) the probability that two unlinked markers have a maximum lod score of 3.0 or greater is $1/10^3$, and (3) the probability that two *linked* markers have a lod of 3.0 or greater is 90%, then the conditional probability that two markers with a lod score of 3.0 or greater are linked is 95% using Bayes theorem (Ott, 1985). However, in the case of the chromosome 4 markers used in this study, the *a priori* chance of linkage is much greater than 1/50, especially if the markers map to the same chromosomal region. For these reasons, we concluded that two chromosome 4 markers were linked if they mapped to the same physical region (Gilliam et al., 1987; MacDonald et al., 1987; and Figure 2.4) and if they produced a maximum lod of 1.5 or greater. Assuming an *a priori* chance of 1/3 that two physically close chromosome 4 markers are linked gives a conditional probability of roughly 95% that they are, in fact, linked. Note, however, that failure to find significant lods between markers within the same physical region does not necessarily exclude linkage; the markers may simply be insufficiently informative in these families.

Second, regarding adRP linkage, although it is standard practice to sum lod scores from genetically independent families, this methodology assumes that the same locus is involved in all the families included in the summation, although not necessarily the same allele. In the case of the two adRP families in this study, both families have a dominant form of RP, but the clinical features differ. These clinical differences may result from differences in environment or genetic background, from allelic differences at the same locus, or from two different, unlinked loci. (We now know that 2 different loci are involved).

We dealt with this potential problem by, first, examining each family alone for suggestive evidence of linkage (arbitrarily taken as a maximum lod of 1.5 or greater) and, second, if no suggestive evidence was found, summing lods between families to produce exclusion ranges. We feel summing lods under these criteria was valid because there is no persuasive evidence for genetic heterogeneity, as opposed to clinical heterogeneity, in adRP. Also, a specific exclusion was likely to apply to both families, even if different loci were involved.

2.3:ii Between-marker Linkages

Table 2.II shows the significant between-marker linkages observed in these families. Loose linkage was found between K082 and G1E5 and between 4F2 and GC. Although the maximum lod score for K082-G1E5 linkage was only 1.53 at 17% recombination, both markers map within the region 4pter->p15.1. 4F2 and GC, with a maximum lod score of 1.75 at 16% recombination, are at least within 75 cM of each other, as determined by physical mapping (see Figure 2.4). However, since the regions within which 4F2 and GC map do not overlap, this linkage should be considered tentative. For these reasons, the linkage of K082 to G1E5 was used for multipoint exclusion of adRP, but 4F2 and GC were analyzed separately.

Tight linkage (i.e., no recombinants) was observed between B3D, B5A, and MNS and between 4F2 and GDS5. For both linkage groups, the physical mapping evidence is consistent with tight linkage.

For 4F2 and GDS5 we observed a maximum lod score of 2.43 at 0% recombination with a 95% confidence range of 0% to 21% recombination. Thus, these two markers may or may not be tightly linked, but loose linkage, at least, is highly likely. Linkage of GDS5 to GC was excluded (lod of -2.0) at a distance of 4% recombination, but this is not inconsistent with the tentative linkage of 4F2 and GC at 16% recombination.

The pair-wise linkages of B3D, B5A, and MNS are consistent with each other, with maximum lods ranging from 3.07 to 5.55. In an unrelated study (unpublished), we observed no recombinants between B3D and MNS in a third family, bringing the summed lod score to 5.96 at 0% recombination. This is equivalent to no recombinants in approximately 20 informative meioses (Ott, 1985). Therefore, although the physical distance between these markers may be several million base pairs, they are very close genetically.

GC and MNS are known to be linked at a distance of approximately 35% to 40% recombination (60-80 cM using Haldane's conversion) (Keats et al., 1979; Donis-Keller et al., 1987). Our observations are consistent with this distance, but our lod scores are not significant (maximum lod of 0.31 at 30% recombination).

Finally, we observed a maximum lod score of 1.24 at 16% recombination between 3E5 and GC. Linkage between these markers is consistent with physical mapping evidence, but they are not within the same chromosomal region, and the lods are less than 1.5. For these reasons, we do not consider this meaningful evidence for linkage, but suggestive, nonetheless.

2.3:iii Haplotype Analysis

K082 haplotypes and B3D-B5A haplotypes were determined in 10 independent individuals, either founding parents or unrelated spouses. Although the sample size is small, our data demonstrated equilibrium between the K082 alleles and between the B3D-B5A alleles. In both cases, all four possible haplotypes were observed, and the observed numbers were approximately those expected, assuming equilibrium.

2.3:iv adRP Exclusion

There was no significant evidence for linkage between adRP and any of the nine markers. Exclusion ranges (i.e. recombination fractions with a lod score of -2.00 or less) are shown in Table 2.III.

Based on the linkage relationship between K082 and G1E5 established in this study and on the previously known GC-MNS linkage, location scores for adRP relative to K082-G1E5 and relative to GC-MNS were calculated using LINKMAP. The other between-marker linkages were either at 0% recombination or were not sufficiently credible to justify multipoint analysis. Results are shown in graphical form in Figures 2.5 and 2.6. These data completely exclude adRP from between G1E5-K082 and from GC-MNS. Table 2.III also lists exclusion ranges for GC and MNS reported in previous studies. The composite exclusion distances and their sums are shown in Table 2.III. The total distance on chromosome 4 from which adRP is excluded is more than 200 cM.

Table 2.III also gives the exclusion distance from the B3D-B5A linkage group, using the four haplotypes defined by this system. Although the result is consistent with the exclusion distance from MNS alone, it must be accepted with caution, since the possibility of an appreciable genetic distance between B3D and B5A cannot be excluded.

2.4 Discussion

Given sufficient numbers of genetic markers and appropriate families, it should be possible, eventually, to find linkage for any genetic disease (Botstein et al., 1980). Even at the time this study was done (1988), with the thousands of polymorphic DNA probes that had been described, there were almost certainly sufficient numbers of probes available (HGM9, 1987) to cover the genome. In addition, the linkage relationships of many of these markers were already known, permitting application of multipoint linkage techniques to the problem (Lathrop et al., 1984). Although the chance of finding linkage with any particular probe was small, by concentrating on probes whose map location was known, it was possible to exclude the disease locus from more and more of the genome with each new probe tested. Eventually, this strategy led to detection of linkage to disease loci in both families.

The central problem remaining in most linkage studies is to find appropriate families. In the case of adRP, the two families used here were particularly appropriate. Both families are multigenerational, have more than 50 living, affected members, and both appear to have clinically similar, though not identical, forms of the disease.

In our combined analysis of the two families using nine chromosome 4 markers, we found no evidence of linkage with adRP. Based on these results, we were able to exclude adRP from over 200 cM of chromosome 4. A reasonable estimate of the genetic length of chromosome 4 is 250 cM (Ott, 1985; Donis-Keller et al., 1987). Thus, we excluded adRP from more than 82% of the chromosome. This exclusion distance, combined with previous data (Goode et al, 1985; Daiger et al., 1987a; Bradley et al., 1989), would exclude adRP from more than 35% of the human genome. This global exclusion, however, must be considered tentative, since several different types of families were included in the composite data set.

In addition to including or excluding a disease locus from a specific chromosomal region, the strategy of analyzing a number of markers in the same families can reveal new between-marker linkages. In our two families we found tentative evidence for loose linkage between K082 (D4S10) and G1E5 (D4S21) and between 4F2 (D4S18) and GC protein. We also found convincing evidence for tight linkage between B3D (D4S44), B5A (D4S40), and the MNS blood group and between 4F2 and GDS5 (D4S23). The first two linkage groups should provide useful multipoint markers for the regions to which they map, 4pter->p15.1 and 4p16.1->q13, respectively. Taken together, these linkage groups added useful new information to the known, detailed maps of chromosome 4 (Donis-Keller et al., 1987; Murray et al., 1988).

The utility of the B3D-B5A-MNS linkage group would depend, in part, on the actual physical distances between the loci. If B3D and B5A are very close, with a low probability of recombination within a family, then their alleles could be combined into haplotypes to increase their information content. If they are more distant from each other, they would be most useful as independent genetic markers. Finally, if B3D and/or B5A are very close to MNS, they could represent genomic clones of glycophorin A (MN) or glycophorin B (Ss) (Siebert and Fukuda, 1986). As such, they could be useful tools for analyzing this complex blood-group system.

Whatever the physical relationship between B3D, B5A and MNS, the two DNA markers would be useful in DNA linkage studies of diseases and traits tentatively linked to MNS. These include sclerotylosis (MIM No. 18160, McKusick, 1983), anterior segment ocular dysgenesis (10725), red hair colour (26630), dentinogenesis imperfecta (12549), and mucopolidosis II (25250).

In conclusion, this was the first systematic chromosomal exclusion study to be completed in the search for the adRP loci in two of our largest pedigrees. As outlined above, using molecular techniques, both genes were subsequently localized (McWilliam et al, 1989; Blanton et al, 1991).

Figure 2.1

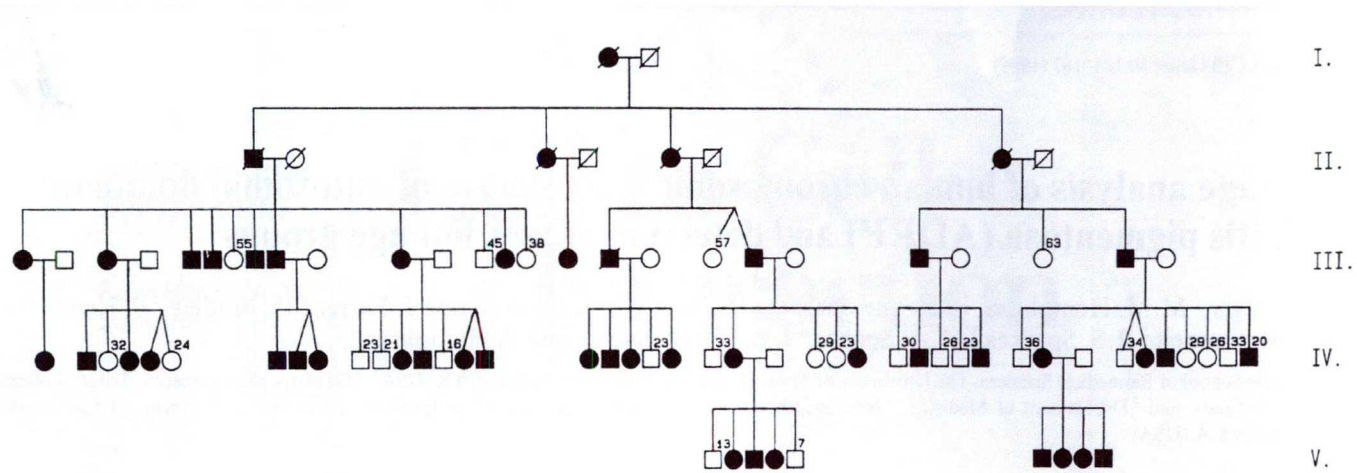
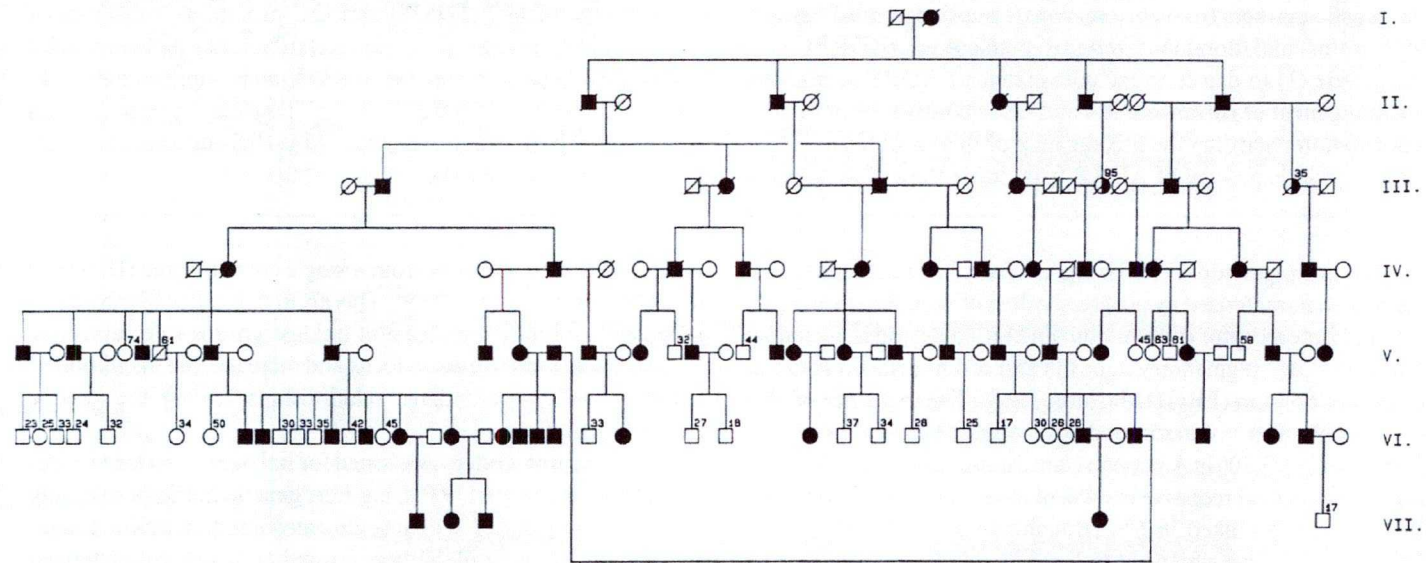
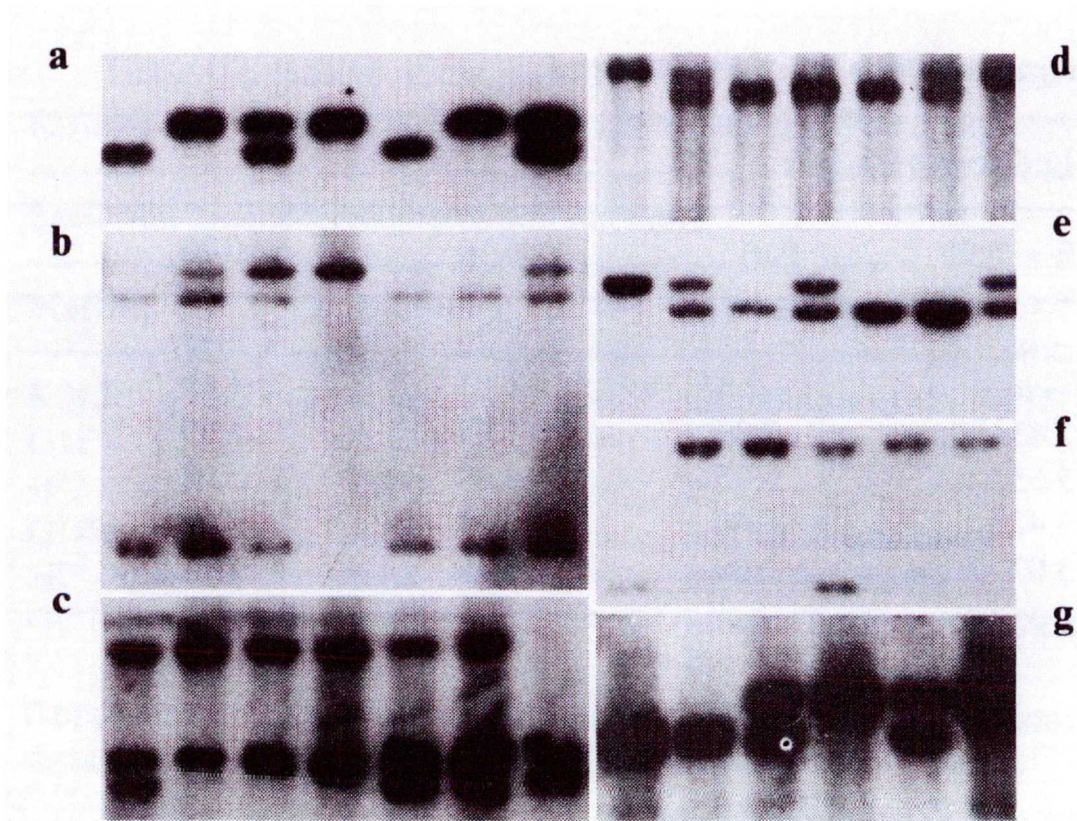


Figure 2.2



Pedigree of the Kentucky adRP family UCLA-RP01. Ages of at-risk, unaffected individuals (and ages at death of obligate carriers) are at the top right of the pedigree symbol.

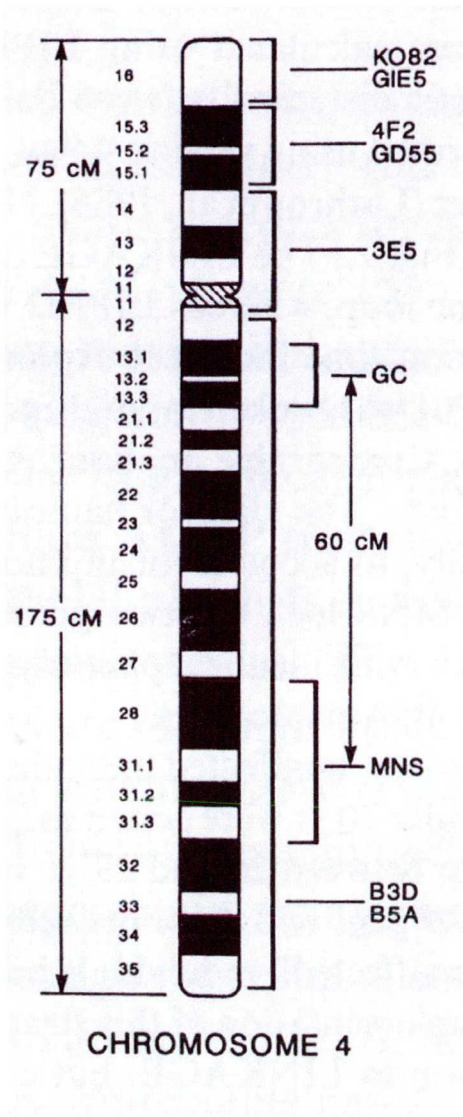
Figure 2.3



Southern gel patterns of the seven chromosome 4 RFLPs tested in these families (see Table II for details). Probes are: (a) GIE5 (D4S21), (b) 3E5 (D4S16), (c) B5A (D4S40), (d) KO82 (D4S10), (e) GDS5 (D4S23), (f) 4F2 (D4S18), and (g) B3D (D4S44).

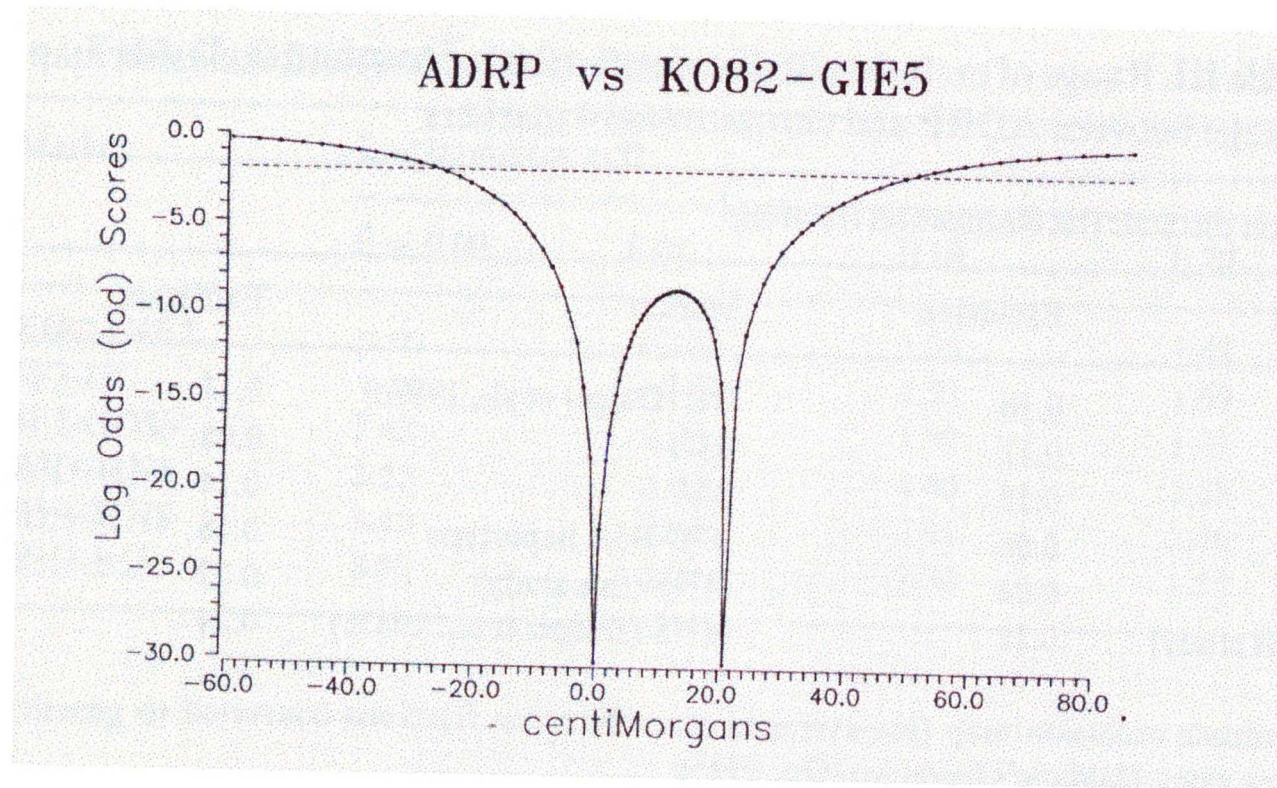


Figure 2.4



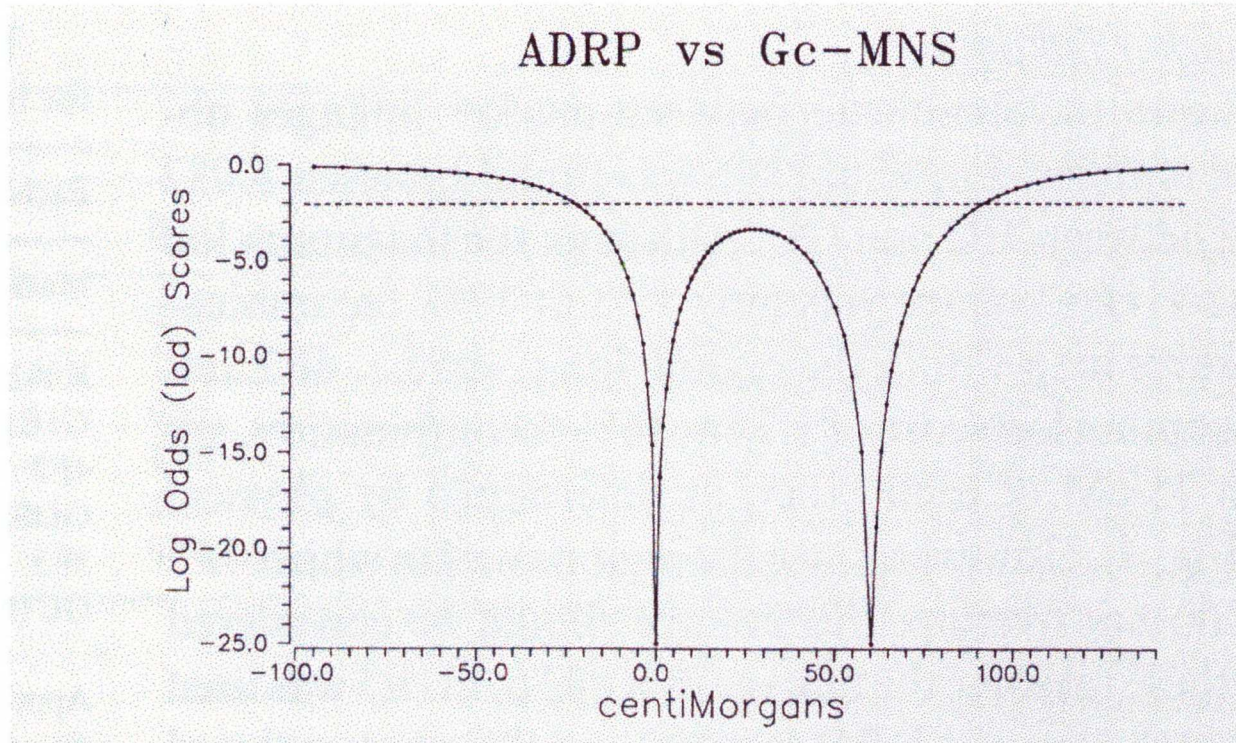
Physical and linkage map of chromosome 4 based on HGM 9 (1987).

Figure 2.5



Multipoint location map for adRP v KO82 - GIE5. KO82 was fixed at 0.0 cM and GIE5 at 21 cM. Lod scores are relative to adRP at a distance of - 10.00 cM. Dashed line is - 2.00 lod exclusion limit.

Figure 2.6



Multipoint location map for adRP v GC-MNS. GC was fixed at 0.00 cM and MNS at 60 cM. Lod scores are relative to adRP at a distance of -10.00 cM. Dashed line is -2.00 lod exclusion limit.

Table 2. I. Chromosome 4 markers included in this study

Chromosomal location	Symbol	DNA probe	Restriction enzyme	Alleles (kb or name)	Frequencies	PIC ^b	Ref.
4p16.3	D4S10	K082	<i>HindIII</i> ^a	17-4.9, 17-3.7, 15-4.9, 15-3.7	0.656, 0.094, 0.219, 0.031	0.46	1, 2
4pter - p15.1	D4S21	GIE5	<i>BamHI</i>	11,9	0.450, 0.550	0.37	2,3
4p16.1 - p15.1	D4S18	4F2	<i>BamHI</i>	10,5	0.720, 0.280	0.32	2,3
4p16.1 - p15.1	D4S23	GDS5	<i>BglII</i>	10,8	0.220, 0.780	0.28	2,3
4p15.1 - q11	D4S16	3E5	<i>MspI</i>	14,11+2.8	0.440, 0.560	0.37	3
4q12 - q13	GC	(protein)	n/a	2, 1f, 1s	0.256, 0.148, 0.596	0.49	4, 5
4q11 - qter	D4S44	B3D	<i>PstI</i>	10, 8.5	0.320, 0.680	0.34	3
4q11 - qter	D4S40	B5A	<i>PstI</i>	16, 5.5	0.710, 0.290	0.33	3
4q28 - q31	MNS ^a	(blood group)	n/a	MS, Ms, NS, Ns	0.259, 0.291, 0.063, 0.387	0.64	4,5

^a Haplotypes.

^b PIC: polymorphic information content (Botstein et al., 1980).

^c References: (1) Youngman et al. (1986); (2) MacDonald et al, (1987); (3) Gilliam et al, (1987); (4) Field et al. (1982); (5) Ferrell et al. (1981).

n/a = Not applicable.

Table 2.II. Significant between-marker linkages

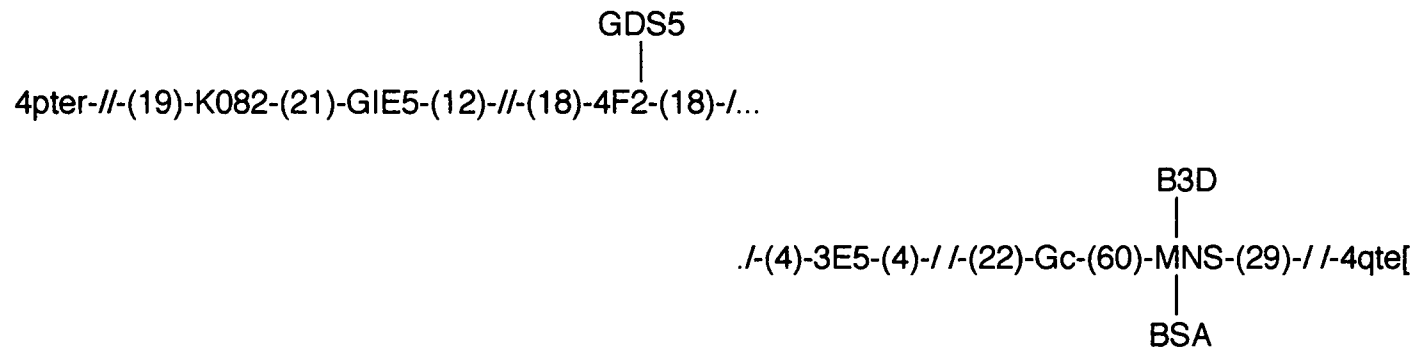
Marker	Lod scores (m = f)						Maximum range			
	0 = 0.00	0.01	0.10	0.20	0.30	0.40	z	o	(± 1.0 lod)	
K082-G1E5	-	-2.31	1.25	1.48	0.99	0.37	1.53	0.17	0.06 - 0.37	
4F2-GC	~	-2.35	1.53	1.69	1.22	0.54	1.75	0.16	0.06 - 0.37	
4F2-GDS5	2.43	2.39	1.99	1.49	0.95	0.42	2.43	0.00	0.00 - 0.21	
B3D-MNS	5.55	5.45	4.40	3.08	1.68	0.46	5.55	0.00	0.00 - 0.08	
B5A-MNS	3.45	3.44	2.91	2.06	1.13	0.30	3.45	0.00	0.00 - 0.15	
B3D-B5A	3.07	3.00	2.36	1.57	0.78	0.17	3.07	0.00	0.00 - 0.13	

Table 2.III. Range of exclusion (lod score of -2.00 or less) and exclusion map for linkage between adRP and chromosome 4 markers

Exclusion distance (recombination fraction)

Marker	Exclusion	Marker	Exclusion
K082	0.16	GC	0.17
GIE5	0.11	B3D	0.08
4F2	0.15	B5A	0.14
GDS5	0.06	B3D-B5A haplotype	0.18
3E5	0.04	MNS (this study)	0.22
GC (this study)	0.15	MNS	0.24

Approximate exclusion map (sex-averaged recombination fractions converted to genetic distances using Haldane's formula) (Ott, 1985):



Total genetic distance excluded: 207 cM

CHAPTER 3

RETINOPATHY INDUCED IN MICE BY TARGETED DISRUPTION OF THE RHODOPSIN GENE.

3.1 Introduction

This Chapter describes the generation of a rhodopsin knockout mouse, and its histopathological and electrophysiological analysis. Additional experiments involving the breeding of these mice onto different genetic backgrounds which may favour photoreceptor survival are also described. My major contribution to this work was the generation and sequencing of the rhodopsin (Rho) targeting vector, the establishment of the Rho^{-/-} colony in Dublin, the PCR and RT-PCR analytical work up of these animals, the crossing of these animals onto pure C57B6 and 129 genetic backgrounds and the establishment of crosses resulting in the generation of Rho^{-/-}cfos^{-/-} genotypes. To make this story a coherent one involved incorporating the data on electroporations, embryonic stem (ES) cell selection, generation of chimeras and electrophysiological analyses. I am the senior author of the manuscript describing the generation and analyses of the Rho^{-/-} mouse, in recognition of my overall contribution to the project. Where data from other people are included, this is clearly stated in the text of the Chapter.

Rhodopsin is the photoreactive pigment of the rod photoreceptors of the retina and the primary constituent protein of such cells. Mutations within the gene encoding rhodopsin have been encountered in retinitis pigmentosa, a disease involving photoreceptor cell death and severe visual impairment, and in congenital stationary night blindness. In order to gain a fuller understanding of the functional and structural consequences of haplo- and homo-insufficiency for rhodopsin in the rod photoreceptor cells, and on the retina as a whole, we

introduced a targeted disruption into the rhodopsin gene, generating mice that are either heterozygous or homozygous for the null allele. $Rho^{+/-}$ mice retain the majority of their photoreceptors, although the outer segments of these cells display varying degrees of disorganisation and become shorter with age. $Rho^{-/-}$ mice do not elaborate functional rod photoreceptor outer segments, and rhodopsin is undetectable by antibody from as early as 3 days of age. The photoreceptor nuclei are lost over a period of three months. These animals should be of substantial value in assessing the feasibility of photoreceptor cell rescue following delivery of a functional rhodopsin gene to degenerating retinal tissues.

Retinitis pigmentosa represents the most common group of mendelian degenerative retinopathies in man (Heckenlively, 1988; Pagon, 1988). A characteristic feature of the disease is the progressive death of the rod photoreceptors. This is followed by more extensive pathological changes within the retina, including cone photoreceptor degeneration, retinal vessel attenuation and the development of pigmentary deposits. Initially, the patient experiences night blindness (nyctalopia), which is usually followed by a gradual constriction of the visual fields. The majority of cases result in severe visual handicap. About fifty percent of cases are sporadic, and the remainder segregate in an autosomal dominant, recessive or X-linked mode. Genetic linkage studies in a large pedigree segregating an autosomal dominant form of the disease initially resulted in the establishment of a location for a causative gene on the long arm of chromosome 3, close to the gene encoding rhodopsin, the photoreactive pigment of the rod photoreceptor cells (McWilliam et al, 1989; Farrar et al, 1990). (For a description of the genetic linkage studies that lead up to this localization, see Chapter 2). A mutation within the rhodopsin gene was subsequently encountered in a family segregating adRP (Dryja et al, 1990). Ongoing genetic linkage studies and direct mutational analysis have resulted in the implication of a number of other genes in the etiology of the disease,

including those encoding *RDS*-peripherin, *Rom1*, the β sub-unit of cyclic GMP phosphodiesterase, the cyclic GMP-gated channel protein and Myosin VIIa, the latter in Usher syndrome (type 1b), a disease incorporating both RP and sensorineural deafness (Farrar et al, 1991a; Farrar et al, 1991b; Kajiwara et al, 1994; McLaughlin et al, 1995; Dryja et al, 1995; Well et al, 1995 and Gibson et al 1998). These genes encode proteins which are either structural components of the rod photoreceptors, or of the rod-mediated visual transduction cascade. In addition, mutations within a ubiquitously expressed gene, *RPGR* (retinitis pigmentosa GTPase regulator) have recently been identified in RP3, one of the two X-linked forms of the disease (Meindl et al, 1996).

Mutations within the rhodopsin gene, of which approximately one hundred have now been identified, account for up to twenty percent of autosomal dominant cases of RP (Humphries et al, 1992a and Humphries et al, 1992b). In addition, a patient has been described who is homozygous for a stop codon mutation near the C-terminus of the protein, and both parents of this patient have few symptomatic vision complaints (Rosenfeld et al, 1992). The majority of mutations are single amino acid substitutions within conserved regions of the rhodopsin protein, although a number of deletions occurring either within or at the carboxy-terminus of the molecule have been described (Bhattacharya et al, 1991 and Horn et al, 1992), [Figure 1.15, Chapter 1]. Mutations within the rhodopsin protein have been classified into two categories according to the functional properties that they display in cells cultured *in vitro* (Sung et al, 1991). Class I mutants [*phe-45-leu*, *gln-334-ter* and *pro-347-lue*, for example] produce proteins in normal levels, which bind the chromophore 11-*cis* retinal and are transported to the plasma membranes following transduction of COS cells by plasmids carrying mutant cDNAs. Class II mutants [*thr-17-met*, *pro-23-his*, for example] result in the production of proteins at lower levels, which do not bind the chromophore and which accumulate in the endoplasmic reticulum (Sung et al, 1991). A sub-set of rhodopsin mutations (*for example*, *lys-296*) result in the

constitutive activation of the protein such that it is capable, *in vitro* and in the absence of the chromophore, of activating the G-protein transducin (Rao et al, 1994). Two constitutively active rhodopsin mutations, *gly-90-asp* and *ala-292-glu*, have also been encountered in autosomal dominant congenital stationary night blindness (Rao et al, 1994 and Sieving et al, 1995).

In order to gain a fuller understanding of the functional and structural role of rhodopsin in the pathogenesis of disease, mice carrying a targeted disruption of the rhodopsin gene have been generated. This work was conducted for a number of reasons, including a question of whether haplo-insufficiency is compatible with survival of rod and cone photoreceptors. This has relevance to possible therapeutic approaches in the eventual treatment of human disease. In addition, the homo-insufficiency model would provide an important background against which to express other rhodopsin mutations, since it has been observed that over-expression of normal wild-type rhodopsin leads to photoreceptor degeneration, even in the absence of a mutated transgene (Olsson et al, 1992). Central questions raised are what are the consequences for the retina of decreasing the expression of wild type rhodopsin or of eliminating rhodopsin altogether?. Can rod photoreceptors survive in the absence of their main constituent protein, which is rhodopsin? In this Chapter I report that mice homozygous for a null rhodopsin allele do not elaborate photoreceptor outer segments, and lose their photoreceptors over a period of 3 months. Heterozygous animals retain the majority of their photoreceptors although the inner and outer segments of these cells display some degree of disorganisation and the outer segments become shorter in older animals. Both $Rho^{+/-}$ and $Rho^{-/-}$ animals should provide a useful model through which the possible therapeutic potential of a normal rhodopsin gene, re-introduced to degenerating retinal tissues, may be evaluated.

3.2 Materials and Methods

3.2:i Materials

General reagents were analytical grade and purchased from the following companies: Dobbs, BDH, and BRL. Phage isolation components were purchased from Stratagene. Nick-translation and radioisotopes were purchased from Amersham. Disposable plastic ware was purchased from Fannins and Dobbs. Restriction enzymes, RNA purification kits, and RT-PCR kits were purchased from Promega. Oligonucleotides were purchased from VH Bio (UK). All components for EM work were supplied by Polyscience (USA).

Methods

3.2:ii Purification of Phage DNA from Single Plaque Forming Units.

A single plaque was placed into 30 μ l of 10mM Tris pH 7.5 which contained proteinase K (1 μ g/ μ l) and was incubated at 37 $^{\circ}$ C for 30 minutes. The proteinase K was deactivated at 99 $^{\circ}$ C for 15 minutes. 5 μ l of the above extracted DNA was used in each PCR.

3.2:iii DNA Digestion, and Gel Electrophoresis of Phage and Genomic DNAs.

DNA was digested in the presence of 4 units of the appropriate restriction enzyme at 37 $^{\circ}$ C overnight using reaction buffers supplied by the manufacturer. Reactions were stopped by phenol/chloroform and chloroform extractions followed by ethanol precipitation in the presence of 3M sodium acetate. DNA was then washed twice in 70% ethanol. The precipitate was redissolved in

sterile H₂O. To visualise the DNA, tracking dye (50% w/v glycerol, 50% w/v TE, 10mM Tris, pH 8, 1mM EDTA, 1mg/ml each of bromophenol blue and xylene cyanol) was added and the DNA fragments were separated according to size on agarose gels (0.8-2%) by electrophoresis in 1 x TAE buffer at 40 volts (Maniatis et al, 1982).

3.2:iv Southern Blotting

Gels were denatured in 1.5M NaCl/0.5M NaOH for 45 minutes and then neutralised for 30 minutes in 1.5M NaCl/0.5M Tris, pH 7.4 at room temperature prior to capillary transfer overnight in 20 xSSC (3M NaCl/0.3M Sodium Citrate). After transfer the membranes were rinsed in 2 xSSC, air dried and fixed by baking at 80°C for 2 hours. Blots were stored at room temperature until required. The transfer membrane used was Hybond-N, a hydrophilic nylon membrane with a high affinity for DNA, which can also be reprobbed.

3.2:v Nick Translation

DNA was labelled using a nick translation kit N500 which contained cold nucleotides, DNA polymerase and salt buffers (Amersham). Reaction mixture contained 1µg of Rhodopsin cDNA, 5µl of dNTP buffer, 100µCi [α -³²P]dCTP, 5µl of DNA polymerase and H₂O to a volume of 100µl. The reaction was incubated at 15°C for 1.5 hours before precipitating the DNA using 10µg yeast RNA, 0.5 volume of 7.5M ammonium acetate pH 4.6, two volumes of ice-cold ethanol and placed at -70°C for 30 minutes. The reaction was centrifuged for 30 minutes at 13,000g and the precipitate was resuspended in 200µl of H₂O. Resuspended probes were denatured by boiling and cooling on ice prior to use.

3.2:vi Prehybridization and Hybridization Conditions

Membranes of recombinant phage DNA or genomic DNA were prehybridized in 25mls of a solution containing 6 x SSC (0.9M NaCl/0.09M Sodium Citrate), 5 x Denhardt's (2% w/v BSA, 2% w/v Ficoll, 2% polyvinylpropylene [PVP]), 0.5% sodiumlaurylsulphate (SDS), with 500µg denatured salmon sperm DNA for 1 hour at 65°C. Hybridization was carried out in the same solution but with nick-translated probe present and incubated overnight at the same temperature.

3.2:vii Membrane Washes

Hybond-N membranes of phage and/or genomic DNA digests were washed in 100ml of 2 x SSC at 65°C for 15 minutes, twice. Membranes were then washed in 2 x SSC, 0.1% SDS at 65°C for 30 minutes. Membranes were finally washed to a higher stringency, 0.1 x SSC for 10 minutes at 65°C.

3.2:viii Ligations, Packaging and Titering Reactions.

Ligations were carried out using a Stratagene ligation kit. For lambda DASH II and lambda TK, 2µg of DNA was used per reaction and between 100ng and 1µg of mouse genomic DNA containing the rhodopsin gene. Reactions were in a volume of 10µl and were incubated at 4°C overnight.

Packaging was performed using Stratagene's Gigapack II Packaging Extracts. To each extract 5µl of ligated DNA was added, mixed very gently and left at room temperature to package for 1.5 hours. 500µl of SM buffer was added to stop the reaction. 20µl of chloroform was added and mixed gently and spun briefly to sediment the debris.

10 fold serial dilutions of the packaged reactions were carried out to 10^{-8} . To this 200 μ l of host cells, (which were resuspended in 10mM MgSO₄ to OD₆₀₀ = 0.5) were added and incubated at 37°C to allow the phage to adhere to the cells. 3 mls of 0.8% soft agarose (which was maintained at 48°C) was added and plated on LB plates. The plates were incubated at 37°C overnight. After incubation, plaque forming units (pfu) were counted and titer estimated.

3.2:ix Large Scale Phage Preparation.

LB broths were inoculated with the appropriate host cells and incubated at 37°C overnight. 5mls of the overnight culture was added to 100mls of tryptone supplemented with 0.2% maltose and 10mM MgSO₄ and grown to an OD₆₀₀ = $1 = 10^8$ cells/ml. The culture was centrifuged and the pelleted cells were resuspended in 5 mls of 10mM MgSO₄. This was added to 10^8 phage, left at room temperature for 15 minutes, added to 400mls of tryptone supplemented with 10mM MgSO₄ (no maltose) and incubated at 37°C until lysis occurred. After lysis, 8mls of chloroform was added, mixed and left at room temperature for 10 minutes. 23.5g of NaCl was added, dissolved and left at 4°C overnight. The lysed cells were centrifuged at 7K, 4°C for 10 minutes to remove debris. PEG6000 was added to 10%, mixed, left at 4°C for 3 hours and centrifuged at 7K, 4°C, 10 minutes. Pellets were dissolved in 8mls of SM buffer and extracted twice with chloroform before centrifugation at 4K for 10 minutes. The solution was put through a CsCl step gradient (1.7, 1.5 and 1.3g/ml) and centrifuged at 26K, 18°C for 1.5 hours. The phage band was removed and further put through a 1.5g/ml CsCl gradient at 40K 4°C overnight. The phage band was harvested and dialysed against SM buffer for 2 hours at room temperature to remove the CsCl. Phage DNA (1ml) was extracted by the addition of 50 μ l of 1M Tris pH8.0, 4 μ l of 5M NaCl, 60 μ l of 0.5M EDTA pH8.0, 100 μ l 10% SDS and 5 μ l of proteinase K (20mg/ml), mixed and incubated at 45°C for 1hour. The DNA was

extracted twice with phenol and chloroform. The DNA was dialysed extensively against TE at 4°C overnight.

3.2:x Large Scale Plasmid Preparations.

The appropriate *E. coli* strains treated with CaCl₂ were transformed with plasmid DNA according to a method described by Maniatis (1982). The transformants were selected on agar plates containing the appropriate antibiotics.

Large scale plasmid preparations were carried out which involved the growth of bacteria in the presence of an antibiotic, amplification of the plasmid, lysis and purification of the DNA through CsCl.

3.2:xi Polymerase Chain Reaction (PCR).

PCR was performed in a 25µl reaction containing 100ng DNA, 50 pmol each of oligonucleotide primers, 200µM each of dGTP, dATP dTTP and dCTP, 50mM KCl, 10mM Tris (pH 9), 1.5mM Mg Cl₂, 0.01% gelatin (w/v), 0.1% triton-X, 0.75 unit Taq polymerase. PCRs were carried out under the following conditions; 94°C, 1'; 55°C, 1'; 72°C, 1.2'; 35 cycles. PCR products were resolved on a 2% agarose gel

3.2:xii Isolation of Total RNA using SV Total RNA Isolation System (Promega).

The retinas of Rho^{+/-}, Rho^{+/+} and Rho^{-/-} were placed in 175µl of RNA lysis buffer (4M guanidine isothiocyanate, 0.01M Tris-HCl pH 7.5 and 0.97% B-Mercaptoethanol) and homogenized. 350µl of RNA dilution buffer was added, mixed by inverting 3 to 4 times, placed at 70°C for 3 minutes and spun for 10

minutes at 14,000g. To the lysate solution 200 μ l of 95% ethanol was added and mixed by pipetting. The solution was transferred to a Spin Basket Assembly (Promega) and centrifuged for 1 minute at 14,000g. 600 μ l of RNA wash solution (162.8mM potassium acetate, 27.1mM Tris-HCl pH 7.5) was added and centrifuged at 14,000g for 1 minute. The eluted solution was discarded. 50 μ l of DNase incubation mix (0.0225M Tris pH7.5, 1.125M NaCl, 0.09M MgCl₂) and DNase 1 (18.35units per 1 μ l]) were added to the spin basket and incubated at room temperature for 15 minutes. 200 μ l of DNase stop solution (4M guanidine thiocyanate, 10mM Tris-HCl pH 7.5) was added to the spin basket and spun at 14,000g for 1 minute. 600 μ l of RNA wash solution was added and spun at 14,000g for 1 minute. The spin basket was then transferred to an elution tube and 100 μ l of nuclease free water was added and centrifuged at 14,000g for one minute. RNA was stored at -70°C until required.

3.2:xiii Reverse Transcriptase Polymerase Chain Reaction (RT-PCR).

Reverse transcriptase PCR (RT-PCR) was carried out on total RNA extracted from whole eyes of Rho^{+/+}, Rho^{+/-} and Rho^{-/-} mice. RT-PCR was performed using 2 μ g RNA, 50 pmol each of oligonucleotide primers, 10mM each of dGTP, dATP dTTP and dCTP, 5 x AMV1Tf1 buffer (Promega), 25mM MgSO₄, AMV reverse transcriptase (5u/ μ l) and nuclease-free H₂O to a volume of 50 μ l. First strand cDNA synthesis is as follows: 48°C, 45 minutes (1 cycle); 92°C, 2 minutes (1 cycle); 94°C for 30 seconds; 60°C, 1 minute; 68°C for 2 minutes (40 cycles).

3.2:xiv Histology

Mice whose eyes were to be used for light and electron microscopy (EM) were perfused with a mixture of 2.5% glutaraldehyde, 2% paraformaldehyde in

0.1M phosphate buffer, pH 7.4. Eyes were removed and a suture tied at the ora serrata on the temporal side of the eye to keep track of orientation. They remained in fixative overnight at 4°C and after trimming, were processed for light or EM microscopy. Eyes for light microscopy were embedded in JB-4 (Polysciences, Warrington, PA). Three mm sections were cut through the optic nerve head, along the vertical meridian of the eye and stained with hematoxylin and eosin. For EM, eyes were post fixed in osmium tetroxide for 1 hour and, after dehydration in a graded series of alcohol, were embedded in Epon. One mm sections were cut from these blocks through the optic nerve head along the vertical meridian of the eye and stained with toluidine blue for light microscopy. The block was further trimmed and thin sections were cut and stained with uranyl acetate and lead citrate for electron microscopy and observed in a Phillips CM100 electron microscope.

3.2:xv Immunocytochemical Analysis of Rhodopsin in Retinal Sections.

Slides containing retinal sections were washed in 0.01M PBS (pH 7.4) and post-fixed in 4% paraformaldehyde for 5 minutes. Slides were washed extensively in 0.01M PBS and incubated with goat serum (Sigma) diluted 1:10 in antibody diluting solution (ADS: 0.25% Triton X-100, 0.01% sodium azide, 1% goat serum in 0.01M PBS pH 7.4). After incubation for 50 minutes at room temperature, blocking solution was replaced by ADS containing the primary antibody (anti-rhodopsin antibody 4D2 [Hicks and Molday, 1986]). After incubation for 12 hours at ambient temperature, sections were washed in 0.01M PBS and incubated with secondary antibody (biotinylated anti-mouse IgG, Amersham) for 6 hours. Sections were then incubated for a further 12 hours with a streptavidin-biotinylated horseradish peroxidase complex in 1% goat serum. Sections were then incubated with 0.05% diaminobenzidine (DAB) (Pierce) in 0.01M PBS pH7.4 for 30 minutes. Colour was developed by

incubation in a solution containing hydrogen peroxide (0.03%) and DAB (0.05%). Sections were also counter-stained with hematoxylin and eosin (Sigma).

3.2:xvi Electoretinographic Recordings.

Electroretinograms (ERG) were recorded on 21 mice from the F1 and F2 generation at ages of 27 days to 4 months. Two were wild type, 8 were heterozygous and 11 were homozygous. ERGs were performed according to previously described procedures (Bush et al, 1995). The animals were dark adapted overnight and prepared for recording in dim red light, after which they were dark adapted for an additional 20 minutes. Anaesthesia was induced with intramuscular injections of 500 mg/kg urethane, 11 mg/kg xylazine and 14 mg/kg ketamine. Pupils were dilated with 0.05% phenylephrine and 0.05% atropine. The mice were positioned with a bite bar and nose clamp and placed on a circulating warm water table at 38°C to maintain body temperature. ERGs were recorded using a 1 mm silver-silver chloride wire loop electrode on the cornea, a stainless steel subcutaneous needle on the forehead as the reference and a ground electrode on the foot of the mice. Signals were amplified 10,000 times at 0.1 to 1000 Hz and passed through a 60 Hz notch filter. One hundred traces were averaged. Single traces were collected over the brightest 2 log units of intensity for animals with large responses, with 50s interstimulus intervals. Intensity of 50ms flashes was regulated with Wratten (Kodak) neutral density (nd) filters over more than 6 log units with a maximum intensity of 130 cd/m². Dark adapted ERGs were recorded beginning at threshold. Light adapted ERGs were recorded at 0 nd flashes on a background of 37 cd/m² to suppress rod responses and reveal cone responses after 10 minutes of exposure to the background light.

3.3 Results

3.3:i Construction of rhodopsin targeting vector, ES cell selection, generation and analysis of chimeric mice.

A 17.1 kb clone was isolated from a Lambda DASH phage library containing I29Sv-derived mouse genomic DNA by PCR using two sets of primers located 5' and 3' of the mouse rhodopsin gene [forward and reverse primers, 5' of the rhodopsin gene - 5'-TTGTCCTGCCTGGATACCTAT-3', 5'-TCTGAGGCTTCAGAACTCTG-3', and forward and reverse primers 3' of the mouse rhodopsin gene 5'-TGGAAACCTTGCCTCATGTC-3' and 5'-GCTTGAGAGCAACAGACCAC-3']. The phage library was titered and 1 million plaque forming units (pfu) were plated over 20 large petri dishes (ie 50,000 pfu per plate), and incubated at 37°C overnight. Plates were overlaid with SM buffer and rotated at room temperature for 3 hours. Supernatant was removed, 100µl of this was used for DNA analysis and the rest was stored at 4°C. PCR was performed on DNA from all plates using the 3' and 5' rhodopsin primers. Phage stock that produced a signal with both sets of primers was further titrated and 50,000 pfu were plated over 20 petri dishes. This selection procedure was repeated down to the 50 pfu stage, and an impression was taken of the plaques onto a Hybond-N filter (Amersham). A human rhodopsin cDNA was used to probe the filter and isolate the 17.1kb fragment. A restriction map of this fragment showing relevant restriction enzyme sites is illustrated in Figure 3.1C. An 11.1 and 3.7kb *Bam* HI and a 2.7kb *Not*I/*Bam*HI fragment derived from the initial 17.1 kb genomic clone were subcloned into Bluescript plasmid (Stratagene) to enable the clones to be fully sequenced for further restriction analysis. The *Bam*HI 11.1kb insert containing all five exons of rhodopsin was ligated into *Bam*HI cut Lambda DASH II. A 3.1 kb *Eco*RV fragment containing the KT3NP4 RNA polymerase II promoter-driven *neo*^r cassette (Deng et al,

1993; Davis and Capecchi, 1994) was ligated into the single *Eco47III* site in the rhodopsin gene, at Codon 135 in Exon II (Figure 3.1A). Following excision with *Sall*, the construct was subcloned into the *XhoI*-cut arms of the Lambda phage targeting vector, λ Syrinx2TK. The rhodopsin genomic sequence, carrying the *neo^f* insert and flanked by the two Thymidine Kinase genes of Lambda Syrinx2TK (Figure 3.1A), was separated from the Lambda phage arms with *Sall*. This was electroporated into R1 embryonic stem (ES) cells by Dr. Mario Capecchi. Positive-negative selection using neomycin and gancyclovir was used to enrich for correctly targeted clones, as described by Mansour et al, (1988). DNAs from 59 selected ES cell clones were digested with *NdeI* and subjected to Southern analysis, (the experiment was undertaken by Dr. Derrick Rancourt at the laboratories of Dr. Mario Capecchi). A 2.7kb 3' flanking fragment, generated by me and provided to Dr. Rancourt for this experiment was used as a probe to detect a 6.7 kb endogenous fragment which increased by 3.1 kb to 9.8 kb in the targeted allele (Figure 3.1b). Four of 59 selected clones (approximately 8%) were identified by this analysis to possess the expected allele.

Two of the correctly targeted cell lines, 1c10 and 1e11, were microinjected by Dr. Mario Capecchi into C57BL/6 blastocysts and each produced one chimeric male mouse that transmitted the targeted allele (mice 2446 and 2461 respectively). A photograph of chimera 2446 is illustrated in Figure 3.2. (Note variegated coat colour indicative of chimerism). Each chimera produced approximately 70% R1-derived offspring, distinguished by agouti coat colour. One half of the R1-derived offspring were identified as heterozygous for the targeted allele both by *NdeI* fragment shift Southern assay (Southern, 1975) and also by a polymerase chain reaction (PCR) screen utilising a mutant-specific primer within the *neo* construct (Figure 3.1d). [Oligo *a* (5'TTCAAGCCCAAGCTTTCGCG3') is a reverse primer for pol-II-*neo*. Oligos *b* and *c* are forward and reverse primers for exon II of the rhodopsin gene (b,

5'AGGTTAGAGCTGGAGGACTG3'; c,5' TAAGACTGATTGGACCATTTC3']. All three primers were used together in the amplification reaction. Mice of the 1c10 and 1e11 sub-lines, representing independently targeted ES clones, were maintained separately. Heterozygotes were crossed to produce litters that included all three rhodopsin genotypes, that is, $Rho^{+/-}$, $Rho^{-/-}$ and wild-type. Targeted homozygotes ($Rho^{-/-}$) of each lineage developed an identical degenerative retinopathy. Since the mutant phenotypes that result in both lineages are the same, we believe that the retinopathy is caused solely by the targeted disruption at the rhodopsin locus, and not to other, unintended mutations that may simultaneously have occurred in the two targeted ES cell clones. I developed a rapid PCR screening assay for genotype assignments (illustrated Figure 3.1D). All mice used in the initial immunocytochemical and electroretinographic studies were one or two generations removed from the founder chimeras, i.e., F₁ or F₂ hybrids from the initial R1 (129Sv-strain) X C57Bl6/J cross.

3.3:ii Reverse Transcriptase PCR (RT-PCR).

Reverse transcription was undertaken on total RNA extracted from retinal tissue of $Rho^{-/-}$, $Rho^{+/-}$ and $Rho^{+/+}$ mice at 10 weeks of age. The primers were derived in exons I and II of the rhodopsin gene, spanning the pol2:neo insertion in exon II. A 461 bp product in $Rho^{+/+}$ and $Rho^{+/-}$ animals was observed, corresponding to the predicted length of the segment of processed rhodopsin transcript. No product was observed using RNA derived from $Rho^{-/-}$ animals, indicating that the rhodopsin transcript, as well as the gene, was absent, [forward and reverse primers of exons 1 and II of the mouse rhodopsin gene are: 5'-TATGTGCCCTTCTCCAACGT-3' and 5'-ATGATCCAGGTGAAGACCAC-3' respectively (Figure 3.3). In addition, primer pairs derived from sequence within exons III and IV of the mouse rhodopsin gene, 3' of the pol2:neo

disruption, amplified 202 bp products in Rho^{+/+} and Rho^{+/-} animals, corresponding to the predicted size of the processed transcript; no amplification was detectable in Rho^{-/-} mice. In addition, primers from the ubiquitously expressed mouse glyceraldehyde-3-phosphate dehydrogenase (GAPDH) gene and spanning an intron of 104 bp, amplified a product in all three genotypes (Figure 3.3). The sequence of the GAPDH forward and reverse primers are: 5'-ACCACAGTCCATGCCATCAC-3' and 5'-TCCACCACCCTGTTGCT-3 respectively.

3.3:iii Retinal Pathology of Rho^{+/-} and Rho^{-/-} mice.

Retinal sections of two 4 month old sibling mice, one wild type and one Rho^{+/-} (carrying one functional copy of the rhodopsin gene) are shown in Figure 3.4 (a,b). This work was undertaken by Dr. Ron Bush, and is included with his permission. The outer nuclear layer is thinner and the rod outer segments (ROS) are somewhat shorter in the Rho^{+/-} mouse than in the wild type sibling. Other than length, the ROS of the heterozygous mouse at this age are normal in appearance. However, close examination of Rho^{+/-} mice at earlier ages revealed some degree of disorganisation, which became more clearly visible under the electron microscope and following immunocytochemical staining (see below).

In Rho^{-/-} mice (Figure 3.4 d,e,f), a progressive decline with age in photoreceptor numbers is evident. At 24 days (Figure 3.4d), the mice have 8-10 nuclei in the outer nuclear layer compared with 10-12 nuclei for wild-type. Since less than 3% of the mouse photoreceptor cells are cones (Carter-Dawson and LaVail, 1979), most of the cells in the outer nuclear layer are rod nuclei. The numbers of nuclei in the 24 day old homozygous mouse are close to the numbers seen in adult wild-type and heterozygous animals. However, the rod outer segment layer is thinner than in either Rho^{+/-} or wild-type mice. By 48

days (Figure 3.4e) the ONL of homozygous mice is reduced to half of the width at 24 days, and the ROS/RIS layer is also thinned further. By ninety days (Figure 3.4f) the ONL is reduced to 1 cell thickness. Thus, at three months of age photoreceptor degeneration is essentially complete. Degeneration was relatively uniform from the periphery to the central retina.

Retinal sections of 27 day old *Rho*^{-/-} mice were also analysed by transmission electron microscopy, (this work was also undertaken by Dr. Ron Bush). The photomicrograph (Figure 3.5a) should be compared to that of *Rho*^{+/+} mice, shown in Figure 1.6, Chapter 1. In *Rho*^{-/-} animals of this age no cellular morphology can be observed in the residual RIS/ROS layers. The region between the outer limiting membrane and the pigment epithelium contains material primarily of inner segment origin, including cilia, basal bodies and mitochondria. No intact outer segment material was seen. Thus, it appears that rod outer segments are not elaborated in animals lacking functional rhodopsin genes.

3.3:iv Immunocytochemical Analysis of Rhodopsin in Retinal Sections.

A preliminary analysis, using non-fluorescent anti-rhodopsin antibodies, was undertaken by Dr. A. Boros, a visitor from the University of Szeged. Retinal sections of 8 week wild-type, *Rho*^{+/-} and *Rho*^{-/-} animals were assayed by immunocytochemistry for rhodopsin (Figure 3.5b,c,d) using the 4D2 antibody which recognises an epitope within the first 39 amino acid residues of the protein (Hicks and Molday, 1986). Strong reactivity was seen in the ROS of both wild type and heterozygous animals (Figure 3.5b,c). The disorganisation of the ROS in heterozygotes of this age is clearly evident. No immunoreactivity was detectable in the homozygote, strongly indicative of a total absence of rhodopsin (Figure 3.5d).

Subsequent to this initial analysis, I employed a fluorescent 4D2 antibody in order to undertake a more sensitive assay for the presence or absence of rhodopsin. (This antibody was kindly supplied by Drs. Lorie and Robert Molday, University of Vancouver). The results of this experiment are illustrated in Figure 3.6a-d. No immunoreactivity towards Rhodopsin was observed in $Rho^{-/-}$ mice consistent with a complete knockout of the rhodopsin gene.

3.3:v Electoretinographic Analysis of $Rho^{+/-}$ and $Rho^{-/-}$ Mice.

Mice were transported to the laboratory of Dr. Paul Sieving (Kellogg Eye Institute, Michigan) who undertook the following ERG studies.

Figure 3.7 shows the mouse electroretinogram (ERG) of a wild type, heterozygote and homozygote at increasing intensities of stimulus for light-adapted and dark-adapted conditions. The mouse ERG reveals different components depending on flash and background intensity. These components reflect the activity of different neurons in the retina (Brown, 1968; Steinberg et al, 1991). In the dark-adapted state the ERG is generated primarily by cells in the rod pathway, including the rod photoreceptors (Penn and Hagins, 1969), rod bipolar cells (Stockton and Slaughter, 1989) and amacrine cells (Sieving et al, 1986). Under bright light adaptation the rod pathway is suppressed and only cells in the cone pathway contribute to the ERG (Aguilar and Stiles, 1954; Peachy et al, 1993 and Sieving et al, 1994). At 10 weeks of age both the heterozygous and wild type mice show similar ERG responses at each intensity. The most sensitive response appearing with very dim flashes, is the scotopic threshold response (STR). Although not reported previously in the mouse, it has been recorded in many other mammals at intensities below b-wave threshold and very near visual threshold (Sieving and Nino, 1988; Bush and Reme, 1992 and Sieving and Wakabayashi, 1991). The STR reflects primarily amacrine cell activity in the proximal retina (Sieving et al, 1986). The STRs

shown in Figure 3.7 were recorded at intensities about one log unit above the STR threshold in rats (Bush et al, 1995) and slightly more than 1 log unit greater than the visual evoked potential threshold recorded in albino and pigmented C57BL/6J mice (Green et al, 1994). In the rat this response was recorded at an intensity at which an estimated 1 in 2500 rods absorbed a single photon (Bush et al, 1995). The 10 week old heterozygous and wild type siblings in Figure 3.7 exhibit an STR at the same intensity, demonstrating that rod sensitivity to very small amounts of light is unaffected by having only a single normal rhodopsin allele.

The other dark adapted ERG potentials of $Rho^{+/-}$ mice also developed in parallel with wild type mice. The ERG b-wave, which reflects bipolar cell activity, and the a-wave, representing rod photoreceptor responses, had similar thresholds in $Rho^{+/-}$ and wild type animals as shown for the 10 week old siblings in Figure 3.7. By contrast $Rho^{-/-}$ mice have no rod ERG responses. ERG responses above -0.3 cd/m^2 (candelas/metre²) are cone responses (Figure 3.7). At higher intensities a small cone b-wave develops but no a-wave is seen. The b-wave response of the $Rho^{-/-}$ mouse is narrower, having a faster time course, and lacks most of the oscillatory potentials seen on the leading edge of the dark-adapted b-waves of the wild type and heterozygous animals.

Light-adapted ERGs in wild type, heterozygous and homozygous mice were recorded using conditions that suppress rod responses and reveal cone signals (Aguilar and Stiles, 1954). Light-adapted responses in 10 week old wild-type and heterozygous siblings were very similar in amplitude and waveform (Figure 3.7). The cone response of the 7 week old $Rho^{-/-}$ mouse was somewhat reduced and lacked an a-wave but otherwise resembled the normal responses. The light-adapted and dark-adapted responses in the $Rho^{-/-}$ mouse had similar amplitude and waveform, indicating that all of the ERG activity recorded in the $Rho^{-/-}$ animal is derived from cone activity.

3.3:vi Breeding of Rho^{-/-} Mice onto Pure C57 and 129 Genetic Backgrounds.

Over the course of approximately two years, I crossed Rho^{-/-} mice with pure C57 and 129 mice (over 12 generations) to ascertain whether one or other genetic background might favour photoreceptor survival. Retinal sections from time points extending up to three months post birth are shown in Figure 3.8. These preliminary data indicate a slower rate of photoreceptor degeneration on the C57 as opposed to 129 genetic background. Notably, at 3 months there are 2-3 rows of nuclei in C57 compared to a single row in 129 retinas. The significance of these results is discussed below.

3.3:vii Generation of Rho^{-/-}c-fos^{-/-} Mice.

It is well established that absence of c-fos is strongly protective against light-induced damage to the photoreceptors, to such an extent that the outer nuclear layer becomes totally resistant to light-induced apoptotic degeneration in c-fos^{-/-} animals (Hafezi et al., 1998). The availability of the Rho knockout enabled crossing of Rho^{-/-}/c-fos^{+/+} mice with Rho^{+/+}/c-fos^{+/-} mice. The PCR assay for diagnosis of c-fos genotype was the same as that reported by the Jackson Laboratory. F1s of genotype Rho^{+/-}/c-fos^{+/-} were interbred to produce an F2 generation of animals half of which, statistically, would be of genotype Rho^{-/-}/c-fos^{-/-}. It should be noted that c-fos animals are very debilitated and in our hands we found it difficult to keep these animals alive much beyond three weeks. A total of 10 Rho^{-/-}/c-fos^{+/+} and 10 Rho^{-/-}/c-fos^{-/-} retinas were examined at 23 days post birth (during the phase of maximal apoptotic cell death in the outer nuclear layer (ONL) as assayed by TUNEL analysis and DNA laddering, (Audrey Hopson and Mary Ann Donovan - personal communication).

Representative retinal sections are shown in Figure 3.9, from which it can be concluded that there is essentially no difference in the thickness of the ONL when $Rho^{-/-}/c-fos^{+/+}$ and $Rho^{-/-}/c-fos^{-/-}$ retinas are compared. The significance of these observations is discussed below.

3.4 Discussion

This Chapter addresses the morphological and functional consequences on the retinas of mice of losing one or both rhodopsin genes. Loss of both alleles for rhodopsin in $Rho^{-/-}$ mice results in a morphological absence of ROS, an inability to identify the presence of opsin using an anti-opsin antibody (Figures 3.5d, 3.6a,b) and no rod ERG response in eight week old $Rho^{-/-}$ animals. This was true even at 27 days when the numbers of rod cell nuclei were near normal and the ROS layer, though reduced in width, still retained significant material. The actual content of this layer in homozygous mice was investigated by transmission electron microscopy and appears devoid of outer segments, but contains structures such as cilia and mitochondria which are associated with the inner segment. This suggests, as would be expected for a protein comprising more than 90% of the outer segment proteins, that disc morphogenesis and maintenance of disc structure are dependent upon the production of rhodopsin. Failure to detect cone outer segments may be due to the fact they are not present in a normal way in these severely structurally compromised ROS layers.

The mouse ERG normally has a near adult waveform and amplitude by 4 weeks of age, so the lack of an ERG response across the normal rod intensity range at 27 days (Figure 3.7) is not due simply to the young age of the animals but indicates a lack of any functioning rods in $Rho^{-/-}$ mice. As illustrated in Figure 3.7, an ERG response was present in young homozygotes at flash intensities above cone ERG threshold. That these responses did not change substantially in the presence of a rod-saturating background indicates that most, if not all, of these high intensity responses are cone-derived.

Loss of photoreceptor cells from the outer nuclear layer of $Rho^{-/-}$ mice is more rapid than that seen in mice homozygous for the retinal degeneration mutant, *rds*, but there are many similar characteristics (Jansen and Sanyal, 1984 and Sanyal and Jansen, 1981)). In the *rds*^{-/-} animals the outer nuclear

layer decreased to 50% thickness in 2-3 months, the decrease slowed after this age, and the ONL was essentially gone at 12 months (Jansen and Sanyal, 1984)). *Rds*^{-/-} mice are similar to *Rho*^{-/-} mice in that their retinas at about 4 weeks have near normal ONL width but the photoreceptors lack outer segments. Only inner segment material including cilia and surrounding plasma membrane can be found in the subretinal space. (Sanyal and Jansen, 1981; Cohen, 1983). Like *Rho*^{-/-} mice the defective gene codes for a major outer segment protein, peripherin, (Connell et al, 1991) thought to be important in morphogenesis and maintenance of disc structure (Arikawa et al, 1992). Rhodopsin can be detected in the inner segment of *rds/rds* mice by immunocytochemistry (Schalken et al, 1985 and Nir and Papermaster, 1986). This suggests that even in the absence of intact outer segments or disc membranes the production of rhodopsin may play a role in prolonging the life of photoreceptors. An additional difference between *Rho*^{-/-} and *rds*^{-/-} mice is that the *rds* degeneration shows a peripheral to central gradient (Jansen and Sanyal, 1984). In the present study degeneration was not quantified. However, qualitatively, no difference in rate of cell loss was observed in different regions along the vertical meridian of the retina from which the sections were taken. For purposes of comparison to clinical retinal degenerations, which often show gradients of rod loss, this is an important area for further study. Our ERG results clearly demonstrate a loss of rod function in *Rho*^{-/-} mice, even in the absence of substantial cell loss from ONL at 4 weeks. The high intensity dark adapted response probably comes from cones since its shape and size is similar to the light adapted response. *Rds/rds* mice of the same age also have a dark adapted ERG b-wave about 10% of normal (Reuther and Sanyal, 1984) but it appears to be broader than that in *Rho*^{-/-} mice and may be of rod origin. No light adapted ERG was recorded. Even though no intact outer segments were found in these mice, rhodopsin which has been detected in the plasma membrane surrounding cilia may initiate phototransduction (Nir and

Papermaster, 1986 and Reuther and Sanyal, 1984). The changes in ERG of $Rho^{-/-}$ mice contrast even more sharply with those of the black eyed RCS rat which has a comparable but somewhat slower rate of ONL cell loss (LaVail and Battelle, 1975). In this degeneration the retina retains measurable rhodopsin which is capable of regenerating, (Perlman, 1978), and intact outer segments for several weeks (Matthes and LaVail, 1989). The presence of rhodopsin in remaining functional rods results in a very different pattern of ERG changes. The b-wave and STR thresholds gradually rise with age and decreasing ONL width. Even at 100 days when only a single layer of photoreceptor nuclei remain in the ONL, rod pathway sensitivity, measured by the STR, is elevated by only 2-3 log units. $Rho^{+/-}$ mice show only limited effects on photoreceptor morphology and function as a consequence of having only a single allele for rhodopsin. Reduced ROS length and a slight thinning of the ONL are the only morphological changes appearing as late as 4 months of age. The functional effect on the ERG is variable for heterozygous siblings, with some having slightly reduced but others having greater than normal responses. The ROS disruptions seen at 4 and 8 weeks in $Rho^{+/-}$ mice are not seen in the 4 month old $Rho^{+/-}$ animal shown in Figure 3.4. It is possible that the damaged tips have been phagocytosed by the pigment epithelium and the remaining ROS are healthy and have reached a stable length. Heterozygotes may not produce enough opsin to support the normal length ROS but may stabilize at a reduced length. Alternatively, the results with $Rho^{+/-}$ mice are consistent with the possibility that reducing rhodopsin expression by eliminating one allele may act as an intracellular signal to reduce ROS length.

Histopathological and electrophysiological consequences of a targeted disruption of a γ sub-unit of the rod cGMP phosphodiesterase, an enzymatic component of visual transduction involved in regulation of levels of cGMP within the rod photoreceptors, have recently been reported (Tsang et al, 1996). In this case, heterozygous animals are histologically normal. Homozygotes thirteen

days post-birth display disorganisation of the rod outer segments, which however remain clearly visible. At three weeks of age a single photoreceptor nuclear layer remains, and the photoreceptor nuclei are completely absent at eight weeks of age. The retinopathy appears therefore to be more rapid in animals homozygous for the γ -phosphodiesterase mutation than in $Rho^{-/-}$ mice.

Recent reports have indicated reporter gene expression in mouse photoreceptors following intravitreal/sub-retinal inoculation of adeno- and adeno-associated viral vectors (Bennett et al, 1994; Tiansen et al, 1994; Borrás et al, 1996 and Ali et al, 1996). In addition, photoreceptor rescue has been reported in the retinas of *rd* mice which carry a naturally occurring mutation of the β subunit of the cyclic GMP phosphodiesterase gene, following sub-retinal inoculation of an adenoviral construct carrying β -phosphodiesterase cDNA driven by a cytomegalovirus promoter (Bennett et al, 1996). It will be of major interest to determine whether in the model described here photoreceptor rescue can be achieved following re-delivery of the missing rhodopsin gene.

The results of crossing $Rho^{-/-}$ mice onto different genetic backgrounds that could influence the rate of degeneration of photoreceptor cells are reported here for the first time. Hafezi et al (1988), have recently shown that the retinas of *c-fos*^{-/-} mice are highly resistant to light induced apoptotic cell death. In other words, when the *c-fos* protein is absent from the photoreceptors they are unable to die by apoptosis. In the $Rho^{-/-}$ mouse and in other animal models such as *rd*^{-/-}, the photoreceptors also die by apoptosis (Hafezi et al, 1997; Hobson et al, 1999 (submitted)). Therefore it is important to know whether or not absence of *c-fos* has any protective effect towards the photoreceptors in $Rho^{-/-}$ animals. From the data we have so far obtained, it is quite clear that the retinas of $Rho^{-/-}/c-fos^{+/+}$ and $Rho^{-/-}/c-fos^{-/-}$ mice show no difference in thickness at 23 days post birth. It was impossible to follow these mice further owing to the reduced viability of *c-fos*^{-/-} mice. Nevertheless these data indicate that as a method of therapeutic intervention, suppression of *c-fos* transcription in photoreceptor

cells, is unlikely to have much protective effect.

In contrast, initial results from the comparative analysis of photoreceptor degeneration in $Rho^{-/-}$ retinas in pure C57/B6 and 129 strains, appear to be interesting. At 3 months, the outer nuclear layer (ONL) of 129s has degenerated to a single row of cone cells, whereas C57s of the same age show 2-3 rows of ONL nuclei. Therefore, it is highly likely that cone cell function will remain for longer periods in C57s as compared to 129s. This could be confirmed by cone ERG analysis and by using antibodies directed, for example to cone transducin. This being the case, identification of those genetic factors pre-disposing to the protective effect will bear relevance to the development of therapies for RP in man. These experiments are ongoing.

4.1 Summary.

The long term objectives of my research are to contribute to the development of methods for the prevention of hereditary retinal diseases, particularly retinitis pigmentosa, given that it is the most prevalent mendelian retinopathy (the disease affects an estimated 1.5 million individuals worldwide). In order to develop effective therapies detailed knowledge of the etiology of RP is obligatory. Today approximately 30 genes involved in the molecular pathology of RP have been identified. With the availability of PCR and microsatellite markers genetic linkage studies on large families segregating RP are relatively straight forward. However, prior to the development of these technologies only classical markers (eg blood groups, enzymes etc) and restriction fragment length polymorphisms (RFLPs) were available for such studies. An enormous drawback to the use of such markers was their lack of information content and the arduous Southern blotting approach. Nevertheless during these times remarkable progress was made. A milestone in such research was the localization of the first autosomal dominant RP gene by this research team in 1989. The first systematic linkage study to be undertaken as part of that research was the linkage study reported in chapter 2 of this thesis (a study never reported as part of a PhD thesis). Nine genetic markers were run in that study, all of these being simple two-allele RFLPs. In spite of the tedium of this approach, an RP locus was excluded from the bulk of chromosome 4 by analysis of DNA from two families, one from Ireland and one from America. It is perhaps ironic to note that the gene in the Irish family was subsequently located on an adjacent chromosome (chromosome 3).

Apart from an extensive knowledge of genetic etiologies, animal models are also an obligatory requirement for the development of genetic therapies. As already emphasized, we chose rhodopsin for targeted disruption for several reasons. The first was historic in that the chromosome 3 linkage turned out to

involve the rhodopsin locus. Secondly however, and clearly of greater scientific importance was the fact that rhodopsin is the most abundant protein of the rod photoreceptors and mutations within the rhodopsin gene have been encountered in an appreciable number of cases of RP. The generation of the rhodopsin knockout mouse (Humphries et al., 1997) has not been reported as a PhD thesis. Already these animals are proving to be of immense value in exploring therapeutic approaches. For example work by others at this research unit has now resulted in long term and highly efficient adeno-associated viral mediated reporter gene expression (green fluorescent protein [GFP] expression driven by a rod opsin promoter). Further studies of this sort may well in the next few months result in a rescue of the photoreceptor cells from degeneration and a partial recovery of the rod electroretinogram. Parallel work is also ongoing in order to assess the neuroprotective effect on the photoreceptors of glial derived neurotrophic factor (GDNF) delivered systemically (via the tail vein) over periods of up to three months. Demonstration of photoreceptor protection in these mice would clearly strengthen the "proof of principle", that gene therapy for degenerative retinal diseases is feasible. Chapter 3 of this thesis describes the building of the rhodopsin knockout mouse and its characterization. The rhodopsin gene was disrupted by targeted integration of a neomycin resistance cassette into exon II of the gene. Double selection using both neomycin and gancyclovir resulted in the identification of a large number of embryonic stem cell lines carrying the null rhodopsin mutation. The resultant retinopathy is intermediate in severity between that of the *Rd* and *Rds* mice. During the course of this year other researchers within this unit have reported the results of experiments in which $Rho^{-/-}$ mice were crossed with mice expressing a normal human rhodopsin transgene. Complete structural and functional rescue of the $Rho^{-/-}$ retinas was obtained (McNally et al., 1999). These experiments have now been taken further by introducing a Pro23His rod opsin mutation onto the wild type human rod opsin background (these animals simultaneously express wild

type and mutant human rod opsins on a $Rho^{-/-}$ background). These mice should serve as ideal models in exploring the effects of ribozymes targeting human rhodopsin transcripts (see Millington-Ward et al., 1997, 1999).

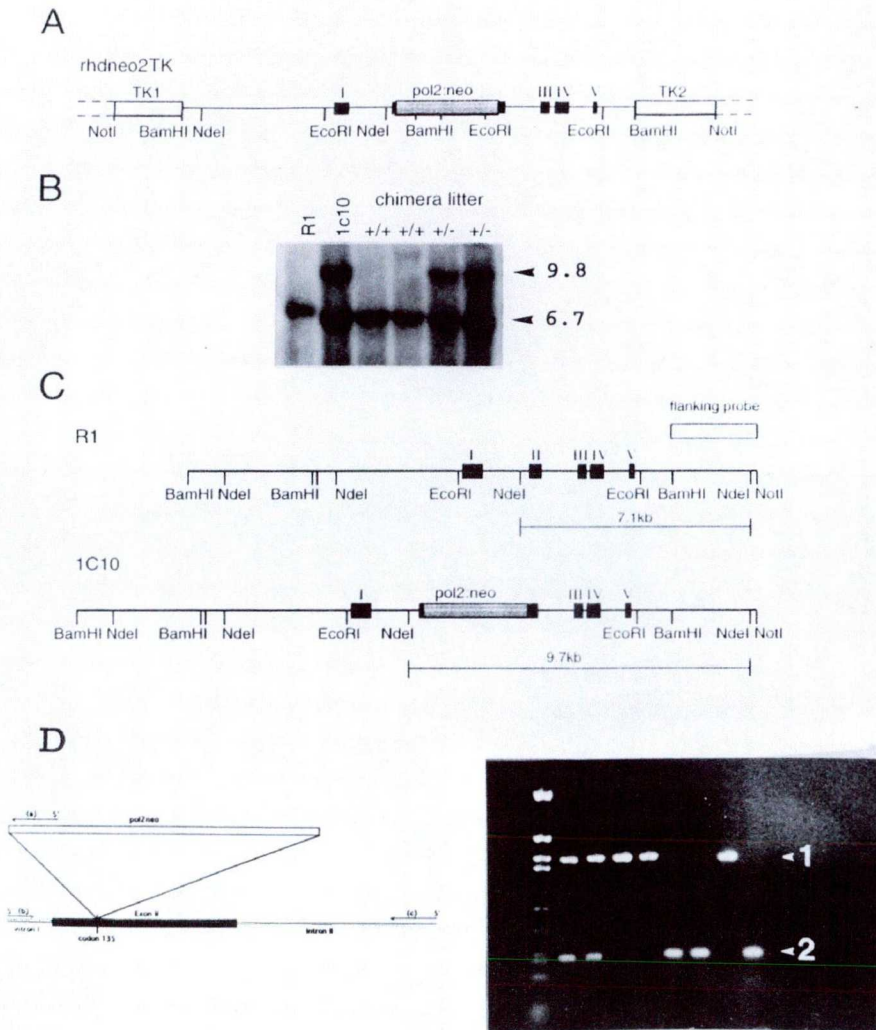
It is interesting to note that while mutations in many genes have been encountered in RP a “common pathway of cell death” appears to be apoptosis. Much is now known of the genetic factors controlling apoptosis. Suppression of *c-fos* activity, over-expression of *bcl-2*, or possibly expression within the photoreceptors of the p35 baculovirus protective protein may all turn out in principle to significantly protect the rod cells of the rhodopsin knockout mouse. Interestingly, while *c-fos*^{-/-} mice are strongly resistant to light induced photoreceptor damage the results of our experiments indicate that the peak of apoptosis is similar in $Rho^{-/-}$ mice on both a *c-fos*^{+/+} or *c-fos*^{-/-} genetic background (Hobson et al, 1999). We are currently building transgenic mice expressing p35 within photoreceptor cells, and it will be interesting to note the effects on the photoreceptors of crossing these mice onto the $Rho^{-/-}$ genetic background.

In addition, some evidence is available to suggest that the photoreceptors of pure-bred C57 mice are more resistant to light damage than many other strains (Danciger et al, 1998, 1999). We crossed $Rho^{-/-}$ mice onto pure C57 and 129 backgrounds over 12 generations. Preliminary data suggest that the degeneration is slower in C57 than in 129s. Should the difference be substantial enough there may be a possibility of identifying such protective genes.

These are some of the investigations currently being undertaken on the $Rho^{-/-}$ mouse in the work up of therapeutic approaches. Embryonic stem cells carrying a targeted 30 base pair (bp) deletion within exon II of the rhodopsin gene have now also been selected. It will be my intention to follow this experiment through to the generation of a mouse model, probably manifesting a rapid dominant segregation pattern. Such animals should be of substantial use in the further work up of ribozyme-based suppression strategies.

In conclusion there is now increasing confidence among the scientific community that some forms of genetic intervention may become available for management of degenerative retinopathies within the near future. The work in this thesis should serve to assist in such endeavours.

Figure 3.1



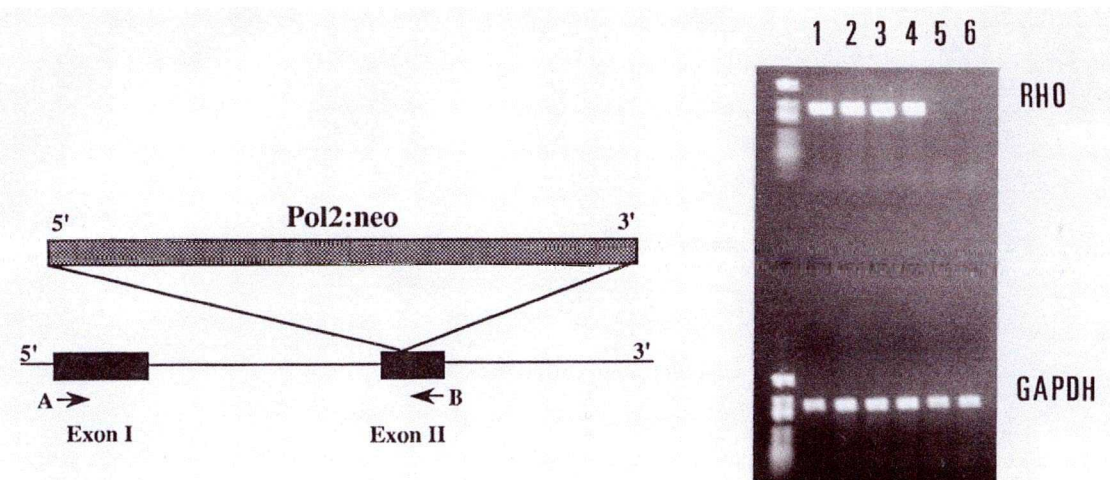
Construction of Rhodopsin gene targeting vector. **a**, targeting vector; **b**, Southern analysis of ES clones by probe flanking targeting vector, showing diagnostic shift-up of *Nde*I restriction fragment, from 6.7 kb to 9.8 kb; **c**, restriction map illustrating *pol2:neo* insertion into exon 2 of the rhodopsin gene, resulting in a 3.1 kb *Nde*I shift-up; **d**, PCR screen using a mutant specific primer within the neomycin construct and primers spanning exon II of the rhodopsin gene. Numbers 1 and 2 are indicative of the rhodopsin wild type and neomycin alleles respectively. Left most lane, *Msp*I-cut pGEM plasmid marker. The positions of primers spanning exon II and the neomycin construct are illustrated.

Figure 3.2



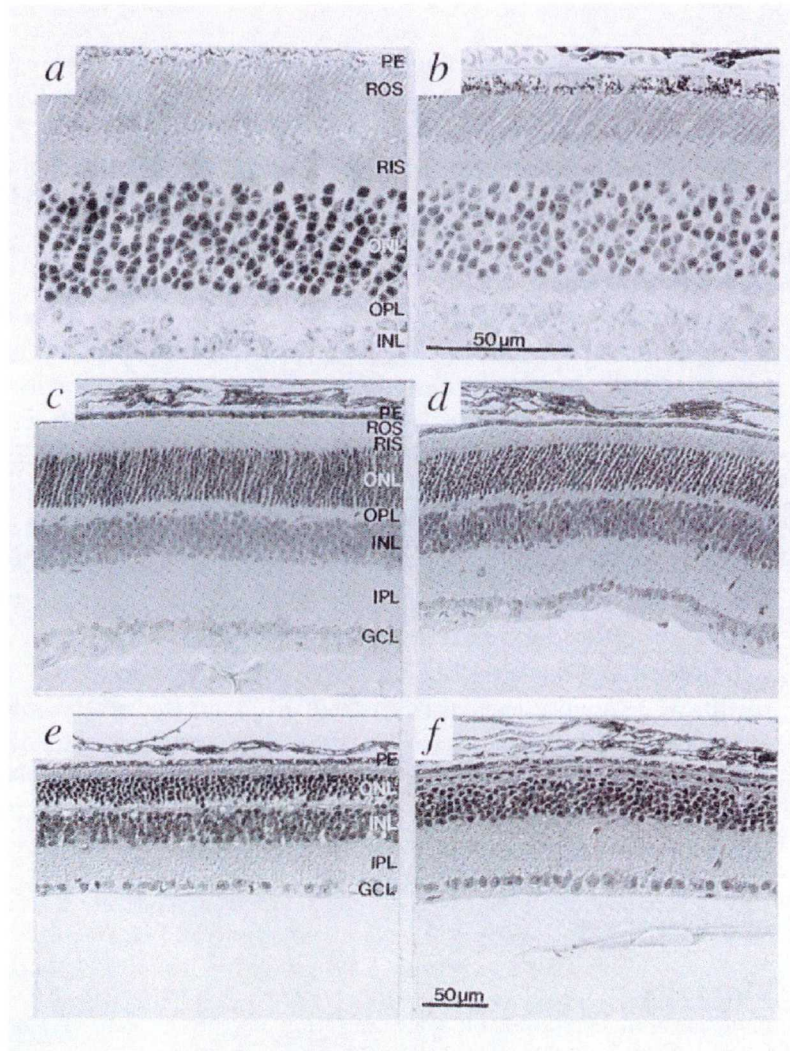
Founder chimeric Rhodopsin knockout mouse.

Figure 3.3



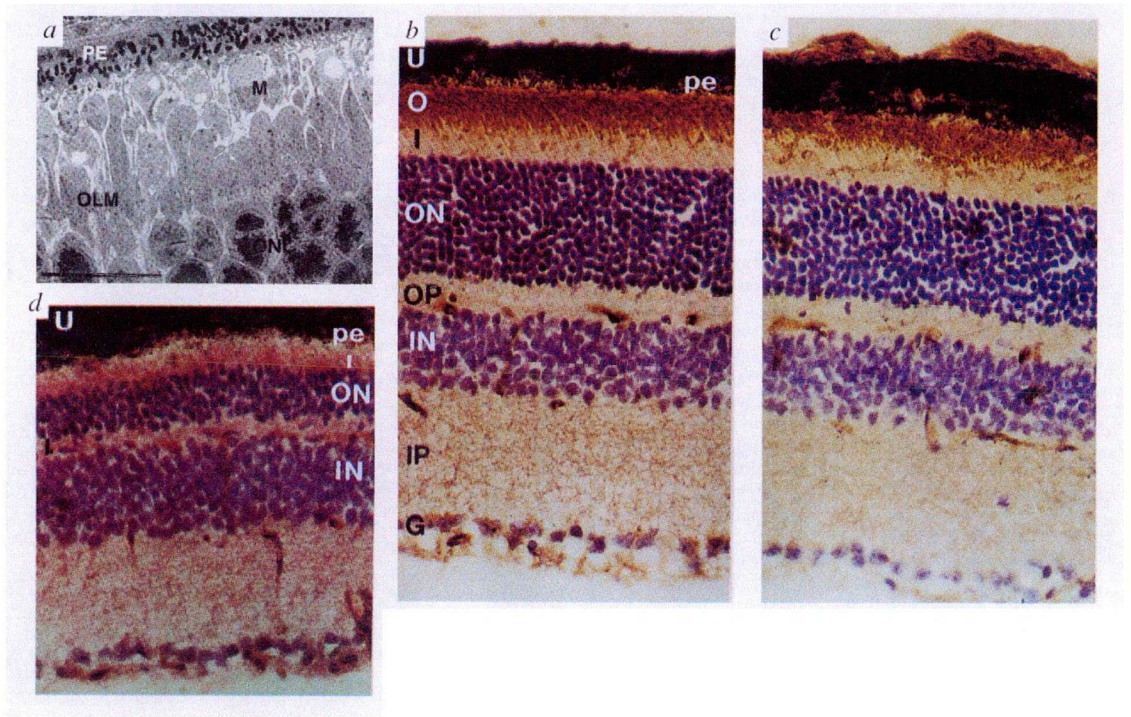
Reverse transcription undertaken on total RNA extracted from retinal tissue of $Rho^{-/-}$ (lanes 5 and 6), $Rho^{+/-}$ (lanes 3 and 4) and $Rho^{+/+}$ (lanes 1 and 2) mice. Primers were derived in exons I and II of the rhodopsin gene spanning the pol2:neo insertion in exon II, producing a 461bp product (top panel). Bottom panel indicates a PCR product of 104bp spanning an intron of the ubiquitously expressed mouse GAPDH gene in all three genotypes.

Figure 3.4



Photoreceptor morphology, **a**, **b**, Retinas from 4 month old wild type and $Rho^{+/-}$ mice respectively. 1μ m thick sections of epon-embedded tissue were cut along the vertical meridian of the eye and stained with toluidine blue. Light photomicrographs were taken of the region approximately 1 mm superior to the optic nerve head. **c – f**, 1 month $Rho^{+/-}$ mouse, and 24, 48 and 90 day $Rho^{-/-}$ respectively. Eyes were embedded in JB-4 (Polysciences) and 3μ m sections were cut through the optic nerve head and stained with haematoxylin and eosin. Light photomicrographs were taken of the region midway between the optic nerve head and periphery. PE, is pigmented epithelium; ROS, rod outer segments; RIS, rod inner segments; ONL, outer nuclear layer; OPL, outer plexiform layer; INL, inner nuclear layer; IPL, inner plexiform layer; GCL, ganglion cell layer.

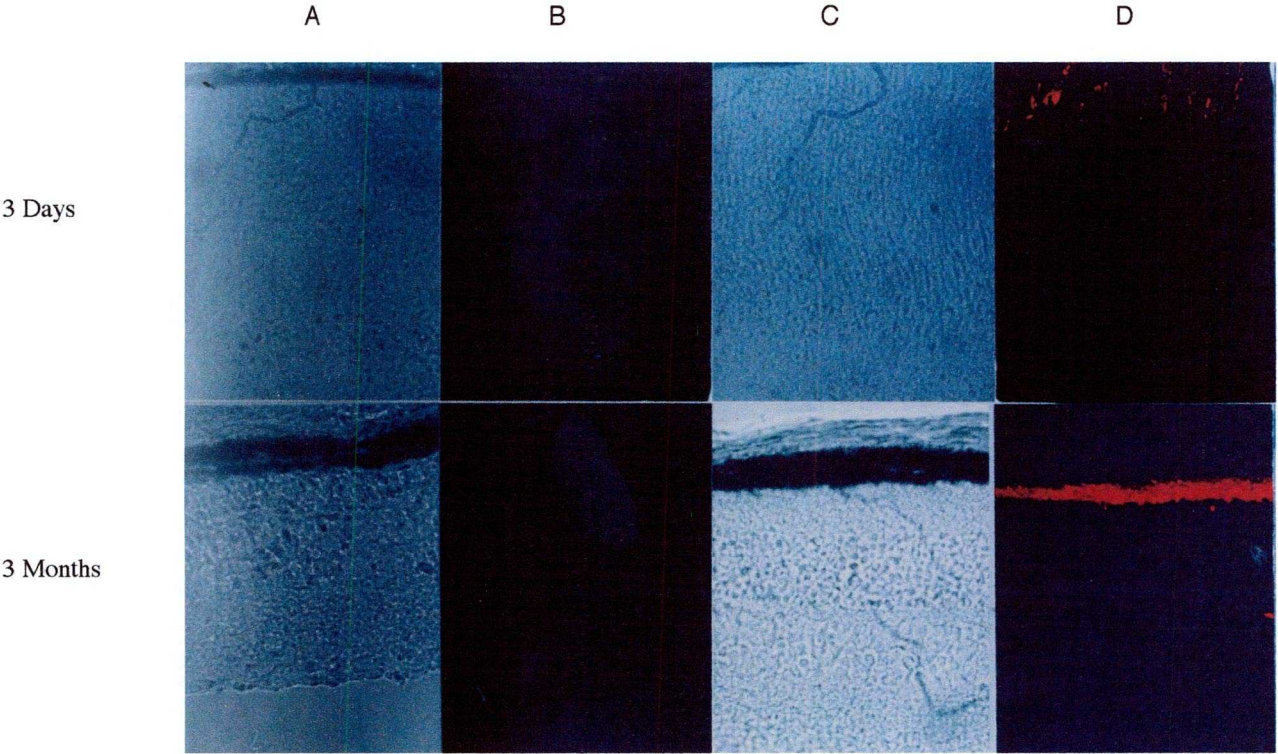
Figure 3.5



a, EM photomicrograph showing the region between the outer limiting membrane and pigment epithelium of a 1 month $Rho^{-/-}$ mouse. M, mitochondria; OLM, outer limiting membrane; ONL, outer nuclear layer; PE, pigmented epithelium. Scale bar = approximately $10 \mu\text{m}$.

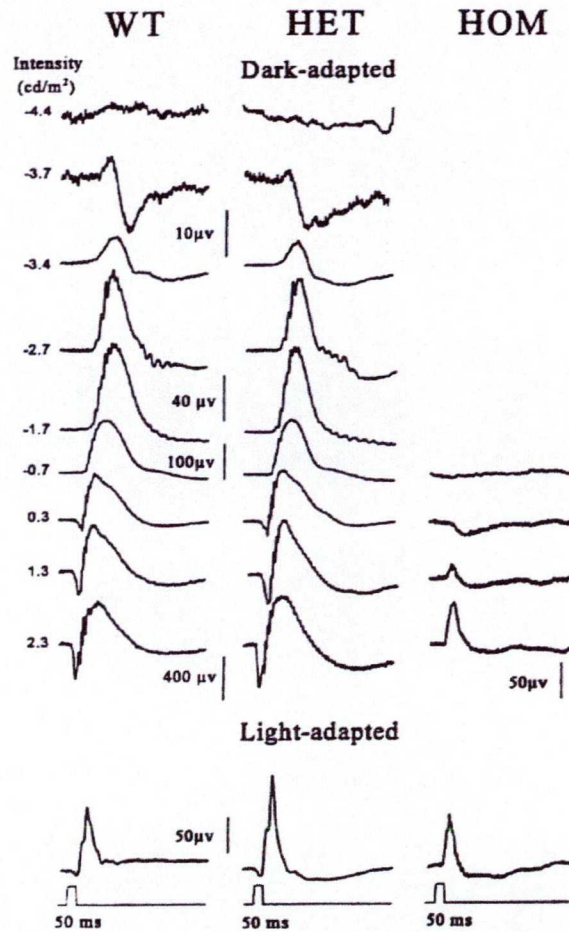
b-d, immunocytochemical analysis of retinal sections from wild type, $Rho^{+/-}$ and $Rho^{-/-}$ mice (b-d respectively). Anti-rhodopsin antibody 4D2 was used. Sections were also stained with haematoxylin and eosin to show the retinal morphology.

Figure 3.6



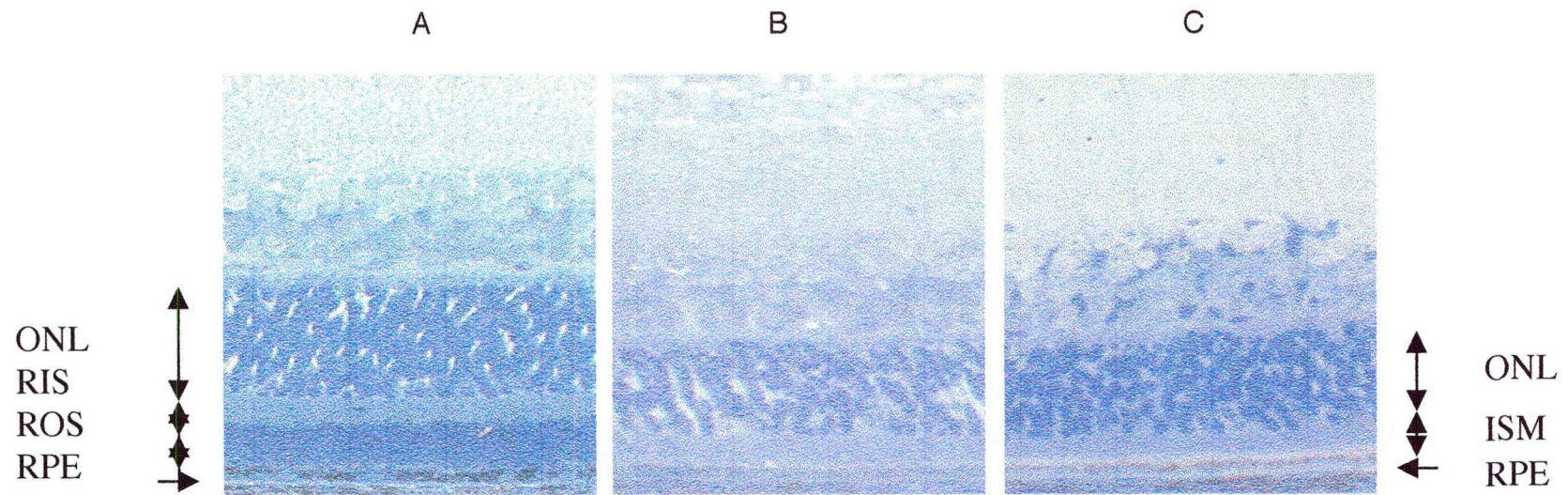
DIC and fluorescent photographs of retinal sections using a rhodopsin antibody (4D2). Lanes A and B are sections from a Rho^{-/-} mouse showing no evidence of fluorescence and absence of Rhodopsin at 3 days (top panel) and 3 months (bottom panel). Lanes C and D are sections from a Rho^{+/+} mouse showing expression of Rhodopsin at 3 days (top panel) and at 3 months (bottom panel).

Figure 3.7



Dark-adapted and light-adapted ERG responses from 13-week-old $\text{Rho}^{+/+}$ and $\text{Rho}^{+/-}$ mice, and from 7-week-old $\text{Rho}^{-/-}$ mouse. ERGs were recorded in a Ganzfeld bowl using a silver wire corneal electrode. The stimulus was a 50ms pulse of 'white' light from a tungsten halogen lamp.

Figure 3.9



Retinal sections from Rho^{+/+}cfos^{+/+} (A), Rho^{-/-}cfos^{+/+} (B) and Rho^{-/-}cfos^{-/-} (C) mice at post-natal day 23.

5.1 References

- Aguilar M and Stiles WS (1954). Saturation of the rod mechanism of the retina at high levels of stimulation. *Opt Acta*, 1, 59-63.
- Ali RR and Bhattacharya S et al (1996). Gene transfer into the mouse retina mediated by an adeno associated viral vector. *Hum Mol Genetics*, 5, 591-594.
- Allikmets R, Singh N, Sun H, Shroyer NF, Hutchinson A, Chidambaram A, Gerrard B, Baird L, Stauffer D, Peiffer A, Rattner A, Smallwood P, Li Y, Anderson KL, Lewis RA, Nathans J, Leppert M, Dean M and Lupski JR (1997). A photoreceptor cell-specific ATP-binding transporter gene (ABCR) is mutated in recessive Stargardt macular dystrophy. *Nat Genet*, 15 (3), 236-246.
- Andreasson S, Ponjavic V, Abrahamson M, Ehinger B, Wu W, Fujita R, Buraczynska M, Swaroop A (1997). Phenotypes in three Swedish families with X-linked retinitis pigmentosa caused by different mutations in the RPGR gene. *Am J Ophthalmol*, 124 (1), 95-102.
- Arden GB, and Barrada A (1962). An analysis of the electrooculograms of a series of normal subjects. *Br J Ophthalmol*, 46, 468-282.
- Arikawa K, Molday LL, Molday RS and Williams DS (1992). Localization of peripherin/rds in the disk membranes of cone and rod photoreceptors: relationship to disk membrane morphogenesis and retinal degeneration. *J Cell Biol* 11, (6), 659-667.
- Baehr W, Devlin MJ and Applebury ML (1979). Isolation and characterization of cGMP phosphodiesterase from bovine rod outer segments. *J Biol Chem*, 254 (22), 11699--77.
- Banerjee P, Kleyn PW, Knowles JA, Lewis CA, Ross BM, Parano E, Kovats SG, Lee JJ, Penchaszadeh GK, Ott J, Jacobson SG and Gilliam TC (1998). 'TULIP1' mutation in two recessive extended Dominican kindreds with autosomal recessive Retinitis Pigmentosa. *Nat Genet* 18, 177-179.
- Bellingham J, Wijesuriya SD, Evans K, Fryer A, Lennon G and Gregory CY (1997). Genetic and physical localization of the gene causing cone-rod dystrophy (CORD2). In 'Degenerative Retinal Diseases', LaVail et al. eds, Plenum Press.
- Bennett J, Wilson J, Sun D, Forbes B and Maguire A (1994). Adenovirus vector-mediated in vivo gene transfer into adult murine retinas. *Invest Oph & Vis Sci*, 35, 2535-2542.
- Bennett J, Tanabe T, Sun D, Zeng Y, Kieldbye H, Gouras P and Maguire AM (1996). Photoreceptor rescue in retinal degeneration (*rd*) mice by in vivo gene therapy. *Nature Medicine*, 2, 649-654.
- Best RZ (1905). Ueber eine hereditare maculaaffektion: Beitrage zur Vererbungslehre Z. Augenheik. 13, 199-212.

Bhattacharya SS, Wright AF, Clayton JF, Price WH, Phillips CI, McKeown CME, Jay M and Bird AC (1984). Close genetic linkage between X-linked retinitis pigmentosa and a restriction fragment length polymorphism identified by recombinant DNA probe L1.28. *Nature*, 309, 253-255.

Bhattacharya SS, Inglehearn CF, Keen J, Lester D, Bashir R, Jay M and Bird A (1991). Identification of novel rhodopsin mutations in patients with autosomal dominant retinitis pigmentosa. *Invest Ophthalmol Vis Sci*, 32, 890.

Blanton SH, Cottingham AW, Giesenschlar N, Heckenlively JR, Humphries P and Daiger SP (1991). Linkage mapping of autosomal dominant retinitis pigmentosa (RP1) to the pericentric region of human chromosome 8. *Genomics*, 11, 857-859.

Borras T, Tamm ER and Zigler JS (1996). Ocular adenovirus gene transfer varies in efficiency and inflammatory response. *Invest Oph & Vis Sci*, 37, 1282-1293.

Botstein D, White RL, Skolnick M, Davis RW (1980). Construction of a genetic linkage map in man using restriction fragment length polymorphisms. *Am. J. Hum. Genet.* 32:314-331.

Bradley DG, Farrar GJ, Sharp EM, Kenna P, Humphries MM, McConnell DJ, Daiger SP, McWilliams P, Humphries P. (1989) Autosomal dominant retinitis pigmentosa: exclusion of the gene from the short arm of chromosome 1 including the region surrounding the rhesus locus. *Am. J. Hum. Genet.* 44:570-576 .

Brown KT (1968). The electroretinogram: Its components and their origins. *Vision Res*, 8, 633-677.

Bush RA and Reme CE (1992). Chronic lithium treatment induces reversible and irreversible changes in the rat ERG in vivo. *Clin Vision Sci*, 7, 393-401.

Bush RA, Hawks KW and Sieving PA (1995). Comparison of rod threshold erg from monkey, cat and human. *Clin Vision Sci*, 6, 171-179.

Carter-Dawson LD and LaVail MM (1979). Rods and cones in the mouse retina I. Structural analysis using light and electron microscopy. *J Comp Neurol*, 188, 245-262.

Chang GQ, Hao Y and Wong F (1993). Apoptosis: final common pathway of photoreceptor death in rd, rds and rhodopsin mutant mice.

Cohen AI (1983). Some cytological and initial biochemical observations on photoreceptors in retinas of rds mice. *Invest Ophthalmol Vis Sci*, 24, (7), 832-843.

Connell G, Bascom B, Molday L, Reid D, McInness RR and Molday RS (1991). Photoreceptor peripherin is the normal product of the gene responsible for retinal degeneration in the rds mouse. *Proc Natl Acad Sci USA*, 88, (3), 723-726.

Cruickshank JK, Klein R and Klein EK (1993). Sunlight and Age-Related Macular Degeneration. *Arch Ophthalmol*, 111, 514-518.

Daiger SP (1988). Appendix H: The Retinitis Pigmentosa (RP) Collection. NIH Publication No. 89-2011, 1988/1989 Catalog of Cell lines, NIGMS Human Genetic Mutant Cell Repository, pp599-608.

Daiger SP, Bertin TK, Smith RJH, Pelias MZ (1987a). Tentative linkage of Usher's syndrome to GC on human chromosome 4. Ninth International Workshop on Human Gene Mapping. *Cytogenet Cell Genet* 46:602

Daiger SP, Brewton GW, Rios AA, Mansell PWA, Reuben JM:(1987b) Genetic susceptibility to AIDS: absence of an association with group-specific component (GC). *New Engl. J. Med.* 317:631-632.

Daiger SP, Heckenlively JR, Lewis RA, Pelias MZ (1987c). DNA linkage studies of degenerative retinal disease, in Hollyfield JG, LaVail MW (eds): *Degenerative Retinal Disorders: Clinical and Laboratory Investigations* (Alan R. Liss, New York.

Daiger SP (1999). RetNet: Disease Table.
<http://www.sph.uth.tmc.edu/RetNet/disease.htm>.

Danciger M, Rickabaugh T, Matthes MT, Yasumura D, Kumar N, LaVail MM, Farber DB (1998). Identification of a QTL on mouse chromosome 3 that influences the severity of light-induced damage of the retina. *Am J Hum Gen*, 63, (4; supplement): abstract, number 1653.

Danciger M, Rickabaugh T, Matthes MT, Yasumura D, LaVail MM, Farber DB (1999). Quantitative trait loci in the mouse influences the severity of light damage. *Invest Ophthalmol Vis Sci*, 40(4): S595, abstract number 3121.

Davis AP and Capecchi MR (1994). Axial homeosis and appendicular skeleton defects in mice with a targeted disruption of *Hoxd-11*. *Development*, 120, 2187-2198.

Deng C, Thomas KR and Capecchi MR (1993). Location of crossovers during gene targeting with insertion and replacement vectors. *Mol Cell Biol*, 13, 2134-2140.

Donis-Keller H, Green P, Helms C, Cartinhou C, Weiffenbach B, Stephens K, Keith TP, Bowden DW, Smith DR, Lander Es, Botstein D, Akots G, Rediker KS, Gravus T, Brown VA, Rising MB, Parker C, Powers JA, Watt DE, Kauffman ER, Bricker A, Phipps P, Muller-Kahle H, Fulton TR, Ng S, Schumn JW, Braman JC, Knowlton RG, Barker DF, Crooks SM, Lincoln Se, Daly MJ, Abrahamson J (1987). A genetic linkage map of the human genome. *Cell* 51: 319-337.

Dowling JE. (1987). "The Retina - An Approach to the Brain". The Belknap Press of Harvard University Press, Cambridge, Massachusetts, and London, England.

Dryja TP, McGee TL, Reichel E, Hohn LB, Cowley GS, Yandell DN, Sandberg MA and Berson EL (1990). A point mutation of the rhodopsin gene in one form of retinitis pigmentosa. *Nature*, 343, 364-366.

Dryja TP, Finn JT, Peng YW, McGee TL, Berson EL and Yau KW (1995). Mutations in the gene encoding the alpha subunit of the rod cGMP-gated channel in autosomal recessive retinitis pigmentosa. *Proc Natl Acad Sci USA*, 92 (22), 10177-10181.

Dryja TP, Hahn LB, Reboul T and Arnaud B (1996). Missense mutation in the gene encoding the alpha subunit of rod transducin in the Nougaret form of congenital stationary night blindness. *Nat Genet*, 13 (3), 358-360.

- Farber MD, Fishman GA, Weiss RA (1985). Autosomal dominant inherited retinitis pigmentosa: visual acuity loss by subtype. *Archs. Ophthalmol.* 103:524-528.
- Farrar GJ, McWilliam P, Bradley DG, Kenna P, Lawler M, Sharp EM, Humphries MM, Eiberg H, Conneally PM, Trofatter JA and Humphries P. (1990). Autosomal Dominant Retinitis Pigmentosa: Linkage to Rhodopsin and Evidence for Genetic Heterogeneity. *Genomics*, Vol. 8:35-40.
- Farrar GJ, Jordan SA, Kenna P, Humphries MM, Kumar-Singh R, McWilliam P, Allamand V, Sharp E and Humphries P. (1991a). Autosomal Dominant Retinitis Pigmentosa: Localization of a Disease Gene (RP6) to the Short Arm of Chromosome 6. *Genomics*, Vol. 11:870-874.
- Farrar GJ, Kenna P, Jordan SA, Kumar-Singh R, Humphries MM, Sharp EM, Sheils DM and Humphries P (1991b). A three-base-pair deletion in the peripherin-RDS gene in one form of retinitis pigmentosa. *Nature*, 354, 478-480.
- Farrar GJ, Kenna P, Redmond R, Sheils D, McWilliam P, Humphries MM, Sharp EM, Jordan S, Kumar-Singh R and Humphries P. (1991c). Autosomal Dominant Retinitis Pigmentosa: A Mutation in Codon 179 of the Rhodopsin Gene in Two Families of Celtic Origin. *Genomics*, Vol. 11:1170-1171.
- Farrar GJ, Findlay JBC, Kumar-Singh R, Kenna P, Humphries MM, Sharp E and Humphries P. (1992). Autosomal dominant Retinitis Pigmentosa: a novel mutation in the rhodopsin gene in the original 3q linked family. *Human Mol. Genet.*, Vol. 1, No. 9:769-771.
- Field LL, Heckenlively JR, Sparkes RS, Garcia CA, Farson C, Zedalis D, Sparkes MC, Crist M, Tideman S, Spence MA (1982). Linkage analysis of five pedigrees affected with typical autosomal dominant retinitis pigmentosa. *J. Med. Genet.* 19:266-270.
- Fishman GA (1976). Fundus flavimaculatus. A clinical classification. *Arch Ophthalmol*, 94 (12)2061-2067.
- Fuchs S, Nakazawa M, Maw M, Tamai M, Oguchi Y and Gal A (1995). A homozygous 1-base pair deletion in the arrestin gene is a frequent cause of Oguchi disease in Japanese. *Nat Genet*, 10 (3)
- Gass JDM (1987). Drusen and disciform macular detachment and degeneration. *Arch Ophthalmol*, 90, 60-96.
- Gibson F, Walsh J, Mburu P, Varela A, Brown KA, Antonio M, Beisel KW, Steel KP and Brown SDM (1998). A type VII myosin encoded by the mouse deafness gene shaker-1. *Nature*, 374, 62-64.
- Gilliam TC, Healey ST, MacDonald ME, Stewart GD, Wasmuth JJ, Tanzi RE, Roy JC, Gusella JF (1987). Isolation of polymorphic DNA fragments from human chromosome 4. *Nucl. Acids Res.* 15:1445-1458.
- Goode ME, Daiger SP, Lewis RA, Rogers WB (1985). Linkage of autosomal dominant retinitis pigmentosa (ADRP) to the Rh blood group. *Am. J. Hum. Genet.* 37:A196.
- Green DG, Herreros de Tejada P and Glover MJ (1994). Electrophysiological estimates of visual sensitivity in albino and pigmented mice. *Visual Neurosci*, 11, 919-925.

Gu SM, Thompson DA, Srikumari CR, Lorenz B, Finckh U, Nicoletti A, Murthy KR, Rathmann M, Kumaramanickavel G, Denton MJ and Gal A (1997). Mutations in RPE65 cause autosomal recessive childhood-onset severe retinal dystrophy. *17* (2) 194-197.

Gusella JF, Wasmuth JJ (1987). Report of the committee on the genetic constitution of chromosomes 3 and 4. Ninth International Workshop on Human Gene Mapping. *Cytogenet Cell Genet.* 46:131-146.

Hafezi F, Steinbach JP, Marti A, Munzck, Wang ZQ, Wagner EF, Aguzzi A and Reme CE (1998). The absence of c-fod prevents light induced apoptotic death of photoreceptors in retinal degeneration in vivo. *Nature Medicine*, 3, (3), 346-349.

Heckenlively JR (1988). "Retinitis Pigmentosa", Pub. JB Lippincott, Philadelphia, 125-149.

Heckenlively JR, Pearlman JT, Sparkes RS, Spence MA, Zedalis D, Field L, Sparkes MC, Crist M, Tideman S (1982). Possible assignment of a dominant retinitis pigmentosa gene to chromosome 1. *Ophthalmic. Res.* 14:46-53.

Hicks D and Molday RS (1986). Differential immunogold-dextran labeling of bovine and frog rod and cone cells using monoclonal antibodies against bovine rhodopsin. *Exp Eye Res*, 42, 55-71.

Hobson AH, Donovan MA, Humphries MM, Carmody R, Tuohy G, Cotter T, Farrar GJ, Kenna P and Humphries P (1999). Apoptotic death of the photoreceptors of the rhodopsin knockout mouse in the presence of c-fos. (submitted).

Horn M, Farrar GJ, Kunisch M, Marchese C, Apfelstedt-Sylla E, Fugl L, Zrenner E, Kenna P, Gal A and Humphries P (1992). Deletions in exon 5 of the human rhodopsin gene causing shift in the reading frame and autosomal dominant retinitis pigmentosa. *Human Genetics*, 90, 255-257.

Huang SH, Pittler SJ, Huang X, Oliveira L, Bersen EL and Dryja TP (1995). Autosomal recessive retinitis pigmentosa caused by mutations in the alpha subunit of rod cGMP phosphodiesterase. *Nat Genet*, 11 (4), 468-471.

Humphries MM, Rancourt D, Farrar GJ, Kenna P, Hazel M, Bush RA, Sieving PA, Sheils DM, McNally N, Creighton P, Erven A, Boros A, Gulya K, Capecchi MR and Humphries P. (1997). Retinopathy induced in mice by targeted disruption of the rhodopsin gene. *Nature Genetics*, 15, 216-219.

News and views article regarding the above in the same edition of *Nature Genetics*, pgs. 116-117.

Humphries P, Kenna P, Farrar GJ (1992a). On the molecular genetics of retinitis pigmentosa. *Science* 256, 8040808.

Humphries P, Farrar GJ and Kenna P (1992b). Autosomal dominant retinitis pigmentosa: Molecular genetic and clinical aspects. *Prog Ret Res*, 12, 231-245.

Humphries P, Kenna P and Farrar GJ (1994). New dimensions in macular dystrophies. *Nat Genet*, 8 (4), 315-317.

Jansen HG and Sanyal S (1984). Development and degeneration of retina in rds mutant mice: electron microscopy. *J Comp Neurol*, 224, 71-84.

Jordan SA, Farrar GJ, Kumar-Singh R, Kenna P, Humphries MM, Allamand V, Sharp EM and Humphries P. (1992). Autosomal Dominant Retinitis Pigmentosa (adRP;RP6): Cosegregation of RP6 and the Peripherin-RDS Locus in a Late-Onset Family of Irish Origin. (1992). *Am. J. Hum. Genet.*, Vol 50:634-639.

Kajiwara K, Berson EL and Dryja TP (1994). Digenic retinitis pigmentosa due to mutations at the unlinked peripherin/RDS and ROM1 loci. *Science*, 264, (5165), 1604-1608.

Keats BJB, Morton NE, Rao DC, Williams W (1979). *A Source Book for Linkage in Man.* :Johns Hopkins University Press, Baltimore.

Klein ML, Mauldin WM and Stoumbos VD (1994). Heredity and age-related macular degeneration. Observations in monozygotic twins. *Arch Ophthalmol*, 112 (7), 932-937.

Kuhn H, Hall SW and Wilden U (1984). Light-induced binding of 48-kDa protein to photoreceptor membranes is highly enhanced by phosphorylation of rhodopsin. *FEBS Lett*, 176 (2), 473-478.

Lathrop GM, Lalouel JM, Julier C, Ott J (1984). Strategies for multilocus linkage analysis in humans. *Proc. Natl. Acad. Sci., USA*, 81:3443-3446.

La Vail MM and Battelle B-A (1975). Influence of eye pigmentation and light deprivation on inherited retina dystrophy in the rat. *Exp Eye Res*, 21, 167-192.

Maniatis T, Sambrook J and Fritsch EF (1982). *Molecular Cloning. A laboratory manual.* First Edition. Cold Spring Harbor Laboratory Press.

Mansour SM, Thomas KR and Capecchi MR (1988). Disruption of the proto-oncogene *int-2* in mouse embryo-derived stem cells: a general strategy for targeting mutations to non-selectable genes. *Nature* 336, 348-352.

Marlhens F, Bareil C, Griffoin JM, Zrenner E, Amalric P, Eliaou C, Lin SY, Harris E, Redmond TM, Arnaud B, Claustres M and Hamel CP (1997). Mutations in RPE65 cause Leber's congenital amaurosis. *Nat Genet*, 17 (2), 139-141.

Marmour MF (1983). Retinitis pigmentosa: a symposium on terminology and methods of examination. *Ophthalmology*, 90, 126-131.

Matthes MT and LaVail MM (1989). Inherited retinal dystrophy in the RCS rat: Composition of the outer segment debris zone. *Inherited and Environmentally Induced Retinal Degenerations* (eds LaVail MM, Anderson RE and Hollyfield JF), 315-330, (Alan R Liss Inc. New York).

Maw MA, Kennedy B, Knight A, Bridges R, Roth KE, Mani EJ, Mukkadan JK, Nancarrow D, Crabb JW, Denton MJ (1997). Mutation of the gene encoding cellular retinaldehyde-binding protein in autosomal recessive retinitis pigmentosa. *Nat Genet*, 17 (2), 198-200.

Meindl A, Dry K, Herrmann K, Manson F, Ciccodicola A, Edgar A, Carvalho MRS, Achatz H, Hellebrand H, Lennon A, Migliaccio C, Portor K, Zrenner E, Brid A, Jay M, Lorenz B, Wittwer B, D'Urso M, Meitinger T and Wright A (1996). A gene (RPGR) with homology to the RCC1 guanine nucleotide exchange factor is mutated in X-linked retinitis pigmentosa (RP3). *Nature Genetics*, 12, 35-42.

Meyers SM and Zachary AA (1988). Monozygotic twins with age-related macular degeneration. *Arch Ophthalmol*, 106 (5), 651-653.

Meyers SM, Greene T and Gutman FA (1995). A twin study of age-related macular degeneration. *Am J of Ophthal*, 120, 757-766.

Millington-Ward S, O'Neill B, Tuohy G, Al-Jandal N, Kiang AS, Kenna P,F, Palfi A, Hayden P, Mansergh F, Kennan A, Humphries P and Farrar GJ (1997). Strategies in vitro for gene therapies directed to dominant mutations. *Hum Mol Genet*, 6, 1415-1426.

Millington-Ward S, O'Neill B, Kiang A-S, Humphries P, Kenna PF and Farrar GJ (1999). A mutation-independent therapeutic strategem for Osteogenesis Imperfecta. *Antisense & Nucleic Acid Drug Development*, 9, 6, 537-542.

Murray J, Buetow KH, smith M, Carlock L, Chakravarti A, Ferrell RE, Gedamu L, Gilliam C, Shiahg R, De Haven CR (1988). Pairwise linkage analysis of 11 loci on human chromosome 4. *Am J Hum Genet*, 42, 490-497.

MacDonald ME, Anderson MA, Gilliam TC, Tranebjaerg L, Carpenter NJ, Magenis E, Hayden MR, Healey ST, Bonner TI, Gusella JF (1987). A somatic cell hybrid panel for localizing DNA segments near the Huntington's disease gene. *Genomics* 1:29034.

McKusick VA (1983). "Mendelian inheritance in man: Catalogues of autosomal dominant, autosomal recessive and X-linked phenotypes", 6th ed., Johns Hopkins University Press, Baltimore.

McLaughlin ME, Ehrhart TL, Berson EL and Dryja TP (1995). Mutation spectrum of the gene encoding the beta subunit of rod phosphodiesterase among patients with autosomal recessive retinitis pigmentosa. *Proc Natl Acad Sci USA*, 92 (8), 3249-3253.

McNally N, Kenna P, Humphries MM, Hobson AH, Khan NW, Bush RA, Sieving PA, Humphries P and Farrar GJ (1999). Structural and functional rescue of murine rod photoreceptors by human rhodopsin transgene. *Hum Mole Genetics*, 8, 7, 1309-1312.

McWilliam P, Farrar GJ, Kenna P, Bradley DG, Humphries MM, Sharp EM, McConnell DJ, Lawler M, Sheils D, Ryan C, Stevens C, Daiger SP and Humphries P (1989). Autosomal dominant retinitis pigmentosa (adRP): Localization of an adRP gene to the long arm of chromosome 3. *Genomics*, 5:619-622.

Newell FW (1982). *Ophthalmology: Principles and Concepts* (5th Edition). The CV Mosby Company.

Nichols BE, Sheffield VC, Vandenburth K, Drack AV, Kimura AE and Stone EM (1993). Butterfly-shaped pigment dystrophy of the fovea caused by a point mutation in codon 167 of the RDS gene. *Nat Genet*, 3, (3), 202-207.

Nir I and Papermaster DS (1986). Immunocytochemical localization of opsin in the inner segment and ciliary plasma membrane of photoreceptors in retinas of rds mutant mice. *Invest Ophthalmol Vis Sci*, 27 (5), 836-840.

Ogden TE (1989). 'Retina: Basic Science and Inherited Retinal Disease', Vol 1. The CV Mosby Company, St. Louis, Baltimore, Toronto.

Olsson JE, Gordon JW, Pawlyk BS, Rood D, Hayes A, Molday RS, Mukai S, Cowley GS, Berson EL and Dryja TP (1992). Transgenic mice with a rhodopsin mutation (Pro23His): A mouse model of autosomal dominant retinitis pigmentosa. *Neuron*, 9, 815-830.

Ott J (1985). *Analysis of Human Genetic Linkage*. :Johns Hopkins University Press, Baltimore.

Pagon RA (1988). Retinitis pigmentosa. *Surv Ophthalmol*, 33 (3), 137-177.

Peachy NS (1993). Properties of the mouse cone-mediated electroretinogram during light adaptation. *Neuroscience Letters*, 162, 9-11.

Pelias MZ, Lemoine Dr, Kossar AL, Ward LJ, Wilson AF, Elston RC (1989). Linkage studies of Usher's syndrome analysis of an Acadian kindred in Louisiana. *Cytogenet. Cell Genet*.

Penn RD and Hagins WA (1969). Signal transmission along retinal rods and the origin of the a-wave. *Nature*, 223, 201-205.

Perlman I (1978). Dark-adaptation in abnormal (RCS) rats studied electroretinographically. *J. Physiol.* 278, 161-175.

Perrault I, Rozet JM, Calvas P, Gerber S, Camuzat A, Dollfus H, Chatelin S, Souied E, Ghazi I, Leowski C, Bonnemaïson M, Le Paslier D, Frezal J, Fugier JL, Pittler S, Munnich A and Kaplan J (1996). Retinal-specific guanylate cyclase gene mutations in Leber's congenital amaurosis. *Nat Genet*, 14 (4), 461-464.

Portera-Cailliau C, Sung CH, Nathans J and Adler R (1994). Apoptotic photoreceptor cell death in mouse models of retinitis pigmentosa. *Proc Natl Acad Sci USA*, 91 (3), 974-978.

Rao VR, Cohan GB and Oprian DD (1994). Rhodopsin mutation G90D and a molecular mechanism for congenital night blindness. *nature*, 367, 639.

Reuther JH and Sanyal S (1984). Development and degeneration of retina in rds mutant mice: the electroretinogram. *Neurosci Lett*, 48, (2), 231-237.

Rose FC (1983). *The Eye in General Medicine*. Printed by University Press, Cambridge, Great Britain.

Rosenfeld PJ, Cowley GS, McGee TL, Sandberg MA, Berson EL and Dryja TP (1992). A null mutation in the rhodopsin gene causes rod photoreceptor dysfunction and autosomal recessive retinitis pigmentosa. *Nat Genet*, 1, (3), 209-213.

Sanyal S and Jansen HG (1981). Absence of receptor outer segments in the retina of rds mutant mice. *Neurosci Lett*, 21, (11), 23-26.

Sarks SF (1980). Drusen and their relationship to senile macular degeneration. *Aust J Ophthalmol*, 8, 117-130.

Sarks SH and Sarks JP (1989). *Medical Retina*, Vol 2. Eds Schachar AP, Murphy RP and Patz A. The CV Mosby Company, St. Louis, Baltimore, Toronto.

Schalken JJ (1985). Immunoassay of rod visual pigment (opsin) in the eyes of rds mutant mice lacking receptor outer segments. *Biochim Biophys Acta*, 839, (1), 122-126.

Siebert PD and Fukuda M (1986). Isolation and characterization of human glycophorin A cDNA clones by a synthetic oligonucleotide approach: nucleotide sequence and mRNA structure. *Proc. Natl. Acad. Sci. USA*, 83:1665-1669.

Sieving PA, Frishman LJ and Steinberg RH (1986). Scotopic threshold response of proximal retina in cat. *J Neurophysiol*, 56, 1049-1061.

Sieving PA and Nino C (1988). Scotopic threshold response (STR) of the human electroretinogram. *Invest Ophthalmol Visual Sci*, 29, 1608-1614.

Sieving PA and Wakabayashi K (1991). Comparison of rod threshold ERG from monkey, cat and human. *Clin Vision Sci*, 6, 171-179.

Sieving PA, Murayama K and Naarendorp F (1994). Push-pull model of the primate photopic electroretinogram: A role for hyperpolarizing neurons in shaping the b-wave. *Visual Neurosci*, 11, 519-532.

Sieving PA, Richards JE, Naarendorp F, Bingham EL, Scott K and Alpern M (1995). Dark-light: Model for nightblindness from the human rhodopsin Gly-90-Asp mutation. *Proc Natl Acad Sci USA*, 92, 880-884.

Silvestri G, Johnston PB and Hughes AE (1994). Is genetic predisposition an important risk factor in age-related macular degeneration? *Eye*, 8, 564-569.

Smith W, Mitchell P and Rochester C (1997). Serum Beta Carotene, Alpha Tocopherol and Age-Related Maculopathy: the Blue Mountains Eye Study. *Am J of Ophthalmol*, 124 (6), 838-840.

Sondheimer S, Fishman GA, Young RS and Vasquez VA (1979). Dark adaptation testing in heterozygotes of Usher's syndrome. *Br J Ophthalmol*, 63 (8), 547-550.

Sorsby AM, Mason MEJ and Gardener N (1949). A fundus dystrophy with unusual features. *Br J Ophthalmol*, 33, 67-97.

Southern EM (1975). Detection of specific sequences among DNA fragments separated by gel electrophoresis. *J Mol Biol*, 98, 503-517.

Spence MA, Sparkes RS, Heckenlively JR, Pearlman JT, Zedalis D, Sparkes M, Crist M, Tidemann S (1977). Probable genetic linkage between autosomal dominant retinitis pigmentosa (RP) and amylase (AMY2): evidence of an RP locus on chromosome 1. *Am. J. Hum. Genet.* 29:397-404.

Steinberg RH, Frishman LJ and Sieving AP (1991). Negative components of the electroretinogram from proximal retina and photoreceptor. *Progress in Retinal Research*, Vol 10, (eds Osborne N and Chader G), Pergamon Press, New York, 121-160.

Stockton RA and Slaughter MM (1989). B-wave of the electroretinogram: a reflection of on bipolar cell activity. *J Gen Physiol*, 93, 101-122.

Stryer L, Huxley JB, Fung B K-K (1981). Transducin: An amplifier protein in vision. *Trends Biochem Sci*, 6, 245-247.

Stryer L (1986). Cyclic GMP cascade of vision. *Annu Rev Neurosci*, 9, 87-119.

Sullivan LS and Daiger SP (1996). Inherited retinal degeneration: exceptional genetic and clinical heterogeneity. *Mol Med Today*, 2 (9), 380-386.

Sung CH, Makino C, Baylor D and Nathans J (1991). A rhodopsin gene mutation responsible for autosomal dominant retinitis pigmentosa results in a protein that is defective in localisation to the photoreceptor outer segments. *J Neurosci*, 14 (10), 5818-5833.

Tiansen L, Adamian M, Roof DJ, Berson EL, Dryja TP, Roessler BJ and Davidson BL (1994). In vivo transfer of a reporter gene to the retina mediated by an adenoviral vector. *Invest Oph & Vis Sci*, 35, 2543-2549.

Tsang SH, Gouras P, Yamashita CK, Kjeldbye H, Fisher J, Farber DB and Goff SP (1996). Retinal degeneration in mice lacking the γ subunit of the rod cGMP phosphodiesterase. *Science*, 272, 1026-1029.

Weber JL and May PE (1989). Abundant class of human polymorphisms which can be typed using the polymerase chain reaction. *Am J Hum Genet*, 44, 388-396.

Weber BHF, Vogt G, Wolz W, Ives EJ and Ewing CC (1994). Sorsby's fundus dystrophy is genetically linked to chromosome 22q13-qter. *Nat Genet*, 8, 352-356.

Well D, Blanchard S, Kaplan J, Builford P, gibson F, Walsh J, Mburu P, Varela A, Levilliers J, Weston MD, Kelley PM, Kimberling WJ, Wagenaar M, Levi-Acobas F, Larget-Piet D, Munnich A, Steel KP, Brown SDM and Petit C (1995). Defective myosin VIIA gene responsible for Usher syndrome type 1B. *Nature*, 374, 60-61.

Yamamoto S, Sippel KC, Berson EL and Dryja TP (1997). Defects in the rhodopsin kinase gene in the Oguchi form of stationary night blindness. *Nat Genet*, 15 (2), 175-178.

Youngman S, Sarfarazi M, Quarrell OWJ, Conneally PM, Gibbons K, Harper PS, Shaw DJ, Tanzi RE, Wallace R, Gusella JF:(1986) Studies of a DNA marker (G8) genetically linked to Huntington's disease in British families. *Hum. Genet.* 73:333-339.

Zuckerman R, Buzdygon B, Philip N, Liebman P and Sitaramayya A (1985). Arrestin: An ATP/ADP exchange protein that regulates cGMP phosphodiesterase activity in retinal rod disk membranes (RDM). *Biophys J*, 47, 37a.